JIMMA UNIVERSITY

JIMMA INSTITUTE OF TECHNOLOGY

SCHOOL OF MECHANICAL ENGINEERING

POST GRADUATE PROGRAM IN DESIGN OF MECHANICAL SYSTEM

ANALYSIS OF THIN-WALLED COMPOSITE BEAMS WITH STIFFER BOX FOR ENHANCING RIGIDITY

By Mesfin Demise

A THESIS SUBMITTED TO SCHOOL OF MECHANICAL ENGINEERING IN PARTIAL FULFILLMENT OF THE REQUIREMENT FOR THE DEGREE OF MASTER OF SCIENCE IN MECHANICAL ENGINEERING (DESIGN OF MECHANICAL SYSTEM STREAM)

Advisor: Seungwon Youn(PhD)

Co-advisor: Mr. Abiyou Solomon (PhD candidate)

JULY 17, 2019

APPROVAL

Name: Mesfin Demise

Degree: Masters of Science

Title: Analysis of thin-walled composite beams with stiffer box for enhancing rigidity

Approved by board of examiners

Mr. Seungwon Youn (PhD)		July 15, 2019
Advisor	Signature	Date
Mr. Abiyou Solomon (PhD candidate)		15 July, 2019
Advisor	Signature	Date
Dr. Mesay Alemu		28/07/19
Internal Examiner	Signature	Date
Professor Hirpa Lemu		26/7-19
External Examiner	Signature	Date
Mr. Yohannis Dabesa	____________	____________
Chairman	Signature	Date

Declaration

I hereby declare that this thesis work is being prepared by Mesfin Demise, entitled "Analysis of thin-walled composite beam with stiffer box for enhancing rigidity" is my own work that has been not submitted in full for a degree in any university/institution, which compiles with the regulations of the university and meets the accepted standards with respect to originality and quality. All relevant resources of information used in this thesis have been fully acknowledged.

Mesfin Demise	____________________	______________________
Student's Name	Signature	Date

This is to certify that the above statement made by the candidate is correct to the best of my knowledge and belief. This thesis has been submitted for examination with my approval.

Seungwon Youn (PhD)	__________________	__________________
Advisor's Name	Signature	Date
Abiyou Solomon (PhD Candidate)	__________________	__________________
Advisor's Name	Signature	Date

Acknowledgement

First of all, I would like to thank Almighty God for the endless blessings and gifts. I would like to thanks my advisor Seungwon Youn(PhD) and Mr. Abiyou Solomon (PhD candidate) for their great effort in terms of supervision, support, dedication and patience from every start and every detailed process until accomplishment of my research.

Finally, I would like to thanks and give my appreciation to all of my family members and my friends those who were supporting and motivating me for the achievement of this study.

Abstract

Fiber reinforced composites have a set of attractive material properties such as higher tensile strength, high stiffness, corrosion resistance, and light weight which make them suitable for a variety of structural applications. In automotive and aerospace industries conventional materials like steel and aluminum replaced by composite materials to improve the automobile/aircraft efficiency and to reduce fuel consumption and overall structural weight. To employ these lightweight composite materials in to engineering applications, these materials are to be designed in such a way that they are safe to use and this safety can be predicted by using the finite element analysis simulations.

The main goal of this study is to investigate the static analysis of thin-walled composite beam with stiffer box of different shapes for enhancing rigidity of thin-walled composite beam by using finite element analysis software. The static analysis considers three types of loads means bending, shear and torsional loads were considered. A general numerical model applicable for thin-walled composite beam subjected to bending, shear and torsional loads were developed. For both thin-walled composite beam fiber angle orientation of $[\pm 30°]_{12}$, ply thickness of 0.25mm, fiber volume fraction of 65% and overall thickness of 3mm with unidirectional carbon/epoxy composite laminate were used. The thin-walled composite beam was considered as cantilever beam with loading conditions of bending, shear and torsion loads with the value of 500N, 500N and 250Nm, respectively, were used in order to deal the effects of rigidity difference on thin-walled composite beam with and without stiffer box. For both symmetric and asymmetric thin-walled composite beam with and without stiffer box static analysis has been done by finite element analysis software. Simulation results shows maximum von Mises stress and resultant displacement for both symmetric and asymmetric thin-walled composite beam without stiffer box. But, symmetric and asymmetric thin-walled composite beam with stiffer box of different shapes subjected to different loading conditions minimum von mise stress and resultant displacement were obtained. Therefore, the rigidity of thin walled composite beam was enhanced by using different stiffer box of different shapes. Finally, for thin-walled composite beam subjected to different loading conditions suitable stiffer box shapes have been selected.

***Keywords**: Thin-walled composite beam, carbon fiber, epoxy, static analysis, Solidworks*

Table of Contents

List of figures

List of tables

Nomenclature

σ	Normal stress
$\left(\sigma_f\right)_{ult}$	Ultimate tensile strength of fiber
$(\sigma_m)_{ult}$	Ultimate tensile strength of matrix
σ_{yc}	Composite yield strength
$(\sigma_m^C)_{ult}$	Ultimate compressive yield strength
ε	Normal strain
$\left(\varepsilon_f\right)_{ult}$	Ultimate failure strain of the fiber
$\left(\varepsilon_f\right)_{ult}$	Ultimate failure strain of the matrix
$(\varepsilon_m^c)_{ult}$	Ultimate compressive failure strain of matrix
E	Young’s modulus
E_1	Longitudinal moduli of the composite lamina
E_2, E_3	Transverse moduli of the composite lamina
E_m	Matrix Young’s modulus
E_f	Fiber Young’s modulus
G_m	Matrix shear modulus
G_f	Fiber shear modulus
G	Shear modulus
G_{12}	In-plane shear modulus
G_{13}	Out-plane shear modulus
G_{23}	Out-plane shear modulus
$\rho_{c,f,m}$	Volume of composite, fiber and matric, respectively
v, u, w	Displacement in the direction of the x, y and z coordinate axis
υ	Poisson’s ratio
V_m	Volume fraction of the matrix
V_f	Volume fractions of the fibers
μ_m	Matrix Poisson’s ratio
$v_{c,f,m}$	Volume of composite, fiber and matric, respectively
$V_{c,f,m}$	Volume fraction of composite, fiber and matric, respectively
$m_{c,f,m}$	Mass of composite, fiber and matric, respectively
μ_{12}	Major Poisson’s ratio
μ_{13}	Major Poisson’s ratio

μ_{23}	Major Poisson's ratio
μ_m	Poisson's ratio
$(\tau_m)_{ult}$	Ultimate shear strength
τ	Shear stress
γ	Shear strain
$(\gamma_{12})_{m\,ult}$	Ultimate shearing strain of the matrix

List of Abbreviations

UD	Unidirectional
PVC	Polyvinyl chloride

1.Introduction

A thin walled beam is a very useful type of beam and it is made up from thin panels connected among themselves to create closed or open cross sections of a beam. Thin walled beams exist because their bending stiffness per unit cross sectional area is much higher than that for solid cross sections such a rod or bar. In this way, stiff beams can be achieved with minimum weight. Thin walled beams are particularly useful when the material is a composite laminate.

The thin-walled composite beam model is widely used to simulate the behavior of engineering structural elements. The thin-walled beam is actually a cylindrical shell whose length is much greater than the dimensions of the cross section which, in turn, are much greater than the thickness of the wall. These specific features of thin-walled beams allows to introduce a system of assumptions which, in turn, enables us to develop a relatively simple and efficient applied theory and to reduce the two-dimensional equations of shell theory to ordinary differential equations providing, as a rule, closed-form analytical solutions [1].

Composite materials are materials made from two or more constituent materials with significantly different physical property that when combined together they produce a material with characteristics different from the individual components. The new materials are superior to those of the constituent materials acting independently [2].

Composite materials are well known to have excellent fatigue resistance, high specific strength and stiffness, good corrosion resistance, excellent fire resistance and lower thermal expansion. High stiffness means that material exhibits low deformation under loading. However, by saying that stiffness is an important property, we do not necessarily mean that it should be high. The ability of a structure to have controlled deformation (compliance) can also be important for some applications (e.g., springs; shock absorbers; and pressure, force, and displacement gauges) [1].

Lack of material strength causes an uncontrolled compliance, i.e., a failure after which a structure does not exist anymore. Usually, we need to have as high strength as possible, but there are some exceptions (e.g., controlled failure of explosive bolts is used to separate rocket stages) [1].

Thus, without controlled stiffness and strength, the structure cannot exist. Naturally, both properties depend greatly on the structure’s design, but are ultimately determined by the stiffness and strength of the structural material, because a good design is only a proper utilization of material properties [1].

Composite materials are also used in other areas such as automobile, sports and civil industries. Most composite structures are designed as assemblies of beams, column, plates and shell [3].

Beams are structural members that carry bending loads and have one dimension much larger than the other two dimensions whereas the plates and shells are two dimensional elements.

In aviation industry, thin-walled beams of isotropic and composite structure with closed and open cross-section are widely used as stiffeners, stringers and as primary load carrying members.

The most commonly used stiffener cross sections are I, C and hat sections. Due to the complexity of the structure and limitations of the closed form analytical solutions composite beam structures are normally validated by testing which is very expensive and tedious process. The other alternate method for validation is using finite element analysis software that can analyses complex composite structures with high accuracy. However, the accuracy of finite element method is dependent upon the quality of modelling and boundary conditions.

This research work is focused on the rigidity increasing of composite thin-walled beams by using different stiffer box inside the thin-walled beam. Depending on the position of neutral axis there are two types of thin-walled beams namely, symmetric and asymmetric. For this research work both symmetric and asymmetric thin-walled composite beams with different stiffer box will be considered.

1.1. History of composite materials

The idea of a composite material is not a new one. In 1500 B.C., early Egyptians and Israelites used a combination of mud and straw to create strong buildings. Nature is another example where the idea of a composite material can be found. Wood is a naturally occurring composite material which falls under the category of fibrous composites, with cellulose fibers embedded in a lignin matrix. Another example is gluing wood strips along different orientations to produce plywood. Concrete can also be considered a composite since it consists of a mixture of stones held together by cement. Ancient Mongolians used composite bows made from wood, bone, and bamboo bonded with a naturally occurring pine resin. These bows are said to be very powerful and accurate [2]. The evolution of modern composites started when researchers developed synthetic resins in the early 1900's. The application of composite materials in the aerospace industry started with the development of the phenolic resin. This development led to the fabrication of transport aircraft. Owens corning had produced the first commercial composite material called fiberglass. Glass fibers combined with a synthetic polymer which created incredibly light weight and strong structures. This invention led to the development of fiber reinforced polymers which resulted in the use of new composite materials to replace traditional metallic materials. Boats that are made of fiberglass offer competitive strength and are not subjected to rusting. Fiberglass has also been used to produce printed circuit boards, helicopter blades, the body of the corvette, sports cars etc. [4]

The US Navy incorporated the use of glass fiber-melamine composite boards in electrical terminal boards since they provide better insulation [5]. In addition, the advancements in science and technology prompted the need for the development of new materials with higher modulus fibers. In the 1960's, new and stronger reinforcing fibers like carbon and graphite were produced using rayon as the precursor. Boron fibers, which were developed around this period also found potential applications in the military and aerospace industries where strength and stiffness are of major concern. Meanwhile, in Japan, high strength graphite fibers were developed using polyacrylonitrile (PAN) as the precursor replacing rayon. In the early 1970's, kevlar fibers based on aramid (aromatic polyamide), were produced and found to be much stiffer and stronger than the existing fibers. The development of these fibers led to replacing of steel belts with polymer based cords in radial tires used in automobiles, thus reducing their overall weight and overall fuel consumption. A small alteration in the chemical structure of the aramid fibers gave rise to another fire resistant fiber called nomex, which is generally used to develop bullet proof vests and protective gear for fire fighters. The use of these strong fibers as skins with some integral honeycomb stiffeners also led to the development of sandwich structures which have been used in the aerospace industry. In recent years, the use of composite materials has widely spread to different industries like aerospace, military, automotive, sporting goods etc. [6]

1.2. Advantages of composites

Composites can be considered as a superior type of material which has a wide range of applications in several industries like aircraft, marine, military, automotive, and medical. One primary characteristic of these composites is the possibility to change the stacking sequence of the plies or lamina to obtain structures with the desired mechanical properties.

The following are some of the advantages of the high performance fiber reinforced polymer matrix composites [2, 4, 6]:

1. **Light weight:** Composite structures are generally lighter than the metallic counterparts which make them suitable for applications in aircraft and automotive industry. The lower weight of the composite materials results in lower fuel consumption and lower emissions.
2. **High strength:** Composites possess high strength compared to many of the conventional metallic materials and have the flexibility to be engineered and be stronger in a specific direction.
3. **High strength-to-weight ratio**: This property is taken in to consideration when building Aircrafts and other structures where high strength and less weight are desirable. The specific strength of composites is superior to that offered by aluminum and steel.
4. **Corrosion resistance:** Composites can withstand harsh environmental conditions and contact with several reactive chemicals. Tubes made from fiberglass can be used for transporting fuel from refineries.
5. **High impact strength:** Composites are engineered in a suitable way to resist the impact from a blast or an explosion. Because of this property composites are used in building military vehicles and bullet proof vests.
6. **Design flexibility and dimensional stability**: Composite materials can be designed for complex shapes and can be molded easily. They have better dimensional stability as they retain their size when hot or cold, thus not allowing any expansions or shrinkage in dimensions which makes them a better fit in applications like airplane wings etc.
7. **Part consolidation:** A single composite structure can replace the existing assemblies made using the conventional metallic materials thus reducing the overall cost.
8. **Low thermal conductivity:** Composite materials do not conduct heat or cold and thus can be used in applications pertaining to harsh weather conditions.
9. **Non-magnetic and non-conductive:** Composite materials do not conduct electricity through them thus making them suitable for applications to develop insulated switch boards, electric poles etc.
10. **Radar transparent:** Structures made from composite materials cannot be detected by the radar signals and thus can be used in several military applications generally as fighter jets.
11. **Durability:** Composite materials, in general, have a long life and requires less maintenance.

1.3 Types of composite materials

1.3.1 Reinforcements

Reinforcements in composites provide the necessary strength and stiffness. In many cases, reinforcements can be fibers or particulates. Particulate reinforcements are weaker, and brittle compared to the fiber reinforcements. Fibers alone cannot be used in structures even though they possess high tensile strength because they cannot alone support the compressive loads. Fibers form the main constituent in the fiber reinforced composites, as they satisfy the required conditions and transfer the strength to the constituent matrix and they take the majority space in a composite structure. The performance of a composite is dependent upon several factors like material of the fiber, length of the fiber, the shape of the fiber, the orientation of the fiber, and composition of the fiber. The orientation of the fiber plays a significant role in indication of the strength of the composite structure. The four types of fibers that are currently in use across different industries are glass, carbon, aramid, and boron. There are other types of fibers like extended chain polyethylene fibers, ceramic fibers apart from the naturally occurring fibers like jute, coir etc. [6].

1.Glass fibers

Glass fibers are the most common type of fibers in the fiber reinforced polymers. Glass fiber primarily consists of silica (SiO_2-Silicon dioxide) apart from the other metallic oxides in minor portions. The raw ingredients are initially fed into a hopper where they are melted and this molten liquid is then fed through electrically heated platinum bushings consisting of 200 small orifices at its base. The molten liquid flows through these orifices because of the gravity thus forming fine continuous filaments. Glass fibers are easily damaged due to the presence of the surface flaws [4]. This can be minimized by providing a proper sizing treatment to the extruded fibers. These protective treatments bind the filaments together into a strand. The Glass fibers are generally available as a strand. These fibers are available in other forms like continuous strand roving, woven roving, chopped strands etc. These fibers can be pre-impregnated with a layer of resin to form a prepreg. Prepregs are easy to stack, cut into required dimensions and easy to shape. There are two types of glass fibers that are widely used as the reinforcements in the fiber reinforced composites. E-glass (named because the chemical composition makes it a better electrical insulator) and S-glass. Another among these is C-glass which is generally known for its superior corrosion resistant properties. Among these fibers, E-glass has the lowest cost and hence it is the main reason for the widespread applications of E-glass. S-glass has the highest tensile strength and higher modulus which makes it suitable for manufacturing aircraft components and missile casings. The density of the glass fibers is low and the strength is high. The modulus is moderate, thus making an average overall modulus to weight ratio. This led to the development of high modulus fibers like carbon fiber, boron fiber etc., The Glass fibers are susceptible to moisture thus decreasing the overall strength of the fibers. These fibers are widely used in building and construction as support for other structural materials, window frames, bathroom units etc. Boat hulls are also made initially with the glass fibers. The Transportation industry, aerospace industry, and chemical industry have huge applications of glass fiber reinforced composites [6].

2. Carbon Fibers

Carbon fibers and graphite fibers are commonly used reinforcements that are generally used in applications which require higher strength and stiffness and higher modulus. The basic difference between the carbon and graphite fibers is the carbon content within the fiber and the process of fabricating the fibers. There are quiet few disadvantages with the carbon fiber like a low strain to failure, poor impact resistance, and very high electrical conductivity. They are generally used in the aerospace applications where weight saving is the key. The carbon fibers have amorphous carbon and a graphitic blend of carbon in almost equal compositions because of which the carbon fibers are usually stronger. The crystal structure of carbon generally has the carbon atoms arranged in parallel planes and these planes are held together by the van der Waals forces, and adjacent carbon atoms in the same plane are held together by a strong covalent bond, thus strengthening the entire carbon crystal. Carbon fibers are basically manufactured from two types of precursors namely polyacrylonitrile (PAN) and pitch. Filaments of PAN are wet spun from a solution of PAN and are stretched at elevated temperatures. These stretched filaments are oxidized at a temperature of 200-300^{0}C for two hours and the filaments are again pyrolyzed for half an hour thus producing filaments of carbon. The key difference between the fabrication of carbon and graphite fibers is the temperature of the pyrolysis process. The result of different pyrolysis temperatures is fibers with different carbon content. Pyrolysis at elevated temperature yields graphite fibers with a carbon content of 99% whereas at a lower temperature, yields carbon fibers with a carbon content of 95%. On the other hand, pitch, generally a byproduct of petroleum refinement, can also be used instead of PAN as a precursor. The carbon fibers produced with the pitch as the precursor usually have the highest modulus compared to PAN carbon fibers. However, tensile strength is lower compared to PAN carbon fibers. Pitch carbon fibers possess better electrical and thermal conductivities over the PAN carbon fibers [6]. Carbon fibers commercially exist as a long and continuous tow, chopped fibers and milled fibers. The long continuous tow usually has an arrangement of parallel strands and is generally used for high performance applications. Carbon fibers are used in numerous applications because of its high modulus and high tensile strength-to-weight ratio. The applications of carbon fibers range from sporting goods to rocket casings in the aerospace industry. Commercial aircrafts also use carbon fiber epoxy composites in few of its structural applications. With increased production of the carbon fiber, the overall price is decreased and the carbon fiber has found a potential use in the medical industry, where carbon fiber may be used to produce certain equipment and as implant materials (joint replacements). Carbon fibers are also used in the production of heavy machinery such as turbines, compressors, windmill blades etc. [6].

3.Aramid fibers

Aramid fibers are generally produced under the tradename of kevlar. There are two distinct types of fibers in kevlar: Kevlar 29 which is used in tires, and the other is kevlar 49 which is used in structural applications that demand high strength and stiffness. Kevlar has a low density but has a better specific strength compared to other reinforcement fibers [7]. Kevlar also possesses superior toughness, good damping characteristics, and impact resistant properties compared to other structural composites. The structure of an aramid fiber comprises of an amide group linked to an aromatic benzene ring. Extruding an acidic solution of a custom precursor through a spinneret results in highly anisotropic kevlar fibers, which possess better physical and mechanical properties. Aramid fibers when exposed to ultraviolet radiations, discolors and loses its mechanical properties. Aramid fibers possess poor compressive properties, which is a major drawback [6].

4.Boron fibers

Boron fibers are usually a coating of boron on a substrate. Boron is usually brittle in nature. Boron is deposited on to the substrate usually by chemical vapor deposition. Since this process involves higher temperatures, a suitable substrate material like a tungsten wire or carbon may be used because of the superior thermal characteristics of the substrate materials. Because of the higher density, higher strength and stiffness than the graphite fibers, boron fibers are preferred for building aerospace structures. However, the cost of the boron fibers is a major setback that prevents the use of them in a variety of structural applications [6].

1.3.2 Matrix Materials

Depending on the strength requirements, polymers, metals, and ceramics are used as a matrix material. Of the three, polymer matrix is preferred widely in making composite structures.

The matrix in fiber reinforced composite materials has the role to hold the fibers together, to transfer load and stresses between the fibers, to prevent the fibers from environmental attacks such as chemicals and mechanical degradation of the surface of the fibers and to offer certain properties like ductility, toughness, and insulation which cannot be possible with fibers alone.

The fiber and matrix material should be chemically non-reactive at any given operating temperature. It is also important to consider the maximum operating temperature of a matrix material. Polymers exist either as a thermoset or a thermoplastic. Epoxy, polyester, phenolics etc., belongs to the thermoset category of polymers. Nylon, polycarbonate, polysulfone, polyether ether ketone (PEEK) belong to thermoplastics [6].

1.Thermoplastic polymers

Thermoplastic polymers are linear polymers in which the molecules are held together by a weak bond and they are not cross-linked to form a rigid structure. The weak bonds break upon the application of heat and the molecules can move to a relatively new position upon the application of heat and or force. Upon cooling, the molecules occupy a new position and the weak bonds are restored thus resulting in a new shape. Therefore, a thermoplastic polymer may be repeatedly melted and processed. However, the thermoplastic polymer may be mechanically degraded because of continuous exposure to elevated temperatures. Because of the linear arrangement of molecules in some thermoplastics, a higher strain to failure can be expected compared to that of cross-linked thermosets making thermoplastics tougher [4]. Common thermoplastic resins that are used as matrix materials are nylon, polypropylene (PP), polycarbonate (PC), and polysulfone (PS). Polyether ether ketone (PEEK), poly phenylene sulfide (PPS) are the new thermoplastics that are used currently as matrix materials. PEEK is preferred widely in a variety of applications because of its superior toughness and impact properties [6].

2.Thermoset Polymers

In a thermoset polymer, molecules are chemically joined together by crosslinking to form a rigid structure. Adjacent molecules are held together by strong covalent bonds. These polymers cannot be softened upon heating because of the crosslinking. Thermosets have higher modulus, high rigidity, and good dimensional stability when compared to thermoplastics. Epoxy is a thermoset resin which is widely used as a matrix material in many of the fiber reinforced composites. Epoxy resins are widely used because of a wide variety of properties like superior resistance to chemical and environmental attacks, good adhesion with the reinforcements and less shrinkage during curing. The major drawback of using epoxy as the matrix is its high cost and long curing time [6].

The ideal matrix materials for high performance polymer matrix composites should have the desirable mechanical properties such as high tensile strength, high modulus, high fracture toughness, resistance to moisture and other solvents, good dimensional stability, higher glass transition temperature

Conventionally, thermoset polymers are preferred for fiber reinforced composites. Low molecular weight chemicals with lower viscosities are preferred as starting materials for the polymerization of the thermoset polymer. Fibers are then pulled through the chemical solution or immersed in them. Because of extremely low viscosity, it is possible to achieve a good wetting between fiber and matrix and this plays a crucial role in the enhanced mechanical performance of the composite. The benefit of using thermoset polymer matrix is enhanced thermal resistance and chemical resistance.

1.4 Applications of composites

1.4.1 Transportation

Composites are widely used materials because of their flexibility and adaptability to severe conditions. They can be easily blended with other materials to fill the desired needs and achieve attractive mechanical properties. Fiber reinforced composites are used in surface transportation because of their superior strength-to-weight ratio compared to the other conventional materials. The stiffness offered by the fiber reinforced composites and the cost makes them a better choice over traditional metallic materials. Carbon fiber reinforced epoxies are used in making racing cars. A polyester resin reinforced with a variety of fibers was the first application of composites in transportation because of the low cost, the simplicity of design and ease of production [6].

1.4.2 Aircraft and military applications

The major structural applications of fiber reinforced composites are in the field of military and commercial aircrafts. Weight reduction is critical in these applications to achieve high speeds and higher payloads. A boron fiber reinforced epoxy was the first composite ever used in the horizontal tail stabilizer of the F14. Since the origination of carbon fibers in the early 1970's, carbon fiber reinforced epoxy composites are continuously being used in aircraft components. Many of the aircraft components like wings, fuselage, and stabilizers are produced using fiber reinforced composites. The structural strength and durability of these composites prompted the development of other aircraft components. The stealth aircrafts today are made of carbon fiber reinforced polymers because of the superior properties of carbon fibers that help reducing heat radiation and radar reflections [6].

Airbus was the first commercial aircraft manufacturer to use composite materials in their aircraft. Airbus incorporated the use of composite materials in their A310 aircraft, where 10% of total weight of the aircraft was made using composite materials [6]. In 1988, Airbus used all composite tail for its A320 aircraft, which include the tail cone, horizontal and vertical stabilizers. In 2006, Airbus introduced A380 Aircraft in which 25% of the total weight of the aircraft is made of composites [8]. Major components that were made from the composites include the empennage, tail cone, wings, landing gear doors, spoiler, flaps, central torsion box and other flight control surfaces. The principal reason fiber reinforced polymers are used in the aircraft and helicopter applications is because of weight reduction which reduces the fuel consumption and increases pay load. The principal advantages of using fiber reinforced polymers include higher strength and stiffness, higher fatigue and corrosion resistance, reduction in a number of components and fasteners.

Boeing also started the use of composite materials in Boeing 777, where 10% of structural weight is made from carbon fiber epoxy composites. The Rutan Voyager was the first all composite aircraft to demonstrate the strength and efficiency by flying nonstop all over the world without refueling [9]. Carbon fiber or glass fiber epoxy composites are used in the helicopter rotor blades. Boeing used most of carbon fiber reinforced composites rather than aluminum alloys in their commercial aircraft, Dreamliner.

1.4.3 Space applications

Reduction of mass is most critical in space applications. The Satellite structure may use the sandwich plates with light alloy honeycomb cores. In few cases, pressure vessels are as well made of the composite tubes. Unidirectional carbon fibers are wound around a mandrel to produce these tubes. Composites are also used as a material for insulation in space vehicles. Space shuttles and Space vehicles use flywheels made from composite materials for the supply of electric power and for controlling the altitude. These flywheels deliver higher levels of power compared to the conventional flywheels because of the reduction in total mass of the flywheel. Composites such as carbon-carbon involves applications at higher temperatures. They are used in producing the structures like nose cap, nose landing gear door and outer edges of the wings. Space shuttles usually experience high temperatures around the nose and the leading edge of the wing. Hence materials like carbon-carbon reinforcements are preferred as they can tolerate high varying environments from launch to reentry. Graphite epoxy composite materials are also used in numerous space applications because of their high strength and stiffness and non-zero coefficient of thermal expansion [10].

1.4.4 Automotive applications

Fiber reinforced composites application in an automobile may be classified in to three categories like body components, chassis, and engine components. These components must sustain the road loads and crash loads. During the early ages of application of fiber reinforced composites in the automotive industry, some specialty cars were produced by the Lotus company which used glass fiber with a polyester resin. In 1938, Ford first produced its fiber reinforced prototype of an automobile. In this, the structure of the automobile was made of graphite fiber epoxy composite. The vehicle was built completely by hand layup of graphite epoxy prepreg. This prototype was compared to the in-production vehicle made of steel. This comparison demonstrated no or a little difference between the two [11]. Body components like a hood, door panel may require high stiffness and should be dent resistant. Also, the exterior body should have a smooth surface finish for appearance. In the engine compartment, glass fiber reinforced polymers may replace certain metallic parts like cylinder head cover and oil pump cover, bearing cages etc. One of the main characteristics of the unidirectional composite is the ability to absorb elastic energy. Therefore, the existing metallic suspension spring maybe replaced with a glass/resin composite spring because they are almost unbreakable [12].

Fiber reinforced composites have become widely used material in motor sports where light weight structures are used for attaining higher speeds. In 1950’s, glass fiber reinforced polymers were used as body panels replacing aluminum body panels. The controlled crush behavior offered by the carbon fiber epoxy composite has found an important application in survival cells and nose cones which protect the driver in the event of the crash [13].

1.4.5 Sporting goods

Sporting goods like tennis rackets, athletic shoes, ski boards etc., use composite materials because of their higher strength and stiffness, and lower weight. Additionally, fiber reinforced composites offer good damping and design flexibility. Bicycles and canoes made of carbon fiber reinforced composites helps in quick maneuvering because of their reduced weights in races. Fiber reinforced composites provide faster damping of vibrations which makes them suitable to produce tennis rackets to eliminate the shock transmission to the player's arm. The capability to store high elastic energy per unit weight of the fiber reinforced composite materials widens the use of the composite materials in archery to produce bows which aid in propelling the arrow through longer distances [6]. Fiber reinforced composites are also found vastly in the production of golf shafts, fishing rods, auxiliary parts of bicycle etc.

1.4.6 Marine Applications

The first composite boat was made in the early 1940's with the invention of the fiber glass reinforcement. Post the invention of the fiber glass, many of the war boats and ships use fiber glass reinforcements. The key advantage of using fiber reinforced composite materials in place of conventional materials is higher cruising speed because of the reduction in weight, easy maneuvering, and higher fuel efficiency. In recent years, the fiberglass has been replaced with kevlar 49 fibers because of their higher strength-to-weight ratio. Carbon fiber reinforced composites are sometimes used in racing boats because of their high strength-to-weight and high modulus-to-weight ratios. The complete hull, deck and other structural components are made of carbon fiber. Sometimes, carbon fibers are blended with other low density polymeric materials to improve the impact resistance of the boats. The hulls of large composite ships are generally made of carbon fiber sandwich structure with PVC as the core. This results in a significant increase in strength and stiffness, and decrease in overall weight. Composite materials cannot be corroded or decayed easily when compared to conventional materials like steel and wood. Few subsea submarines use composite materials for improved stealth capability.

1.4.7 Miscellaneous Applications

Fiber reinforced composites are gradually replacing conventional materials like concrete, steel etc., used in civil applications. The main advantage of using fiber reinforced composites is the weight reduction of the total structure and resistance to corrosion. Apart from these advantages, fiber reinforced composites would reduce the overall cost for installations, consolidation of fabrication processes, reduced transportation costs, reduced maintenance cost due to improved corrosion resistance [4]. Application of fiber reinforced composites for the construction of bridges is a large-scale application of the composite materials. The conventional bridges must support their own dead weight and therefore use light weight fiber reinforced composites would allow the bridge to accommodate a number of vehicles and heavier trucks as well [6].

Fiber reinforced composites are also used in producing small components like windows, doors, canopies etc., Composites are also used to produce large self-supporting structures like curved domes. Glass fiber reinforced composite has been used as a structural shell member in constructing the dome of Sharjah international airport. Composite materials today are also used as pultruded frames which form the skeleton of buildings. Load bearing members in civil engineering structures like pedestrian and vehicle bridges, bridge decks, energy absorbing guard rails, building systems, modular roof tops, electric poles, light towers etc., are made predominantly from fiber reinforced composites. Fiber reinforced composites are also used as reinforcement bars, columns, panels, beams etc. [14].

Composite materials are also used in the medical field to build new medical devices and artificial human bones. Composite materials are used as cladding materials, moderators and control rods in nuclear reactors. They are used widely in electronics as printed circuit boards and because of the better insulation properties of composite materials, they are also used in making electrical panel boards [4].

1.5. Problem statement

Thin-walled composite beam can be an advantageous alternative to thin-walled metal beam for internal and external reinforcement of mechanical structures, especially in environments exposed to corrosion. In these type of environments, the use of composite stirrups, that are normally located as an outer reinforcement, has even more sense as it can be more susceptible to severe environmental effects, due to the minimum galvanized cover provided.

Replacing metal thin-walled beam by thin-walled composite beam has advantages of high specific stiffness, high specific strength and less weight. Because metal thin-walled beam in the automotive and aerospace industries leads to high weight structure which consumes more fuel than thin-walled composite beam.

Composite material properties perpendicular to the fiber directions are not good. The poor properties of the basic unit are transverse to the length wise direction of the fiber. Therefore, to load a composite material perpendicular to the fiber direction is to load the fiber in the soft and weak diametrical direction of the fiber. In addition, if a composite material is loaded perpendicular to the fiber direction commonly referred to as the transverse direction not all the load transmitted through the fiber. A portion of load goes around the fiber and is entirely in the matrix material. The fact that the fibers do not touch means some of the load must be transferred through the matrix. The poorer transverse properties of the fiber coupled with the softer and weaker properties of the matrix lead to poor properties of the composite in the direction perpendicular to the fibers. The transverse properties of composite materials are poor and a poor interface leads to poor transverse strength, low stiffness in the transverse direction, poor transverse and shear properties of fiber-reinforced materials. Because of poor loading capacity of composite materials leads thin-walled composite beam to poor loading in the transverse direction. Therefore, to increasing the rigidity of thin-walled composite beam in the transverse direction by using stiffer box of different shapes will be necessary.

1.6. Objective of the study

1.6.1. General objective

The general objective of this research is to analyse thin-walled composite beam with stiffer box of different shapes for enhancing rigidity of thin-walled composite beam.

1.6.2. Specific objective

- To investigate von mise stress and resultant displacement distribution in the thin-walled composite beam with and without stiffer box of different shapes.
- To compare bending, shear and torsional load capability of thin-walled composite beam with and without stiffer box of different shapes.
- To investigate critical location of the thin-walled composite beam.
- To select suitable stiffer box that enhances rigidity of thin-walled composite beam for different loading conditions.

1.8. The Scope of the study

The scope of this study to analyze symmetric and asymmetric thin-walled composite beam with and without stiffer boxes for enhancing rigidity by using finite element software. The thin-walled composite beam will be modelled and analyzed using finite element software. Finally, for the thin-walled composite beam critical location will be identified, stress and displacement distribution of the structure will be performed. From the result of finite element analysis, suitable stiffer box for thin-walled composite beam of different loading condition will be identified.

2.Literature review

There are so many literatures done on thin-walled composite beams and most of the literature related with dynamic analysis such as vibration analysis, buckling analysis, stability analysis and optimization. But in this research, literatures that related with static analysis such torsional analysis, flexural-torsional analysis, flexural-shear-torsional analysis, bending analysis etc. have been selected.

Pavassa [15] an approximate analytical solution for torsion of short thin walled beams by taking the influence of shear on torsion for both stresses and displacements were obtained in a closed analytical form. Various types of thin-walled beams with general shapes of cross sections, loading and types of boundary conditions were considered. Cross sections with two axes of symmetry of the beam will be subjected to torsion with respect to the shear canter and with that one axis of symmetry of the beam will be subjected to torsion and bending. In the general case, the beam will be subjected to torsion, bending and tension.

Kim and Shin [16] a numerical method that evaluates exactly the element stiffness matrix, determines eigen modes and derives exact displacement functions was presented for thin walled composite beams. Then, the exact stiffness matrix was determined using the member force deformation relationships. The developed theory was validated by comparing various torsional responses to the finite element beam model for all displacement parameters and two-dimensional analysis results using the shell elements of ABAQUS. It was demonstrated that the effect of boundary condition on the twist angle of box beams subjected to a torsional moment is negligible.

Vo and Lee [17,18] an analytical model that is capable of predicting accurate deflection as well as angle of twist for various configuration including boundary conditions, laminate stacking sequence and fiber angle orientation was developed to study the flexural torsional behavior of a laminated composite beam with box section. Numerical results were obtained for thin walled composites beams under vertical and torsional loading, addressing the effects of fiber angle and laminate stacking sequence.

Kim and Lee [19] presented an effective numerical beam model capable to analyze the flexural and torsional responses of thin walled functionally graded beams with single and double-cell sections. The beam model is based on the Euler-Bernoulli beam theory and considers elastic couplings and constrained warping. The governing equations are derived from the strain energy and the Hermite cubic interpolation polynomials as shape functions were employed to discretize the governing equations for the finite beam element.

Günay and Timarci [20] developed analytical model to investigate the flexural torsional behavior of thin walled laminated composite beams with variable stiffness by using the curvilinear fibers. The numerical results were initially obtained by use of a displacement based finite element method with 2 node beam elements for thin walled having straight. New numerical results involving displacements and rotations for the same type of the beam with same conditions but with variable stiffness layers were also obtained to see the effect of changing the orientation of fiber angle. The numerical results obtained was very good agreement with the results of the finite element analysis software

Günay and Timarci [20] investigated static behavior of thin walled laminated composite beams of variable stiffness. The analytical model used accounts for flexural torsional coupling and variable stiffness effects along the contour of the cross section of the beam. The variable stiffness was acquired by constructing the laminates with curvilinear fibers having certain specific paths. The orientation of fibers varies depending on the fiber path along the contour of the cross section in each layer. A displacement based finite element method was developed to solve the analytical model and to predict displacements and rotations under the effect of different types of loading conditions. Numerical results were obtained for different fiber paths and lay-up configurations and compared with the available solutions in the literature with the results of a finite element analysis software using shell element.

Kim and Lee [21] an effective numerical beam model capable to study the flexural torsional behavior of shear flexible thin walled sandwich I-beams with functionally graded material. The thicknesses in flanges and web are almost proportional to the location of center of gravity and the distance between center of gravity and shear center. For flexural deflection decreases logarithmically as the material ratio increases. The shear effect increases with the increase of thickness ratios in flanges, but vice versa in the web. For the torsional analysis, the thickness ratios in flanges and material ratio significantly reduce the twist angle, but its ratio in web has no strong influence on the twist angle.

Jang [22] the finite element analysis of tapered thin walled box beams subjected to out of plane bending and torsional loads was presented. The procedure to derive the element stiffness matrix of the tapered box beam was developed with an explicit formula. The tapering effects were reflected in the development of the tapered box beam element. The accuracy and convergence of the developed tapered beam finite elements were tested using several numerical examples. The results for the tested problems showed that the error by the developed tapered higher order beam elements was comparable to the shell elements within 2~3%.

Correia [23] a new beam element derived using a normalized version called Legendre polynomials for the analysis of beams with solid rectangular cross sections based on higher order cross sectional displacement modes. The higher order displacement field contains the six common displacement modes of classical beam theory and the usual cross-sectional stress resultants. The proposed model includes the interaction between the axial force, bi-directional shears, bending moments, and torsion with all higher order generalized forces. Since explicit normal shear stress interaction is directly accounted for, such element is also deemed suitable for shear critical member analysis.

Barrientos [24] developed one dimensional element that considers all the resistance modes: axial, bending, torsion and distortion, both homogeneous and nonhomogeneous. It provides a breakdown of the stresses by each mode which helps us to understand how the structures under analysis behave and to apply the corresponding codes or standards to each mode on a separate basis when required. It is applicable to any cross-sectional shape, with or without symmetry axes. The results of the element were validated by comparison with other calculation methods and with the results of other authors, obtained good convergence for the analytical solutions when those solutions could be obtained.

Ahmed and Ahmed [25] the structural performance of composite beams of cantilever configuration with torque applied at free end subjected to constrained torsion has been analyzed. The torsional response of the beams has been determined. Axial forces were found significant with high forces close to the restrained end, which are not present in case of free torsion. The constrained effects are mostly present in the region close to the restrained end and vanish as we move away from the re-strained end. The Normal stress intensity was higher close to restrained end due to constraint warping. The simple engineering analytical approach used for determining the constrained torsional response of composite beams is thus duly supported whereby it has been shown that the use of the appropriate equivalent engineering elastic constants in the theory is able to adequately predict actual behavior.

Pavazzaa and Matoković [26] presented a general case of asymmetric beam subjected to bending with influence of shear and in addition to torsion and tension/compression due to shear. In the case of mono-symmetrical the beam will be subjected to bending with influence of shear and in addition to tension/compression due to shear and in the case of loads through the shear center the beam will be subjected to bending with influence of shear and to torsion due to shear. Finally, in the case of bi-symmetrical cross-section, the beam will be subjected to bending with influence of shear only.

Zhong [27] developed a new transfer matrix method for the static analysis of thin walled space frame structures, that is, thin walled beam transfer matrix method, which expands the advantages of the general transfer matrix method. Using this method, the transfer matrix of single beam was obtained through Laplace transform and inverse Laplace transform at first, and then gets the coupling equations of the whole structure with respect to coordinate transformation matrices and joint coupling matrices. Some numerical examples are given and compared with the general transfer matrix method and the finite element method results to validate the developed method.

Lee [28] an analytical model of a laminated composite beam with an I-section was developed to study the flexural behavior of a laminated composite beam that capable of predicting accurate deflection for various configuration including boundary conditions, laminate orientation and span to height ratio. The shear effects become significant for lower span to height ratio and higher degrees of orthotropic of the beam. The orthotropic solution is accurate for lower degrees of material anisotropy, but, becomes inappropriate as the anisotropy of the beam gets higher, and fully coupled equations should be considered for accurate analysis of thin walled composite beams.

VO and Thai [29] a two nodded finite element model with six degree of freedom per node with shear deformation effects and anisotropy coupling was developed to study the static behavior of composite beams with arbitrary lay ups under vertical loads. The model is capable of predicting accurately static responses for various configuration including boundary conditions, span to height ratio and laminate orientation. The orthotropic solution is accurate for lower degrees of material anisotropy, but, becomes inappropriate as the anisotropy of the beam gets higher, and fully coupled equations should be considered for accurate analysis of composite beams.

Luoa [30] modeled based on the Hodges generalized Timoshenko beam theory can be applied to model composite beams with box cross sectional shape, arbitrary material distribution and large deflection. The calculation shows that there is tension, shear and bending twist elastic coupling in the symmetric thin walled composite box beam, while bending shear and tension twist elastic coupling in the anti-symmetrical thin walled composite box beam.

The influence of Timoshenko beam theory on the static deformation of the composite box beam is related to the aspect ratio of beam length to section dimension. The greater the aspect ratio, the smaller the effect of Timoshenko beam theory. When the aspect ratio reaches a certain value, the effect of Timoshenko beam theory on the static deformation is negligible.

Ghafari and Rezaeepazhand [31] the importance of dimensional reduction method and beam cross sectional analysis is well recognized for beams. The beam cross-sectional properties can be computed by 2D and 1D sectional analysis. The 2D analysis benefits from arbitrary section features and geometry and better accuracy due to considering all warping displacements. On the other hand, 1D methods are enjoyed from simplicity of analysis which do not need mesh generation of numerical 2D approaches. Reducing 3D problem, the refined 1D beam model is obtained by involving the transverse shear effects. The discussed beam analysis can significantly reduce the time cost in contrast to 3D FEM and provide the chance of accurate and fast structural optimization.

Kim and Jang [32] proposed the thin walled beam element to solve static problems of beams with varying cross sections that generates coupling among cross sectional deformation modes. The coupling among the deformations was significant when more than two thin walled beams are connected at an angled joint such as in a T-joint structure. The extensional distortions and quadratic warping’s are easily excited at the joint. The use of the proposed method might be effective to solve jointed thin walled beam problems, though matching conditions of the deformation modes for an angled joint need further consideration

3. Mathematical modeling

3.1. General equation of linear elastic analysis of solid mechanics

Problems in solid mechanics deal with states of stress, strain and displacement in deformable solids. The basic relationships which govern these states and are the basis for finite element applications have been summarized. For a linear elastic solid under static equilibrium, the general equations for any three dimensional body:

3.1.1. Static equilibrium equations for stresses.

Generally, the direct and shear stresses on opposite faces of an element are not equal but differ by small amounts. Therefore if, say, the direct stress acting on the z plane is σ_z, then the direct stress acting on the $z + \delta_z$ plane is, from the first two terms of a Taylor's series expansion, $\sigma_z + (\frac{\partial \sigma_z}{\partial z})\delta_z$.We now investigate the equilibrium of an element at some internal point in an elastic body where the stress system is obtained by the method just described. In Fig.3.1.the element is in equilibrium under forces corresponding to the stresses shown and the components of body forces (not shown).

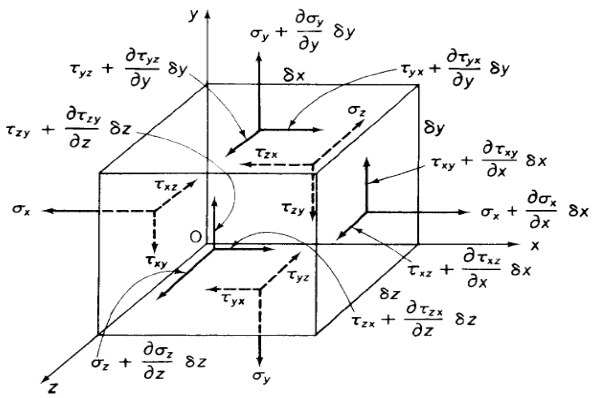

Figure 3.1. Stresses on the faces of an element at a point in an elastic body [33].

Surface forces acting on the boundary of the body, although contributing to the production of the internal stress system, do not directly feature in the equilibrium equations.

Taking moments about an axis through the center of the element parallel to the z axis

Dividing by $\delta_x\delta_y\delta_z$ and taking the limit as δ_x and δ_y approach zero.

which gives, $\tau_{xy} = \tau_{yx}$

Similarly, $$\left.\begin{array}{l}\tau_{xy} = \tau_{yx}\\ \tau_{xz} = \tau_{zx}\\ \tau_{yz} = \tau_{zy}\end{array}\right\} \quad \ldots\ldots\ldots\ldots\ldots\ldots\ldots\ldots\ldots\ldots \quad (3.2)$$

Therefore a shear stress acting on a given plane $\tau_{xy}, \tau_{yz}, \tau_{zx}$ is always accompanied by an equal complementary shear stress $\tau_{yx}, \tau_{zx}, \tau_{zy}$ acting on a plane perpendicular to the given plane and in the opposite sense.

Now considering the equilibrium of the element in the x direction

which gives

Similarly,
$$\left.\begin{aligned} \frac{\partial \sigma_{xx}}{\partial x} + \frac{\partial \tau_{yx}}{\partial y} + \frac{\partial \tau_{zx}}{\partial z} + X = 0 \\ \frac{\partial \tau_{xy}}{\partial x} + \frac{\partial \sigma_{yy}}{\partial y} + \frac{\partial \tau_{zy}}{\partial z} + Y = 0 \\ \frac{\partial \tau_{xz}}{\partial x} + \frac{\partial \sigma_{yz}}{\partial y} + \frac{\partial \sigma_{zz}}{\partial z} + Z = 0 \end{aligned}\right\} \ldots \ldots (3.3)$$

Or in tensor form, $\sigma_{ij,j} + f_i = 0$

The equations of equilibrium must be satisfied at all interior points in a deformable body under a three-dimensional force system.

3.1.2. Static equilibrium equations for strains

The external and internal forces cause linear and angular displacements in a deformable body. These displacements are generally defined in terms of strain. Longitudinal or direct strains are associated with direct stresses σ and relate to changes in length, while shear strains define changes in angle produced by shear stresses. These strains are designated, with appropriate suffixes, by the symbols ε and γ respectively, and have the same sign as the associated stresses.

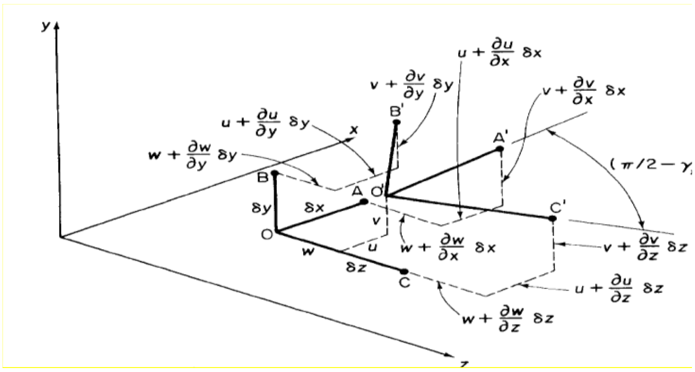

Figure 3.2. Displacement of line elements OA, OB, and OC [33].

$$\left.\begin{aligned} \varepsilon_{xx} &= \frac{\partial u}{\partial x} \\ \varepsilon_{yy} &= \frac{\partial v}{\partial x} \\ \varepsilon_{zz} &= \frac{\partial w}{\partial z} \end{aligned}\right\} \ldots \ldots (3.4)$$

The shear strain at a point in a body is defined as the change in the angle between two mutually perpendicular lines at the point.

$$\left.\begin{aligned}\gamma_{xz} &= \frac{\partial w}{\partial x} + \frac{\partial u}{\partial z}\\ \gamma_{xy} &= \frac{\partial v}{\partial x} + \frac{\partial u}{\partial y}\\ \gamma_{yz} &= \frac{\partial w}{\partial y} + \frac{\partial v}{\partial z}\end{aligned}\right\} \quad \ldots\ldots\ldots\ldots\ldots\ldots\ldots\ldots \text{(3.5)}$$

Or in tensor form, $\varepsilon_{ij} = \frac{1}{2}\left(u_{i,j} + u_{j,i}\right)$ ……………………………………… (3.6)

3.1.3. Compatibility equations

Compatibility equations can be derived by differentiating strain equation of eqn (3.5)

$$\frac{\partial^2 \varepsilon_{xx}}{\partial y^2} + \frac{\partial^2 \varepsilon_{xx}}{\partial y^2} = \frac{\partial^2 \gamma_{xy}}{\partial x \partial y} \quad \ldots\ldots\ldots\ldots \text{(3.7)}$$

$$\frac{\partial^2 \varepsilon_{yy}}{\partial z^2} + \frac{\partial^2 \varepsilon_{zz}}{\partial y^2} = \frac{\partial^2 \gamma_{yz}}{\partial y \partial z} \quad \ldots\ldots\ldots\ldots \text{(3.8)}$$

$$\frac{\partial^2 \varepsilon_{zz}}{\partial x^2} + \frac{\partial^2 \varepsilon_{xx}}{\partial z^2} = \frac{\partial^2 \gamma_{zx}}{\partial z \partial x} \quad \ldots\ldots\ldots\ldots \text{(3.9)}$$

$$\frac{\partial}{\partial z}\left(\frac{\partial \gamma_{yz}}{\partial x} + \frac{\partial \gamma_{zx}}{\partial y} - \frac{\partial \gamma_{xy}}{\partial z}\right) = 2\frac{\partial^2 \varepsilon_{zz}}{\partial x \partial y} \quad \ldots\ldots\ldots\ldots \text{(3.10)}$$

$$\frac{\partial}{\partial x}\left(\frac{\partial \gamma_{zx}}{\partial y} + \frac{\partial \gamma_{xy}}{\partial z} - \frac{\partial \gamma_{yz}}{\partial x}\right) = 2\frac{\partial^2 \varepsilon_{xx}}{\partial y \partial z} \quad \ldots\ldots\ldots\ldots \text{(3.11)}$$

$$\frac{\partial}{\partial y}\left(\frac{\partial \gamma_{xy}}{\partial z} + \frac{\partial \gamma_{yz}}{\partial x} - \frac{\partial \gamma_{zx}}{\partial x}\right) = 2\frac{\partial^2 \varepsilon_{yy}}{\partial x \partial z} \quad \ldots\ldots\ldots\ldots \text{(3.12)}$$

Or in tensor form, $\varepsilon_{ij,kl} + \varepsilon_{kl,ij} - \varepsilon_{lj,ki} - \varepsilon_{ki,lj} = 0$ ……………………………… (3.13)

3.1.4. Constitutive equations

$$\sigma_{xx} = \frac{E}{(1+\mu)(1-2\mu)}\left[(1-\mu)\varepsilon_{xx} + \mu\varepsilon_{yy} + \mu\varepsilon_{zz}\right] \quad \ldots\ldots\ldots\ldots \text{(3.14)}$$

$$\sigma_{yy} = \frac{E}{(1+\mu)(1-2v)}\left[\mu\varepsilon_{xx} + (1-\mu)\varepsilon_{yy} + \mu\varepsilon_{zz}\right] \quad \ldots\ldots\ldots\ldots \text{(3.15)}$$

$$\sigma_{zz} = \frac{E}{(1+\mu)(1-2\mu)}\left[\mu\varepsilon_{xx} + \mu\varepsilon_{yy} + (1-\mu)\varepsilon_{zz}\right] \quad \ldots\ldots\ldots\ldots \text{(3.16)}$$

$$\tau_{xy} = \frac{E}{(1+\mu)}\gamma_{xy} \quad \ldots\ldots\ldots\ldots \text{(3.17)}$$

$$\tau_{xz} = \frac{E}{(1+\mu)}\gamma_{xz} \quad \ldots\ldots\ldots\ldots \text{(3.18)}$$

$$\tau_{yz} = \frac{E}{(1+\mu)}\gamma_{yz} \quad \ldots\ldots\ldots\ldots \text{(3.19)}$$

Generalized Hooke’s for stress-strain

$$\sigma_{ij} = E_{ijkl}\varepsilon_{kl} = \lambda\varepsilon_{mm}\delta_{ij} + 2\eta\varepsilon_{ij} \quad \ldots (3.20)$$

where $\eta = \frac{E}{2(1+\mu)}$ and $\lambda = \frac{\mu E}{(1+\mu)(1-2\mu)}$

Alternately, for the strain-stress equations:

$$\varepsilon_{xx} = \frac{1}{E}(\sigma_{xx} - \mu(\sigma_{yy} + \sigma_{zz}) \quad \ldots (3.21)$$

$$\varepsilon_{yy} = \frac{1}{E}(\sigma_{yy} - \mu(\sigma_{xx} + \sigma_{zz}) \quad \ldots (3.22)$$

$$\varepsilon_{zz} = \frac{1}{E}(\sigma_{zz} - \mu(\sigma_{xx} + \sigma_{yy}) \quad \ldots (3.23)$$

$$\gamma_{xy} = \left(\frac{1+\mu}{E}\right)\tau_{xy} \quad \ldots (3.24)$$

$$\gamma_{xz} = \left(\frac{1+\mu}{E}\right)\tau_{xz} \quad \ldots (3.25)$$

$$\gamma_{yz} = \left(\frac{1+\mu}{E}\right)\tau_{yz} \quad \ldots (3.26)$$

3.1.5. Hooke's law for orthotropic material

Combined with six simultaneous linear equations of Hooke's law, six strain-displacement relations and three equilibrium equations give 9 equations for the solution of 9 unknowns. Because strain-displacement and equilibrium equations are differential equations, they are subject to knowing boundary conditions for complete solutions.

$\varepsilon_{ij} = S_{ijkl}\sigma_{kl}$ where i, j, k, l=1,2,3

$$\begin{bmatrix}\varepsilon_{xx}\\ \varepsilon_{yy}\\ \varepsilon_{zz}\\ \gamma_{yz}\\ \gamma_{zx}\\ \gamma_{xy}\end{bmatrix} = \begin{bmatrix}\frac{1}{E_1} & \frac{-v_{xy}}{E_1} & \frac{-v_{xz}}{E_1} & 0 & 0 & 0\\ \frac{-v_{yx}}{E_2} & \frac{1}{E_2} & \frac{-v_{yz}}{E_2} & 0 & 0 & 0\\ \frac{-v_{zx}}{E_3} & \frac{-v_{zy}}{E_3} & \frac{1}{E_3} & 0 & 0 & 0\\ 0 & 0 & 0 & \frac{1}{G_{yz}} & 0 & 0\\ 0 & 0 & 0 & 0 & \frac{1}{G_{zx}} & 0\\ 0 & 0 & 0 & 0 & 0 & \frac{1}{G_{xy}}\end{bmatrix}\begin{bmatrix}\sigma_{xx}\\ \sigma_{yy}\\ \sigma_{zz}\\ \tau_{yx}\\ \tau_{zx}\\ \tau_{xy}\end{bmatrix} \ldots (3.27)$$

$$\sigma_{ij} = C_{ijkl}\varepsilon_{kl} \qquad , i, j, k, l = 1, 2, 3$$

where C_{ijkl} =stiffnes matrix, σ_{ij} =stress tensor, ε_{kl} =strain tensor

$$\begin{bmatrix}\sigma_{xx}\\ \sigma_{yy}\\ \sigma_{zz}\\ \tau_{yx}\\ \tau_{zx}\\ \tau_{xy}\end{bmatrix} = \begin{bmatrix} \frac{1-v_{yz}v_{zx}}{E_yE_z\Delta} & \frac{v_{yx}+v_{yz}v_{zx}}{E_yE_z\Delta} & \frac{v_{zx}+v_{yx}v_{zy}}{E_yE_z\Delta} & 0 & 0 & 0\\ \frac{v_{yx}+v_{yz}v_{zx}}{E_yE_z\Delta} & \frac{1-v_{xz}v_{zx}}{E_xE_z\Delta} & \frac{v_{zy}+v_{xy}v_{zx}}{E_xE_z\Delta} & 0 & 0 & 0\\ \frac{v_{zx}+v_{yx}v_{zy}}{E_yE_z\Delta} & \frac{v_{zy}+v_{xy}v_{zx}}{E_xE_z\Delta} & \frac{1-v_{yz}v_{yx}}{E_xE_y\Delta} & 0 & 0 & 0\\ 0 & 0 & 0 & G_{yz} & 0 & 0\\ 0 & 0 & 0 & 0 & G_{zx} & 0\\ 0 & 0 & 0 & 0 & 0 & G_{xy}\end{bmatrix} \begin{bmatrix}\varepsilon_{xx}\\ \varepsilon_{yy}\\ \varepsilon_{zz}\\ \gamma_{yz}\\ \gamma_{zx}\\ \gamma_{xy}\end{bmatrix} \dots\dots (3.28)$$

where $\Delta = \left(1 - v_{xy}v_{yx} - v_{yz}v_{zy} - v_{xz}v_{zx} - 2v_{yx}v_{zy}v_{xz}\right)\Big/(E_1E_2E_3)$

3.4. Micromechanical analysis of a lamina [2]

3.4.1. Volume fractions

Consider a composite consisting of fiber and matrix. Define the fiber volume fraction V_f and the matrix volume fraction V_m as

$$V_f = \frac{v_f}{v_c} \quad \text{and} \quad V_m = \frac{v_m}{v_c} \dots\dots (3.29)$$

Note that the sum of volume fractions is

$$V_f + V_m = 1 \dots\dots (3.30)$$

from eqn (3.29) as

$$v_f + v_m = v_c \dots\dots (3.31)$$

3.4.3. Density

The derivation of the density of the composite in terms of volume fractions is found as follows. The mass of composite m_c is the sum of the mass of the fibers m_f and the mass of the matrix m_m given as:

$$m_c = m_f + m_m \dots\dots (3.32)$$

After simplified eqn (3.32) gives:

$$\rho_c = \rho_f V_f + \rho_m V_m \dots\dots (3.33)$$

3.4.5. Evaluation of the elastic moduli

There elastic moduli of a unidirectional lamina can be found by the following formula:

a) Longitudinal young's modulus, (E_1)

$$E_1 = E_f V_f + E_m V_m \dots\dots (3.34)$$

b) Transverse young's modulus (E_2)

$$\frac{1}{E_2} = \frac{V_f}{E_f} + \frac{V_m}{E_m} \quad \ldots \ldots (3.35)$$

Note: For unidirectional lamina $E_2 = E_3$

c) Major Poisson's ratio (μ_{12})

$$\mu_{12} = \mu_f V_f + \mu_m V_m \quad \ldots \ldots (3.36$$

Minor Poisson's ration

$$\mu_{21} = \mu_{12}\frac{E_2}{E_1} \quad \ldots \ldots (3.37)$$

$$\mu_{32} = \mu_{23} = \mu_{12}\left(\frac{1-\mu_{21}}{1-\mu_{12}}\right) \quad \ldots \ldots (3.38)$$

Note: For unidirectional lamina $\mu_{12} = \mu_{13}$

d) In-plane shear modulus G_{12}

$$\frac{1}{G_{12}} = \frac{V_f}{G_f} + \frac{V_m}{G_m} \rightarrow G_{12} = \frac{G_f * G_m}{G_f V_m + G_m V_f} \quad \ldots \ldots (3.39)$$

where, $G_f = \frac{E_f}{2(1+\mu_f)}$ $\qquad G_m = \frac{E_m}{2(1+\mu_m)}$

Note: For unidirectional lamina $G_{12} = G_{13}$

3.5.6. Ultimate strengths of a unidirectional lamina

The ultimate strength parameters for a unidirectional lamina can be found from the individual properties of the fiber and matrix by using the mechanics of materials approach.

(a) Longitudinal tensile strength

A simple mechanics of materials approach to find longitudinal tensile strength was presented. Then the ultimate failure strain of the fiber:

$$(\varepsilon_f)_{ult} = \frac{(\sigma_f)_{ult}}{E_f} \quad \ldots \ldots (3.40)$$

and the ultimate failure strain of the matrix:

$$(\varepsilon_m)_{ult} = \frac{(\sigma_m)_{ult}}{E_m} \quad \ldots \ldots (3.41)$$

Because the fibers carry most of the load in polymeric matrix composites, it is assumed that, when the fibers fail at the strain of $(\varepsilon_f)_{ult}$, the whole composite fails. Thus, the composite tensile strength is given by

$$(\sigma_1^T)_{ult} = (\sigma_f)_{ult} V_f + (\varepsilon_f)_{ult} E_m (1 - V_f) \quad \ldots \ldots (3.42)$$

(b) Longitudinal compressive strength

Using maximum strain failure theory, if the transverse strain exceeds the ultimate transverse tensile strain, $(\varepsilon_2^T)_{ult}$the lamina is considered to have failed in the transverse direction.

$$(\varepsilon_2^T)_{ult} = (\varepsilon_m^T)_{ult}\left(1 - V_f^{1/3}\right) \ldots\ldots\ldots\ldots\ldots\ldots\ldots\ldots\ldots (3.43)$$

$$(\sigma_2^c)_{ult} = \frac{E_1(\varepsilon_2^T)_{ult}}{\mu_{12}} \ldots\ldots\ldots\ldots\ldots\ldots\ldots\ldots\ldots (3.44)$$

(c) Transverse tensile strength

The ultimate transverse tensile strength

$$(\sigma_2^T)_{ult} = E_2(\varepsilon_2^T)_{ult} \ldots\ldots\ldots\ldots\ldots\ldots\ldots\ldots\ldots (3.45)$$

(d) Transverse compressive strength

Using compressive parameters in equation $(\sigma_2^T)_{ult}$,

$$(\varepsilon_m^c)_{ult} = \frac{\sigma_m^c}{E_m} \ldots\ldots\ldots\ldots\ldots\ldots\ldots\ldots\ldots (3.46)$$

$$(\varepsilon_2^c)_{ult} = (\varepsilon_m^c)_{ult}\left(1 - V_f^{1/3}\right) \ldots\ldots\ldots\ldots\ldots\ldots\ldots\ldots\ldots (3.47)$$

$$(\sigma_2^c)_{ult} = E_2(\varepsilon_2^c)_{ult} \ldots\ldots\ldots\ldots\ldots\ldots\ldots\ldots\ldots (3.48)$$

(e) In-plane shear strength

The ultimate shear strength for a unidirectional lamina using a mechanics of materials approach.

$$(\gamma_{12})_{mult} = \frac{(\tau_{12})_{mult}}{G_m} \ldots\ldots\ldots\ldots\ldots\ldots\ldots\ldots\ldots (3.49)$$

$$\frac{d}{s} = \sqrt{\frac{4V_f}{\pi}} \ldots\ldots\ldots\ldots\ldots\ldots\ldots\ldots\ldots (3.50)$$

$$(\gamma_{12})_{ult} = \left[\frac{d}{s}\left(\frac{G_m}{G_f} - 1\right) + 1\right](\gamma_{12})_{mult} \ldots\ldots\ldots\ldots\ldots\ldots (3.51)$$

The ultimate shear strength is then given by

$$(\tau_{12})_{ult} = G_{12}(\gamma_{12})_{ult} = G_{12}\left[\frac{d}{s}\frac{G_m}{G_f} + (1 - \frac{d}{s})\right](\gamma_{12})_{mult} \ldots\ldots\ldots (3.52)$$

(f) Composite yield strength

The yield strength of composite material of unidirectional lamina using mechanics of materials approach.

$$\sigma_{yc} = [V_f E_f + V_m E_m]\left(\frac{\sigma_{ym}}{E_m}\right) \ldots\ldots\ldots\ldots\ldots\ldots\ldots\ldots\ldots (3.53)$$

Table 3.1 shows the value of elastic moduli that calculated from properties of carbon fiber and epoxy matrix of Table 5.1 by using equations under section 3.4.

Table 3. 1.Elastic moduli of a unidirectional lamina from fiber and matrix property

Density of composite material (ρ_c)	$2.172\ g/cm^3$
Longitudinal young's modulus(E_1)	162.82GPa
Transversal young's modulus(E_2)	80.113GPa
Transversal young's modulus(E_3)	80.113GPa
Major poisons ratio(v_{12})	0.39
Poisons ratio(v_{23})	0.42
Poisons ratio(v_{13})	0.39
In-plane hear modulus(G_{12})	28.26GPa
Out-plane hear modulus(G_{23})	26.215GPa
Out-plane hear modulus(G_{13})	28.26GPa
Composite yield strength(σ_{yc})	2.59GPa

4. Materials and methods

Selecting appropriate materials is an important part of the design process for mechanical engineering products, particularly for load bearing components and structures. For a given loading system, the performance of an engineering structure is limited by the properties of the material of which it is made, and by the shapes to which this material can be formed. However, compared to conventional engineering materials, the use of composites complicates the situation because these materials are actually a combination of different materials, comprising of reinforcement, matrix, and possibly fillers and additives. Composites provide an enhanced shaping capability and an ability to tailor the reinforcement, thus leading to efficient material utilization and high performance structures.

4.1. Materials Selected for thin-walled composite beam

Thin-walled beam can be manufactured from different types of materials. That means it can be made from metals and composite materials. For this research carbon fiber and epoxy matrix with properties in table 4.1 have been selected.

Table 4. 1.Properties of carbon fiber and epoxy [34].

Fiber: T-300 12K carbon fiber	Matrix: Epoxy adhesive
Density$\left(\rho_f\right) = 1.76\,g/cm^3$	Density$(\rho_m) = 1.33\,g/cm^3$
Ultimate tensile strength$(\sigma_f)_{ult} = 3650MPa$	Ultimate tensile strength$(\sigma_m)_{ult} = 33MPa$
Tensile modulus$\left(E_f\right) = 231GPa$	Tensile modulus$(E_m) = 36.2GPa$
Poisson's ratio$\left(\mu_f\right) = 0.4$	Yield tensile strength$(\sigma_m)_{yield} = 576MPa$
Fiber volume fraction$\left(V_f\right) = 0.65$	Ultimate shear strength$(\tau_m)_{ult} = 80.2MPa$
	Ultimate compressive yield strength$(\sigma_m^C)_{ult} = 359MPa$
	Compressive modulus $(E_m^C) = 45.2GPa$
	Poisson's ratio$(\mu_m) = 0.389$
	Matrix volume fraction$\left(V_f\right) = 0.35$

4.2. Thesis workflow chart

Figure 4.1. shows the schematic work flows of the thesis that have been given as follow:

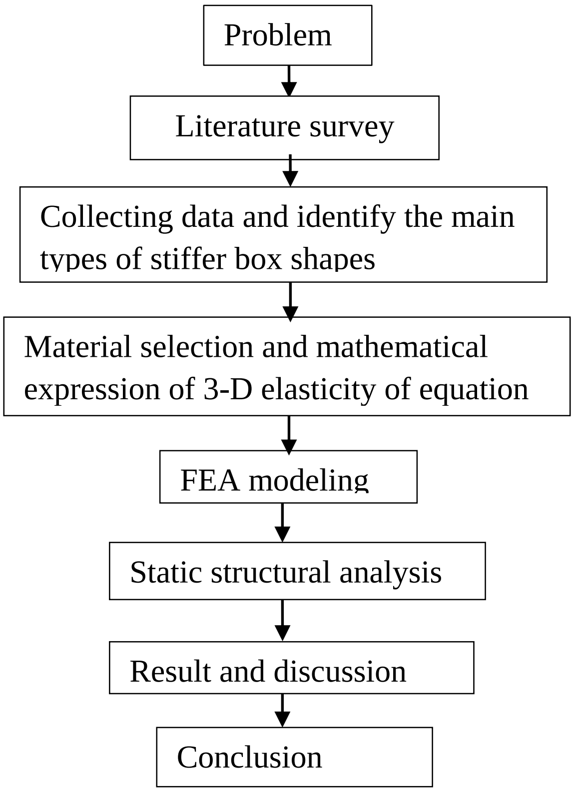

Figure 4.1. The schematic of the work flows of the thesis.

5. Modeling and conditions

5.1. Thin-walled composite beam

Figure 5.1 shows the two types of thin-walled composite beams namely symmetric and asymmetric thin-walled composite beams with open and closed sections. In this research work, both symmetric and asymmetric thin-walled composite beams of cantilever nature with closed section were considered.

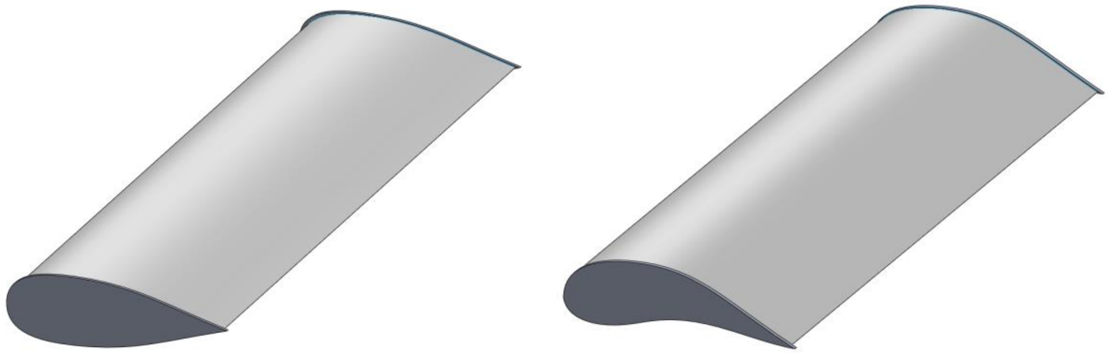

a) Symmetric thin-walled beam b) Asymmetric thin-walled beam

Figure 5.1. Thin-walled composite beam

5.2. Stiffer box

Figure 5.2. shows the stiffer box is the box of different shapes used to enhance the rigidity of composite thin-walled beam. There so many types of stiffer box shapes that can be made from different materials, but for this research five different stiffer box shapes that can easily manufactured have been considered. For asymmetric thin-walled composite beam all five different stiffer boxes were used. But, for symmetric thin walled composite beam three different stiffer box shapes were used because the effect of load is the same for symmetricity of shapes.

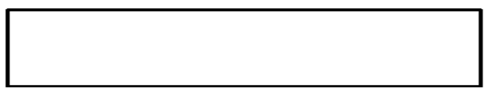

a) Rectangle

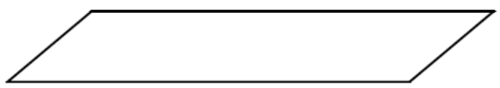

b) Right slanted rectangle c) Left slanted rectangle

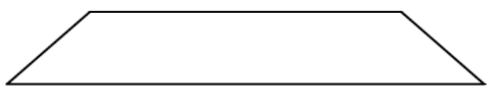

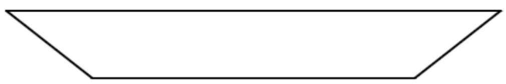

d) Downward trapezoid e) Upward trapezoid

Figure 5.2. Stiffer box with different shapes

5.3. Load condition

For both thin-walled composite beams seven types of loading condition means pure bending, pure shear, pure torsion, bending-shear, bending-torsion, shear-torsion and bending-shear-torsion load were considered. The loading condition of thin-walled composite beam specified as bending load of 500N, shear load of 500N and torsional load of 250Nm

5.4. Total number of cases to be considered

The total number of cases to be considered for thin-walled composite beam depend on the number of stiffer boxes, loading conditions and symmetricity of the thin-walled composite thin-walled beam. Depending on these three conditions twenty-eight (28) number of cases for symmetric thin-walled composite beam and forty-two (42) number of cases for asymmetric thin-walled composite beam have been considered. Totally seventy (70) number of cases for both thin-walled composite beam were considered.

5.5. Boundary condition

The boundary conditions are the known conditions on the surfaces of the thin-walled composite beam which must be prescribed in advance in order to obtain the solution of a particular problem. Such conditions include the load applied on the faces of the thin-walled composite beam however, the load has been taken into account in the formulation of the general problem of bending, shear and torsion of thin-walled composite beam. For this study thin-walled composite beam was considered as cantilever.

5.6. Overall initial speciation

Table 5.1 shows the overall initial specification for both symmetric and asymmetric composite thin-walled beams were presented in table form as follows.

Table 5. 1.Overall initial specification of thin-walled composite beam

Overall specification for thin-walled composite beam	
Chord length of thin-walled composite beam	100mm
Maximum height of thin-walled composite beam	30mm
Depth of thin-walled composite beam	350mm
Single ply thickness of thin-walled composite beam	0.25mm
Total number of plies	12
Ply orientation	$\pm 30°$
Total ply thickness of thin-walled composite beam	3mm
Stiffer box thickness	2mm

6. Result and discussion

6.1. Results

In this research work static analysis of symmetric and asymmetric thin-walled composite beam with and without stiffer box of different shapes were done by using finite element analysis software. And from finite element analysis software, the results of von mise stress and resultant displacement were generated. The generated von Mises stress and resultant displacement distribution of symmetric and asymmetric thin-walled composite beam of all loading cases have been given in appendix A and appendix B.

Generally, the results of maximum von mise stress and resultant displacement of symmetric and asymmetric thin-walled composite beam with and without stiffer box of different shapes for all loading conditions have been summarized in table 6.1-6.4 as follow. Table 6.1 shows maximum von mise stress results of symmetric thin-walled composite beam with and without stiffer box of different shapes subjected to different loading conditions.

Table 6. 1 Von mise stress analysis result of symmetric thin-walled composite beam

Load type	Symmetric thin-walled beam			
	No stiffer box	Rectangular stiffer box	Slanted rectangular stiffer box	Trapezoid stiffer box
	Stress (MPa)	Stress (MPa)	Stress (MPa)	Stress (MPa)
Bending	79.6	51.09	55.59	55.89
Shear	79.82	55.77	55.31	55.60
Torsion	192.3	148.6	161.6	150.5
Bending-shear	159.4	116.1	110.9	111.4
Bending-torsion	217.5	153.4	157.4	153.7
Shear-torsion	77.42	55.78	158.8	55.57
Bending-shear-torsion	244.7	171.5	171.9	171.8

Figure 6.1 shows maximum von mise stress values of symmetric thin-walled composite beam with and without stiffer box of different shapes subjected to different loading conditions from appendix A.

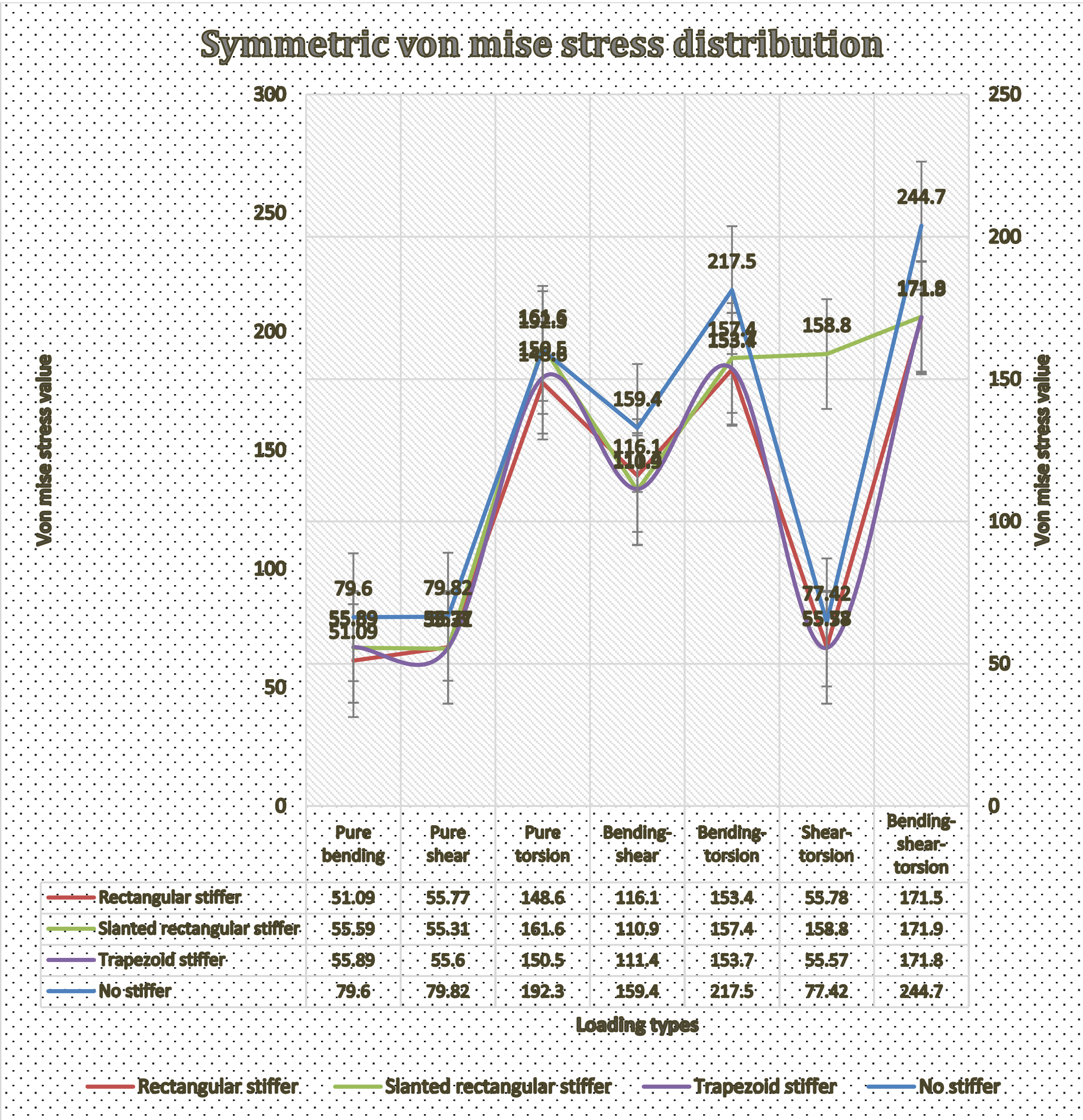

Figure 6.1. Symmetric thin-walled composite beam with and without stiffer box maximum von mise stress under different loading condition

Table 6.1 shows resultant displacement results of symmetric thin-walled composite beam with and without stiffer box of different shapes subjected to different loading conditions.

Table 6. 2 Resultant displacement analysis result of symmetric thin-walled composite beam

Load type	Symmetric thin-walled beam			
	No stiffer box	Rectangular stiffer box	Slanted rectangular stiffer box	Trapezoid stiffer box
	Displacement (mm)	Displacement (mm)	Displacement (mm)	Displacement (mm)
Bending	1.714	1.307	1.309	1.309
Shear	1.709	1.296	1.298	1.298
Torsion	1.599	1.277	1.280	1.276
Bending-shear	3.414	2.597	2.601	2.601
Bending-torsion	3.270	2.549	2.553	2.550
Shear-torsion	1.787	1.296	2.561	1.298
Bending-shear-torsion	4.952	3.828	3.834	3.831

Figure 6.2 shows resultant displacement distribution of symmetric thin-walled composite beam with and without stiffer box of different shapes subjected to different loading conditions that generated in appendix A.

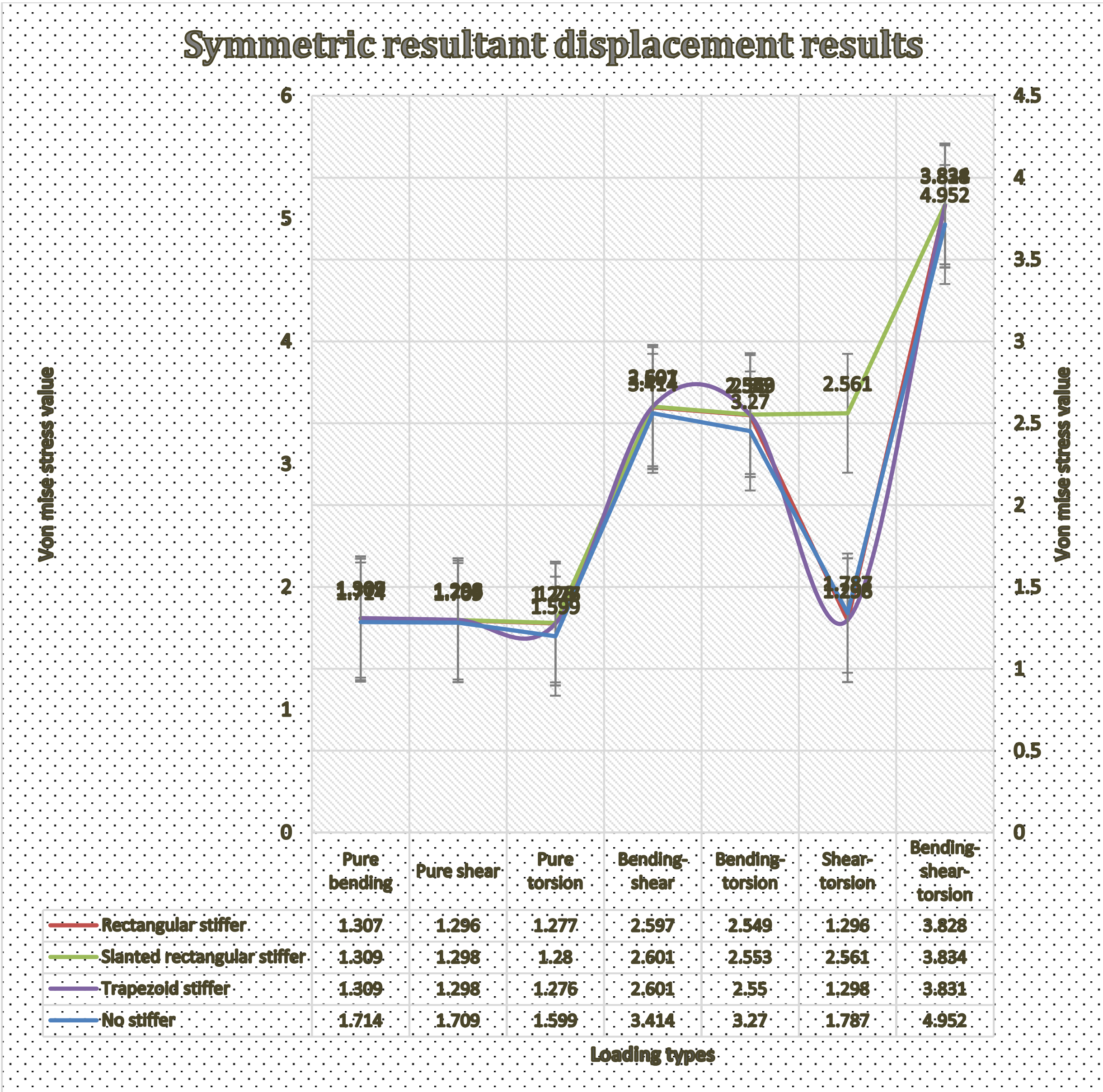

Figure 6.2 Symmetric thin-walled composite beam with and without stiffer box resultant displacement under different loading condition

Table 6.3 shows maximum von mise stress results of asymmetric thin-walled composite beam with and without stiffer box of different shapes subjected to different loading conditions.

Table 6. 3 Von mise stress analysis result of asymmetric thin-walled composite beam

Load type	Asymmetric thin-walled composite beam					
	No stiffer box	Rectangular stiffer box	Left slanted rectangular stiffer box	Right slanted rectangular stiffer box	Upward trapezoid stiffer box	Downward trapezoid stiffer box
	Stress (MPa)	Stress (MPa)	Stress (MPa)	Stress (MPa)	Stress (MPa)	Stress (MPa)
Bending	84.24	61.48	63.71	61.66	68.01	60.50
Shear	84.59	64.41	64.24	62.03	68.70	60.74
Torsion	187.5	164.0	165.6	181.7	162.3	165.6
Bending-shear	168.8	123.2	128.0	123.7	136.8	121.4
Bending-torsion	257.8	180.5	182.5	181.4	187.4	180.5
Shear-torsion	261.4	182.9	185.1	184.0	188.3	183.2
Bending-shear-torsion	307.4	228.3	236.3	230.2	136.8	226.9

Figure 6.3 shows maximum von mise stress distribution value of asymmetric thin-walled composite beam with and without stiffer box that subjected to different loading conditions generated from simulation results found in appendix B.

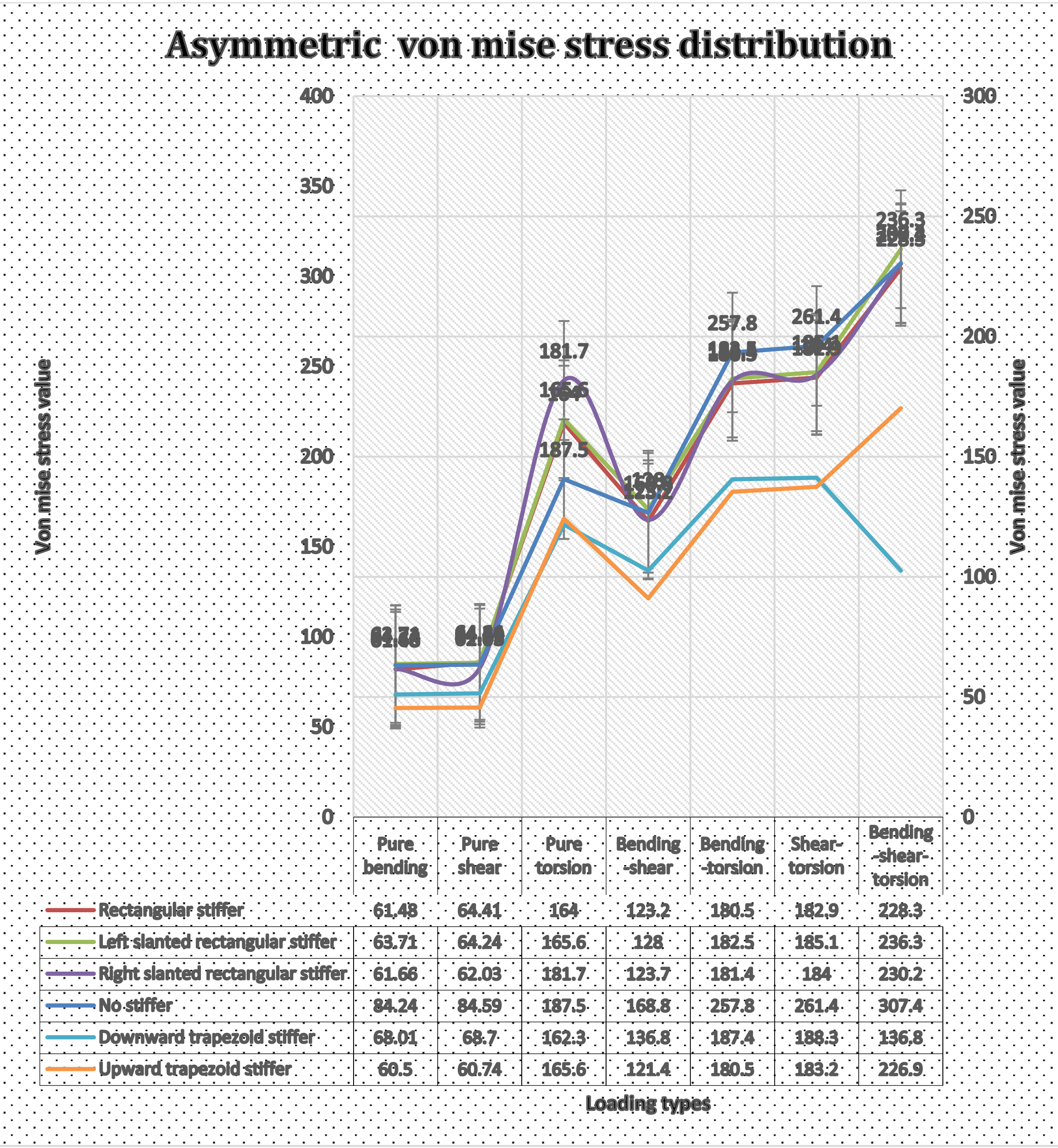

	Pure bending	Pure shear	Pure torsion	Bending -shear	Bending -torsion	Shear-torsion	Bending -shear-torsion
Rectangular stiffer	61.48	64.41	164	123.2	180.5	182.9	228.3
Left slanted rectangular stiffer	63.71	64.24	165.6	128	182.5	185.1	236.3
Right slanted rectangular stiffer	61.66	62.03	181.7	123.7	181.4	184	230.2
No stiffer	84.24	84.59	187.5	168.8	257.8	261.4	307.4
Downward trapezoid stiffer	68.01	68.7	162.3	136.8	187.4	188.3	136.8
Upward trapezoid stiffer	60.5	60.74	165.6	121.4	180.5	183.2	226.9

Figure 6.3 Asymmetric thin-walled composite beam with and without stiffer box maximum von mise stress under different loading condition

Table 6.4 shows resultant displacement results of asymmetric thin-walled composite beam with and without stiffer box of different shapes subjected to different loading conditions.

Table 6. 4 Resultant displacement analysis result of asymmetric thin-walled beam with stiffer box

Load type	Asymmetric thin-walled beam					
	No stiffer box	Rectangular stiffer box	Left slanted rectangular stiffer box	Right slanted rectangular stiffer box	Upward trapezoid stiffer box	Downward trapezoid stiffer box
	Displacement (mm)	Displacement (mm)	Displacement (mm)	Displacement (mm)	Displacement (mm)	Displacement (mm)
Bending	1.918	1.485	1.508	1.484	1.510	1.478
Shear	1.897	1.456	1.479	1.456	1.482	1.449
Torsion	3.133	2.473	2.512	2.462	2.610	2.448
Bending-shear	3.797	2.933	2.979	2.932	2.983	2.920
Bending-torsion	4.979	3.891	3.953	3.883	3.958	3.859
Shear-torsion	4.995	3.904	3.967	3.896	3.971	4.005
Bending-shear-torsion	6.837	5.323	5.405	5.315	2.983	5.284

Figure 6.3 shows resultant displacement distribution value of asymmetric thin-walled composite beam with and without stiffer box that subjected to different loading conditions generated from simulation results found in appendix B.

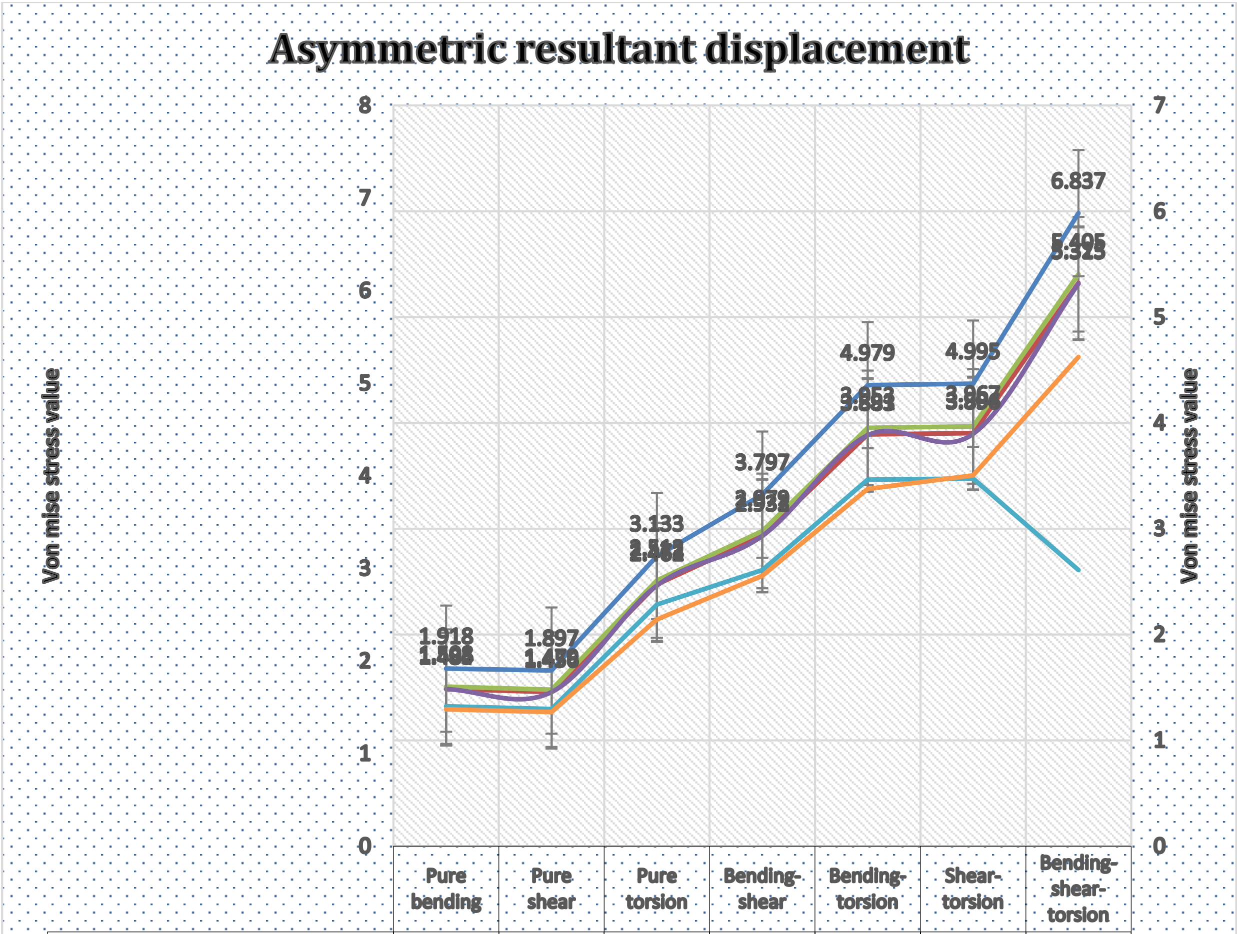

	Pure bending	Pure shear	Pure torsion	Bending-shear	Bending-torsion	Shear-torsion	Bending-shear-torsion
Rectangular stiffer	1.485	1.456	2.473	2.933	3.891	3.904	5.323
Left slanted rectangular stiffer	1.508	1.479	2.512	2.979	3.953	3.967	5.405
Right slanted rectangular stiffer	1.484	1.456	2.462	2.932	3.883	3.896	5.315
No stiffer	1.918	1.897	3.133	3.797	4.979	4.995	6.837
Downward trapezoid stiffer	1.51	1.482	2.61	2.983	3.958	3.971	2.983
Upward trapezoid stiffer	1.478	1.449	2.448	2.92	3.859	4.005	5.284

Loading types

Figure 6.4 Asymmetric thin-walled composite beam with and without stiffer box maximum von mise stress under different loading condition

6.2. Discussion

Static analysis results summary for both symmetric and asymmetric thin-walled composite beam without and with stiffer box of different shapes that tabulated in table 6.1-6.4 were presented in appendix A and appendix B as follow.

6.2.1. Static analysis results summary for symmetric thin-walled beam

The symmetric composite thin-walled beam without stiffer box subjected to pure bending load results maximum von mise stress value of 79.60MPa and maximum resultant displacement value of 1.714mm. But, symmetric thin-walled beam with rectangular stiffer box results minimum von mise stress of 51.09MPa and resultant displacement1.307mm.

The symmetric composite thin-walled without stiffer box subjected to pure shear load results maximum von mise stress value of 79.82MPa and resultant displacement value 1.709mm. But, symmetric thin-walled beam with slanted rectangle results minimum von mise stress value of 55.31MPa and symmetric thin-walled beam with rectangular stiffer box results minimum resultant displacement value of 1.296mm.

The symmetric composite thin-walled without stiffer box subjected to pure torsion load results maximum von mise stress value of 192.30MPa and resultant displacement value of 1.599mm. On the other hand, symmetric thin-walled beam with rectangular stiffer box results minimum von mise stress value of 148.60MPa and symmetric thin-walled beam with trapezoid stiffer box minimum resultant displacement value of 1.276mm.

The symmetric composite thin-walled without stiffer box subjected to bending-shear load results maximum von mise stress value 159.40MPa and resultant displacement value of 3.414mm. But, symmetric thin-walled beam with slanted rectangular stiffer box results minimum von mise stress value of 110.90MPa and symmetric thin-walled beam with rectangular stiffer box results minimum resultant displacement value of 1.307mm.

The symmetric composite thin-walled without stiffer box subjected to bending-torsion load results maximum von mise stress value of 217.5MPa and resultant displacement value of 3.270mm. But, symmetric thin-walled beam with rectangular stiffer box results minimum von mise stress value of 153.50MPa and resultant displacement value of 2.549mm.

The symmetric composite thin-walled with slanted rectangle stiffer box subjected to shear-torsion load results maximum von mise stress value of 158.8MPa and resultant displacement value of 2.561mm. But, symmetric thin-walled beam with trapezoid stiffer box results minimum von mise stress value of 55.57MPa and symmetric thin-walled beam with rectangular stiffer box results resultant minimum displacement value of 1.296mm.

The symmetric composite thin-walled without stiffer box subjected to bending-shear-torsion load results maximum von mise stress value of 244.70MPa and resultant displacement value of 4.952mm, but, symmetric thin-walled beam with rectangular stiffer box results minimum von mise stress value of 171.50MPa and resultant displacement value of 3.828mm.

Generally symmetric composite thin-walled without stiffer box subjected all types of loads have maximum value of von mise stress and resultant displacement.

6.2.2. Static analysis results summary for asymmetric thin-walled beam

The asymmetric composite thin-walled beam without stiffer box subjected to pure bending load results maximum von mise stress value of 84.24MPa and resultant displacement value of 1.918mm, but, asymmetric thin-walled beam with rectangular stiffer box results minimum von mise stress value of 50.04MPa and asymmetric thin-walled beam with downward trapezoid stiffer box results minimum resultant displacement value of 1.478mm.

The asymmetric composite thin-walled beam without stiffer box subjected to pure shear load results maximum von mise stress value of 84.59MPa and resultant displacement value of 1.897mm, but, asymmetric thin-walled beam with downward trapezoid stiffer box minimum von mise stress value of 60.74MPa and minimum resultant displacement value of 1.449mm.

The asymmetric composite thin-walled beam without stiffer box subjected to pure torsion load results maximum von mise stress value of 231.40MPa and resultant displacement value of 3.463mm, but, asymmetric thin-walled beam with upward trapezoid stiffer box results minimum von mise stress value of 162.30MPa and asymmetric thin-walled beam with downward trapezoid stiffer box results minimum resultant displacement value of 2.448mm.

The asymmetric composite thin-walled beam without stiffer box subjected to bending-shear load results maximum von mise stress value of 168.80MPa) and resultant displacement value of 3.797mm, but, asymmetric thin-walled beam with rectangular stiffer box results minimum von mise stress value of 123.20MPa and asymmetric thin-walled beam with downward trapezoid stiffer box results minimum resultant displacement value of 2.920mm.

The asymmetric composite thin-walled beam without stiffer box subjected to bending-torsion load results maximum von mise stress value of 257.8MPa and resultant displacement value of 4.979mm, but, to asymmetric thin-walled beam with rectangular stiffer box results minimum von mise stress value of 180.50MPa and asymmetric thin-walled beam with downward trapezoid stiffer box minimum resultant displacement value of 3.859mm.

The asymmetric composite thin-walled beam without stiffer box subjected to shear-torsion load results maximum von mise stress value of 261.40MPa and resultant displacement value of 4.995mm, but, asymmetric thin-walled beam with rectangular stiffer box results minimum von mise stress value of 182.90MPa and asymmetric thin-walled beam with right slanted rectangular stiffer box results minimum resultant displacement value of 3.896mm.

The asymmetric composite thin-walled beam without stiffer box subjected bending-shear-torsion load results maximum von mise stress value of 307.400MPa and resultant displacement value of 6.837mm, but, asymmetric thin-walled beam with upward trapezoid stiffer box minimum von mise stress value of 226.90MPa) and resultant displacement value of 2.983mm.

7.Conclusion and future work

7.1. Conclusion

In this research work static analysis of symmetric and asymmetric thin-walled composite beam with and without stiffer box of different loading conditions have been done by finite element analysis software. The simulation results of von mises stress and resultant displacement were generated from finite element analysis software and summarized briefly as follows.

Static analysis simulation results presented for symmetric thin-walled composite beam without stiffer box subjected to pure bending, shear and torsion load, bending-torsion and bending-shear-torsion load and symmetric thin-walled composite beam with slanted rectangular stiffer box subjected to shear-torsion load results maximum von mise stress and resultant displacement for the given loading conditions. From these results thin-walled composite beam without stiffer box and with slanted rectangular stiffer box were not suitable described loading conditions.

Generally, static analysis simulation results shown for symmetric thin-walled composite beam with rectangular stiffer box subjected to pure bending and torsion load, bending-torsion and bending-shear-torsion load and symmetric thin-walled composite beam with slanted rectangle stiffer box subjected to pure shear and bending-shear load and symmetric thin-walled composite beam with trapezoid stiffer box subjected to shear-torsion load results minimum von mise stress. Symmetric thin-walled composite beam with rectangular stiffer box subjected to pure bending and shear load, bending-shear, bending-torsion, shear-torsion and bending-shear-torsion load and thin-walled composite beam with trapezoid stiffer box subjected to shear-torsion load results minimum resultant displacement from other thin-walled composite beam with stiffer box another shapes subjected under different loading conditions. From these results symmetric thin-walled composite beam with rectangular, slanted rectangle and trapezoid were suitable for the specified loading conditions.

Static analysis simulation results showed that asymmetric thin-walled composite beam without stiffer box subjected all seven loading conditions results maximum von mise stress and resultant displacement from other asymmetric thin-walled composite beam with stiffer box shapes subjected under all loading conditions. From these results thin-walled composite beam without stiffer box was not suitable for all loading conditions.

Generally, static analysis simulation results showed that asymmetric thin-walled composite beam with rectangular stiffer box subjected to pure bending, bending-shear, bending-torsion and shear-torsion load and asymmetric thin-walled composite beam with downward trapezoid stiffer box subjected to pure shear load and asymmetric thin-walled composite beam with upward trapezoid stiffer box subjected to bending-shear-torsion load results minimum von mise stress. Asymmetric thin-walled composite beam with downward trapezoid stiffer box subjected to pure bending, shear and torsion load, bending-shear, bending-torsion and shear-torsion load and thin-walled composite beam with right slanted rectangle stiffer box subjected to bending-shear-torsion load results minimum resultant displacement from other thin-walled composite beam with stiffer box another shapes subjected under different loading conditions. From these results asymmetric thin-walled composite beam with rectangular, downward and upward trapezoid were suitable for the specified loading conditions.

7.2. Future work

The aim of this study was to investigate the static analysis of thin-walled composite beam using unidirectional composites by finite element method for various stiffer box of different shapes for increasing the rigidity of thin-walled composite beam under bending, shear and torsion loading. This study can be further expanded by considering different fiber angle orientation, by doing experimental and by using hybrid composites.

- Finite element analysis on thin-walled composite beam with the different fiber orientation can be conducted.
- Effect of matrix/fiber debonding can be studied by applying bending, shear and torsion load.
- Stress analysis of thin-walled composite beam under thermal loading can be performed.
- Stress analysis on nanoparticles thin-walled composite beam can be conducted.
- Failure prediction of thin-walled composite beam can be investigated.

Reference

[1]. Valery V.V, Evgeny V.M, Advanced mechanics of composite materials and structural elements, 3rd edition, United Kingdom, Elsevier, 2013

[2] Kaw, A.K., Mechanics of composite materials, 2nd Edition, Boca Raton FL, CRC Press, 2006.

[3]. Mahmoud Y.O, Osama M. E. S. Free vibration analysis of laminated composite beams using finite element method, International journal of engineering research and advanced technology.3(2017):2454-6135.

[4] Chawla, K.K., Composite materials: Science and engineering, 2nd Edition, New York, Springer, 1998.

[5] Palucka, Tim., Bensaude-Vincent, B., Composites overview, 2002.

[6] Mallick, P.K., Fiber reinforced composites material, Manufacturing and design, 3rd Edition, Boca Raton FL, CRC Press, 2007.

[7] Gibson, Ronald F., Principles of composite material mechanics, 3rd Edition, Boca Raton FL, CRC Press, 2011.

[8] Pora, Jerome. Van Forest, Arnold., and Sippel, Martin., "The Logistical challenges of Spaceliner Concept," 1st International academy of astronautics symposium on private human access to space, 2008.

[9] Roncz, J., "Propeller development for the Rutan Voyager," SAE technical paper No. 891034, 1989.

[10] Van Forest, Arnold., and Sippel, Martin., "The logistical challenges of Spaceliner Concept," 1st International academy of astronautics symposium on private human access to space, 2008.

[11] Peijs, Ton., "Natural fiber based composites," Journal of materials technology, 15(2000), pp. 281-285.

[12] Gay, Daniel., Composite materials: Design and applications, 3rd Edition, Boca Raton FL, CRC Press, 2014.

[13] Heimb S., "Crash Simulation of an F1 Racing Car Front Impact Structure," 7th LS-Dyna conference, Stuttgart, 2009.

[14] Mohite P.M., "A course on composite materials," NPTEL.

[15]. Pavassa R, Torsion of thin-walled beams of open cross-section with influence of shear, International journal of mechanical sciences, 47 (2005):1099–1122

[16]. Kim. N. I and Shin. D. K, Torsional analysis of thin-walled composite beams with single- and double-celled sections, Engineering Structures, 31 (2009):1509-1521

[17]. Vo T. P and Lee J., Flexural–torsional behavior of thin-walled closed-section composite box beams, Engineering Structures, 29 (2007):1774–1782

[18]. Vo T. P and Lee J, Flexural–torsional behavior of thin-walled composite box beams using shear-deformable beam theory, Engineering Structures, 30 (2008):1958–1968.

[19]. Kim. N. I and Lee. J, Theory of thin-walled functionally graded sandwich beams with single and double-cell sections, Composite Structures, 157 (2016):141–154

[20]. Günay. M. G and Timarci. T, Static analysis of thin-walled laminated composite closed-section beams with variable stiffness, Composite Structures, 182 (2017):67–78

[21]. Kim. N. I and Lee. J, Flexural-torsional analysis of functionally graded sandwich I-beams considering shear effects, Composites Part B, 108 (2017):436-450.

[22] Jang. G. W, Kim. Y. Y, Shin. D and Choi. S, Finite element beam analysis of tapered thin-walled box beams, Thin-walled structures, 102(2016):205–214

[23]. Correia. A. A, Almeida. J. P and Pinho. R, Force-based higher-order beam element with flexural–shear–torsional interaction in 3D frames. Part I: Theory, Engineering Structures, 89 (2015):204–217

[24]. Barrientos. F. C, Valle J. D and Martinez. J. A, Beam element for thin-walled beams with torsion, distortion, and shear lag, Engineering Structures,143 (2017):571–588

[25] Ahmed. M. N and Ahmed, S, Torsional analysis of multi-cell multi-tapered composite beams with cantilever configuration, Thin-walled structures, 96(2015):75–81

[26]. Pavazzaa. R and Matoković. A, Bending of thin-walled beams of open section with influence of shear, part I: Theory, Thin-walled structures, 116 (2017):357–368

[27] Zhong. H, Liu. Z, Qin. H and Liu. Y, Static analysis of thin-walled space frame structures with arbitrary closed cross-sections using transfer matrix method, Thin-walled Structures, 123 (2018):255–269

[28] Lee. J, Flexural analysis of thin-walled composite beams using shear-deformable beam theory, Composite Structures, 70 (2005):212–222

[29]. Vo. T. P and Thai. H. T, Static behavior of composite beams using various refined shear deformation theories, Composite Structures, 94 (2012):2513–2522

[30] Luoa. D, Zhonga. D. Y, Lia. B and Denga. B, Static and dynamic analysis of composite box beam based on geometrically exact nonlinear model considering non-classical effects, Composite Structures, 204 (2018):689–700

[31] Ghafari. E and Rezaeepazhand. J, Two-dimensional cross-sectional analysis of composite beams using Rayleigh-Ritz-based dimensional reduction method, Composite structures, 184 (2018):872–882

[32]. Kim. H and Jang. G. W, Higher-order thin-walled beam analysis for axially varying generally shaped cross sections with straight cross-section edges, Computers and Structures, 189 (2017):83–100.

[33]. Megson, T. H. G, An introduction to aircraft structural analysis. (Burlington, MA 01803, USA, Elsivier,2010)

[34]. http://www.Matweb.com

Appendix A

Symmetric thin-walled composite beam static analysis results

Pure bending von mises stress distribution of different stiffer box

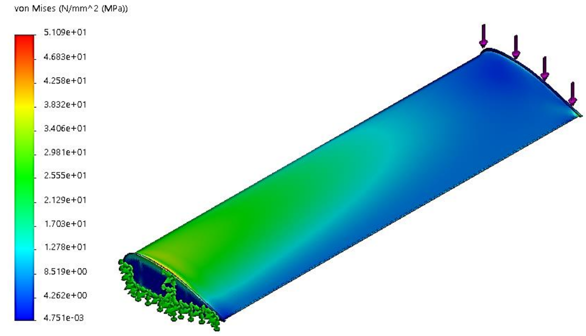

Rectangular stiffer box

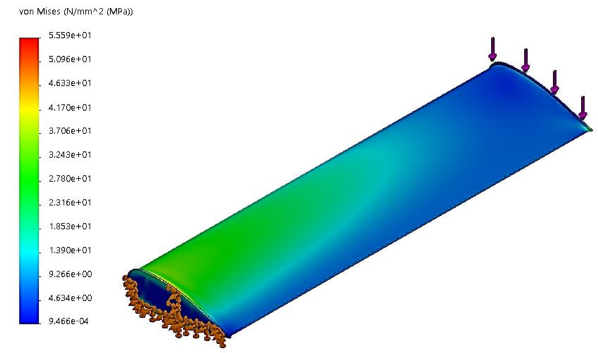

Slanted rectangular

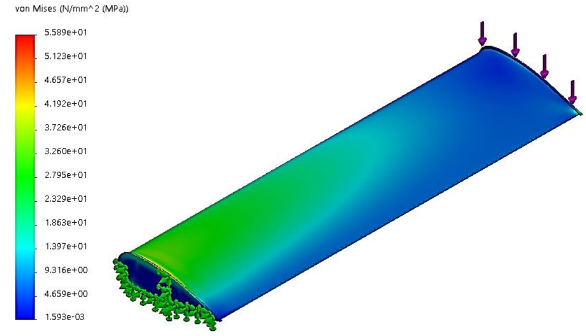

Trapezoid stiffer box

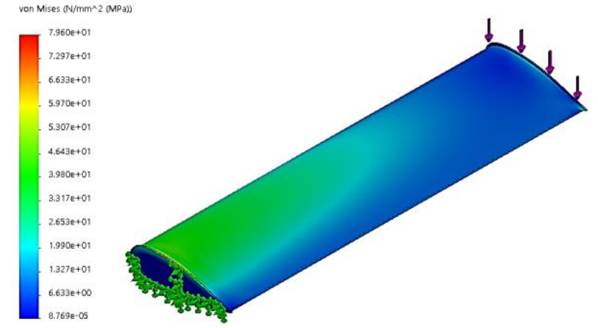

No stiffer box

Pure bending resultant displacement distribution of different stiffer box

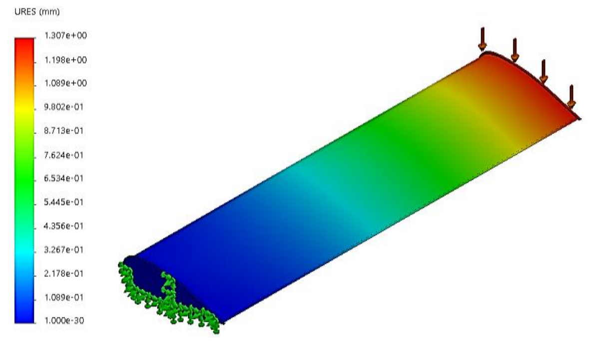

Rectangular stiffer box

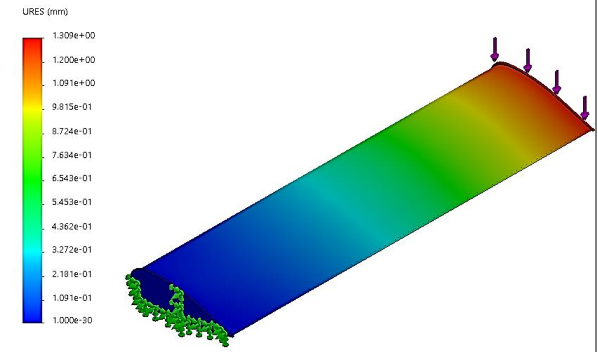

Slanted rectangular stiffer box

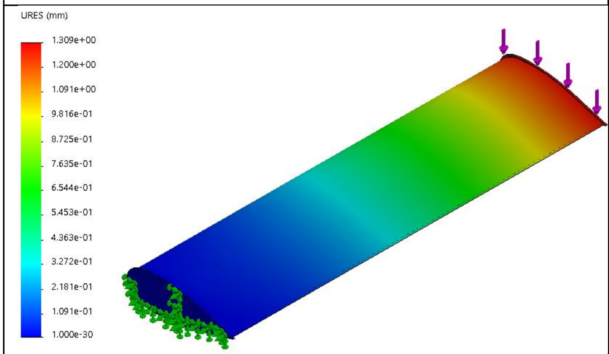

Trapezoid stiffer box

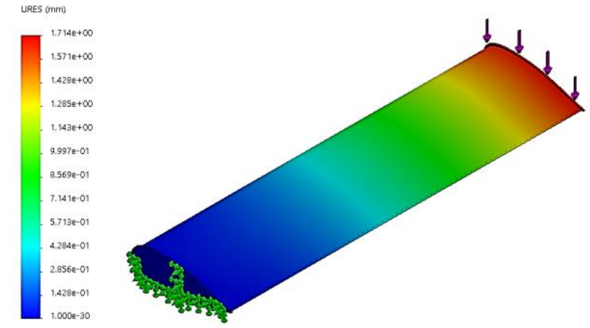

Without stiffer box

Pure shear von mises stress distribution of different stiffer box

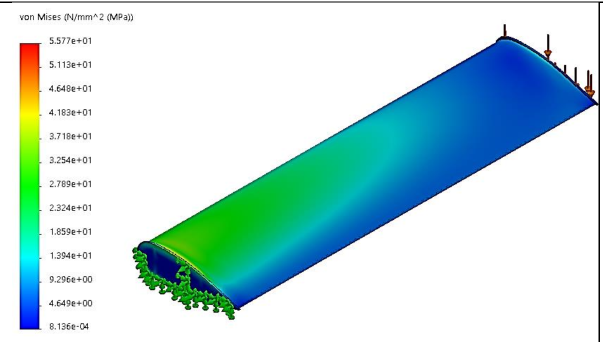

Rectangular stiffer box

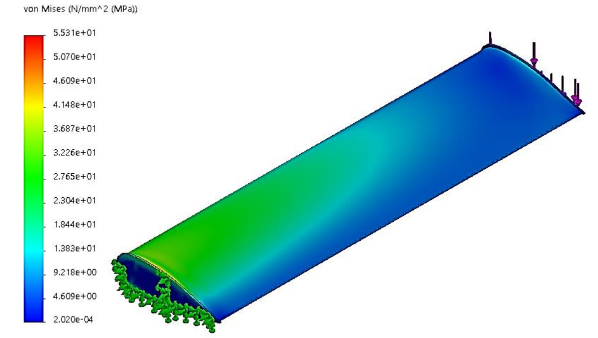

Slanted rectangular stiffer box

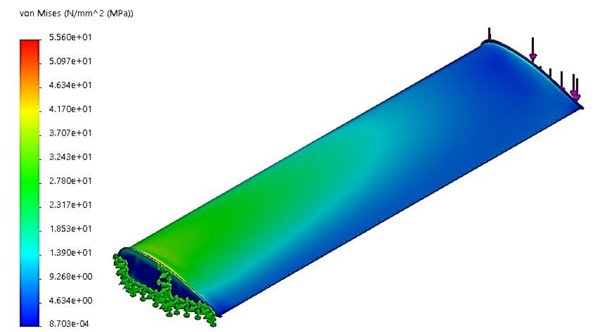

Trapezoid stiffer box

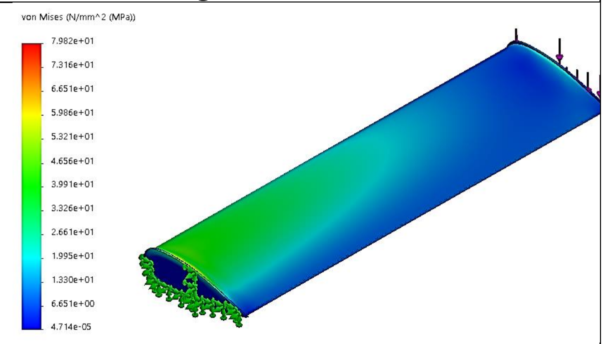

Without stiffer box

Pure shear resultant displacement distribution of different stiffer box

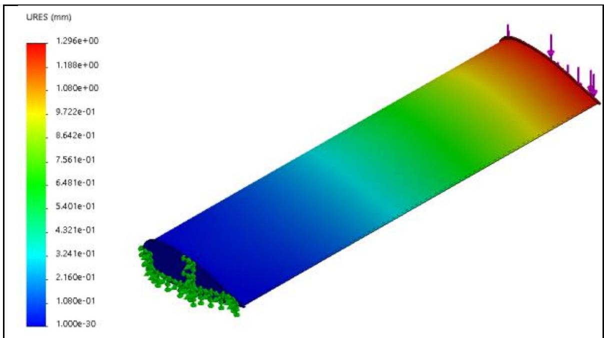

Rectangular stiffer box

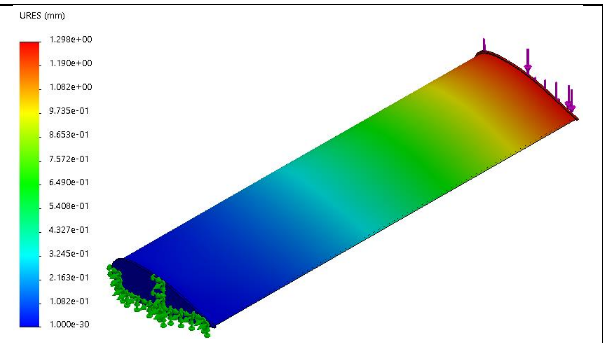

Slanted rectangular stiffer box

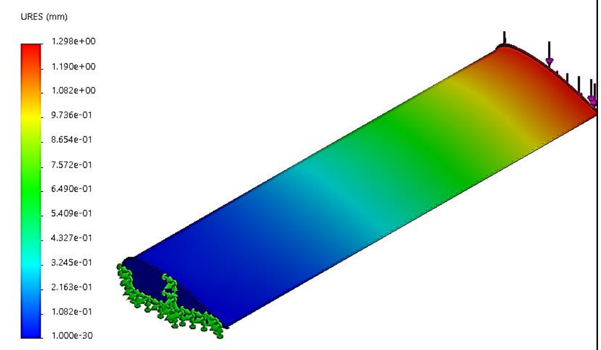

Trapezoid stiffer box

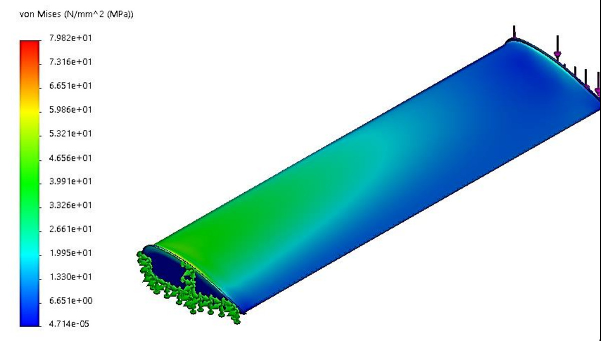

Without stiffer box

Pure torsion von mise stress distribution of different stiffer box

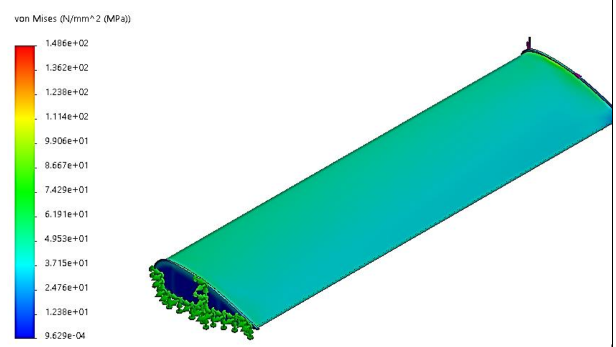

Rectangular stiffer box

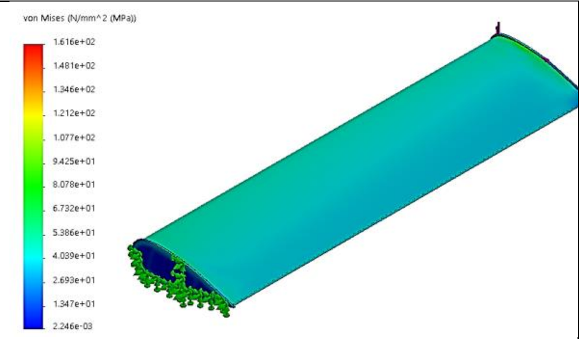

Slanted rectangular

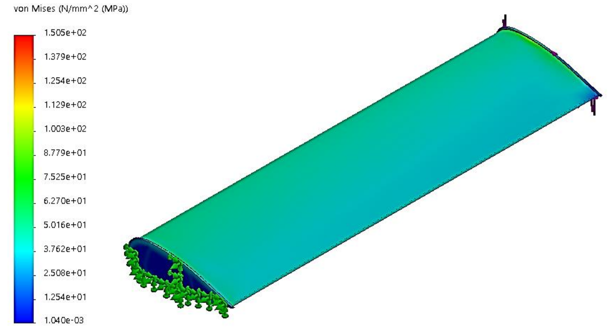

Trapezoid stiffer box

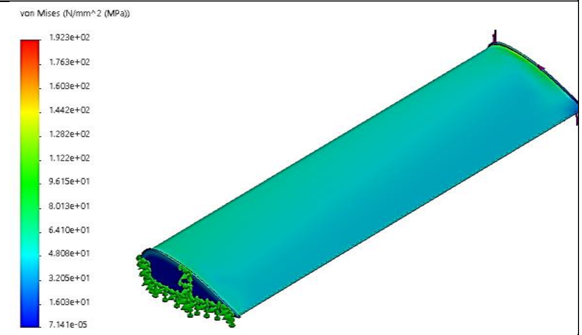

No stiffer box

Pure torsion resultant displacement distribution of different stiffer box

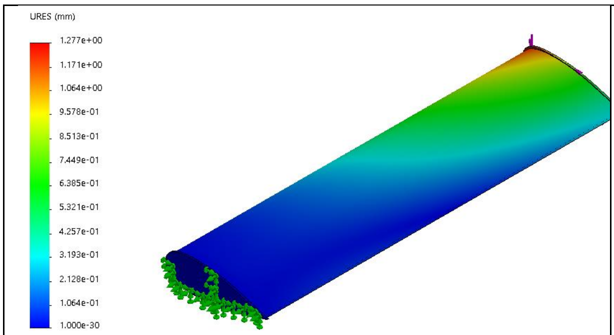

Rectangular stiffer box

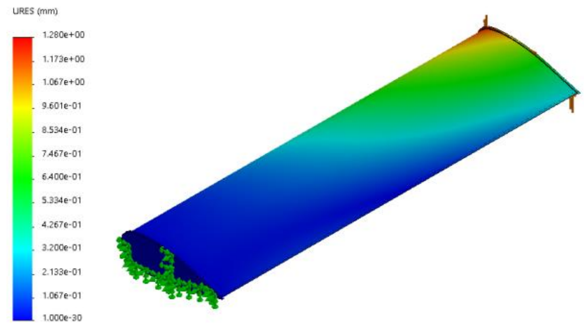

Slanted rectangular stiffer box

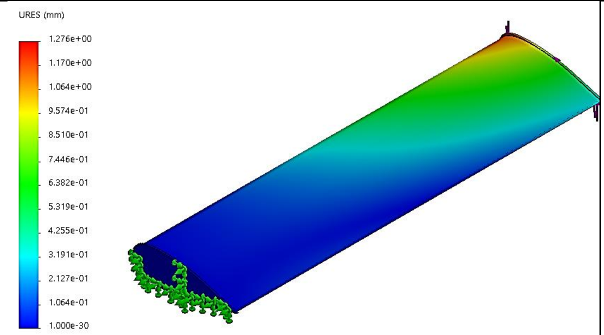

Trapezoid

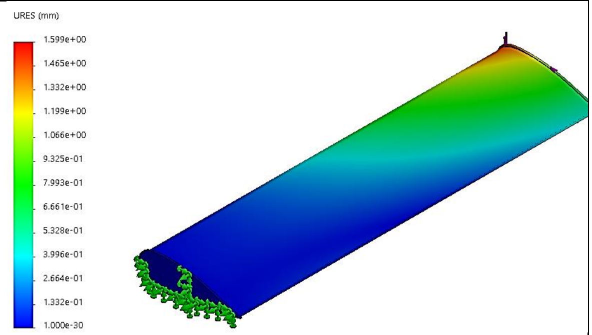

Without stiffer box

Bending-shear von Mises stress distribution of different stiffer box

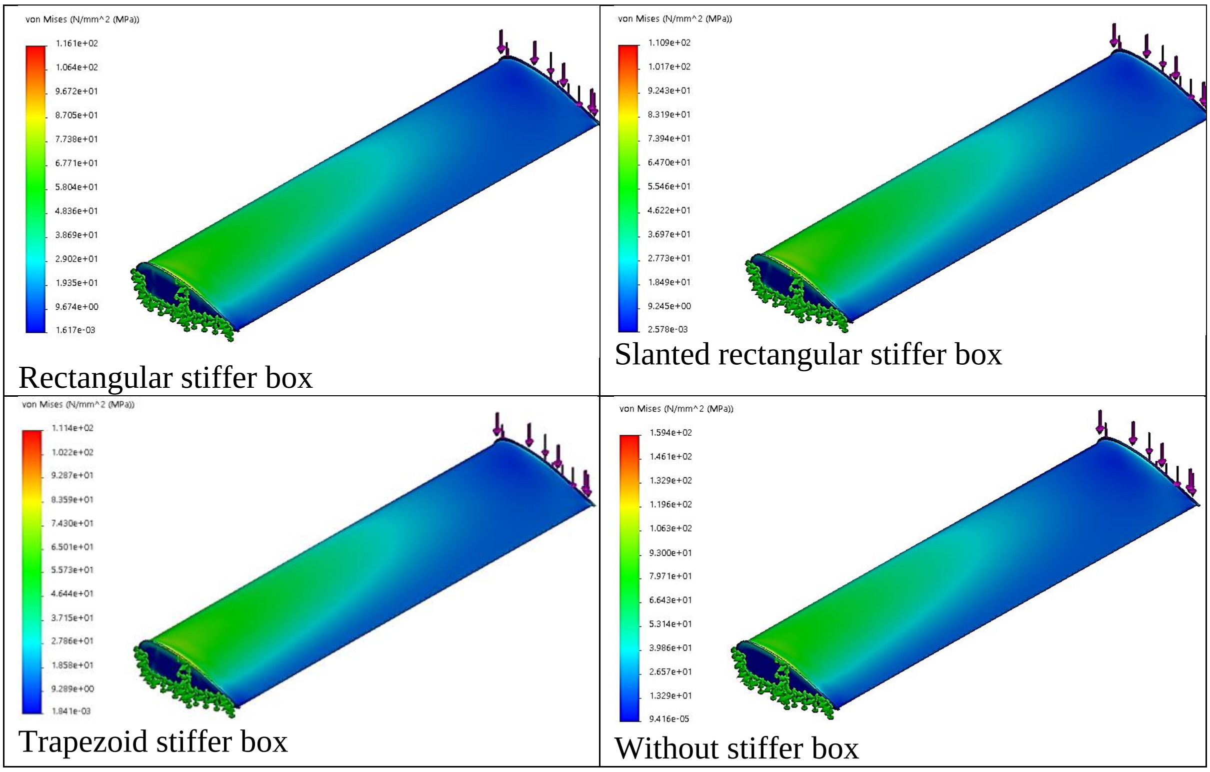

Bending-shear resultant displacement distribution of different stiffer box

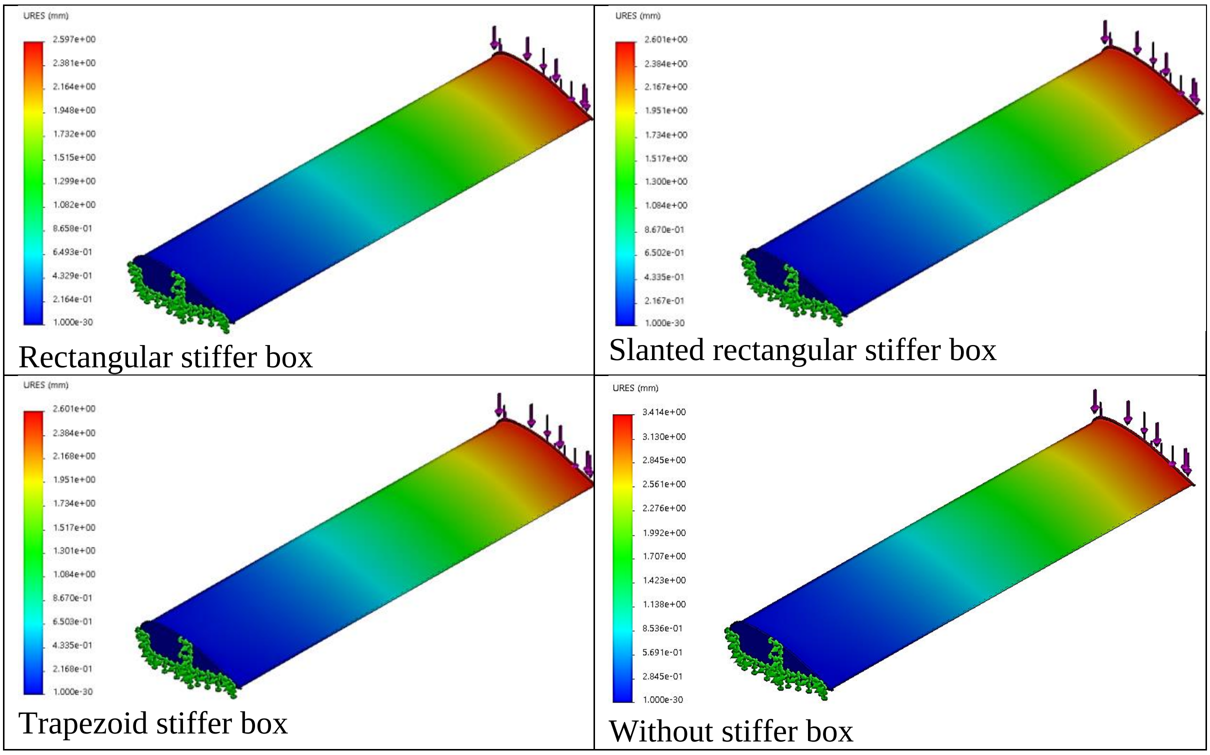

Bending-torsion Von mise stress distribution of different stiffer box

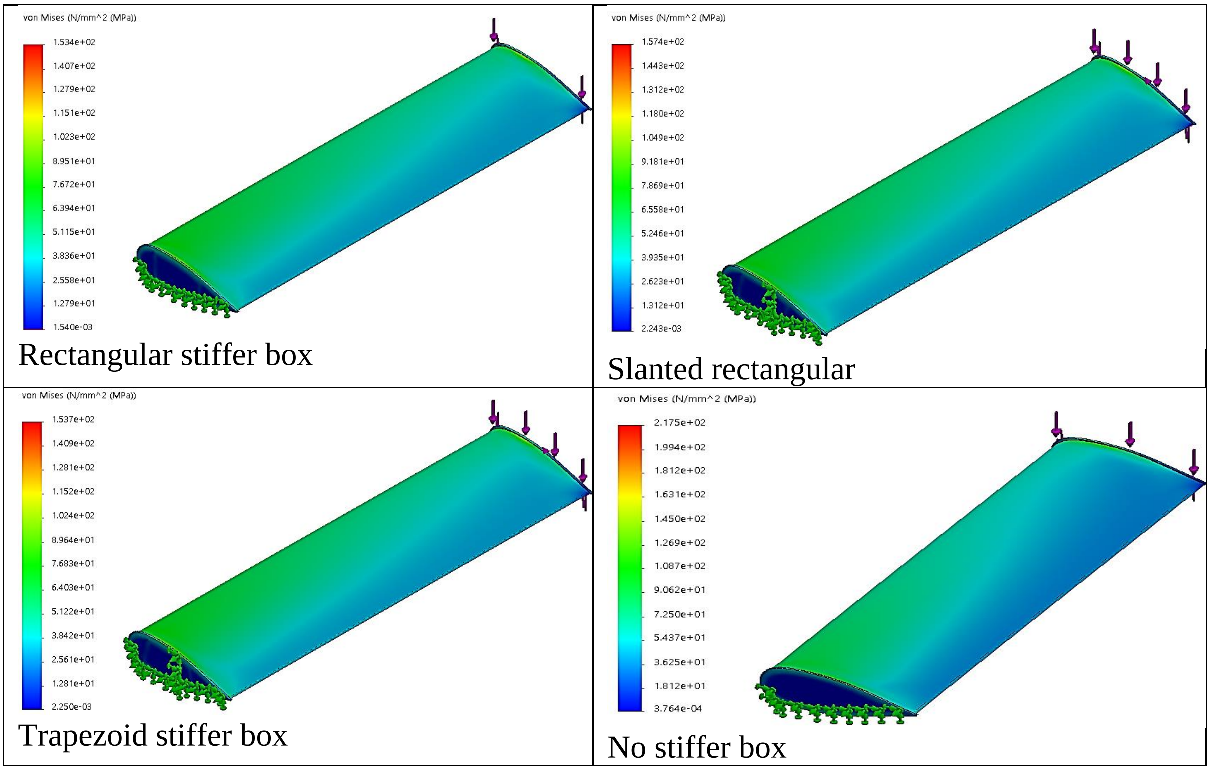

Bending-torsion resultant displacement distribution of different stiffer box

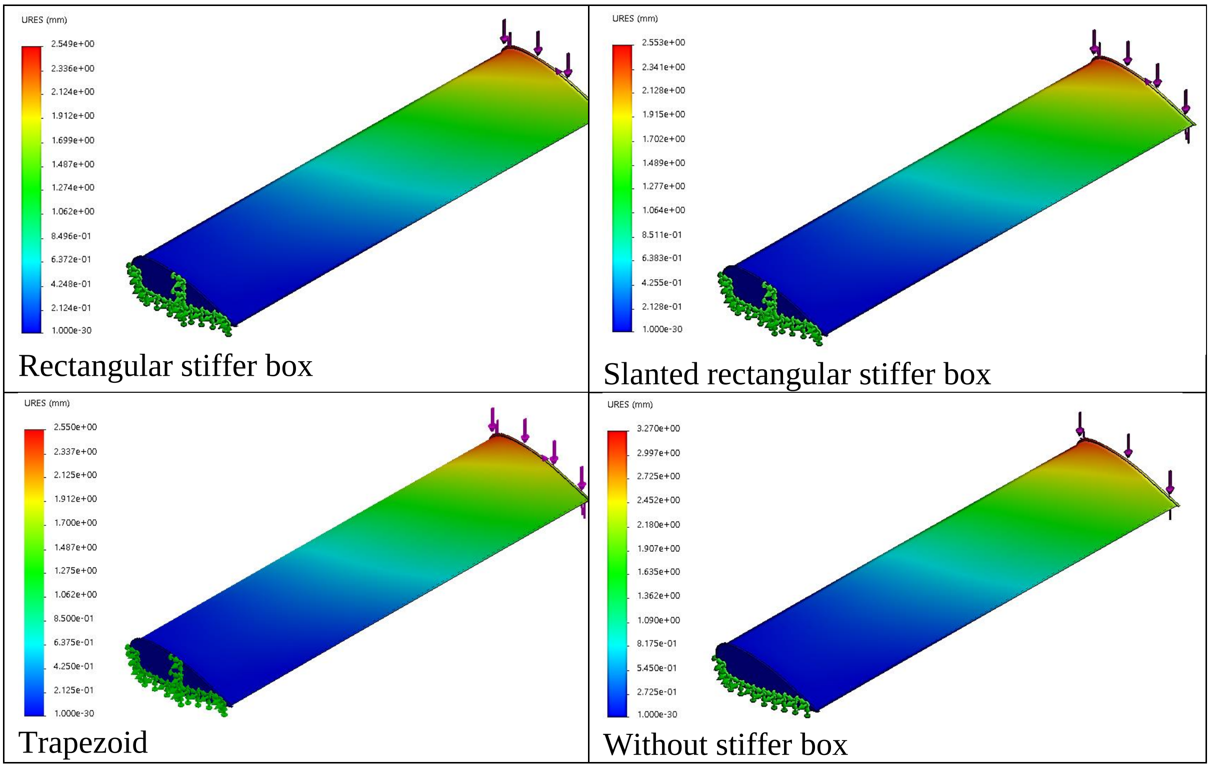

Shear-torsion Von mise stress distribution of different stiffer box

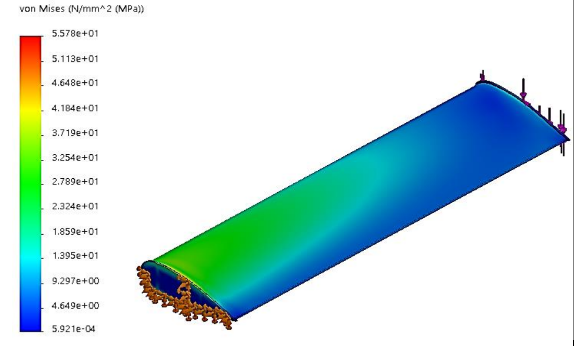

Rectangular stiffer box

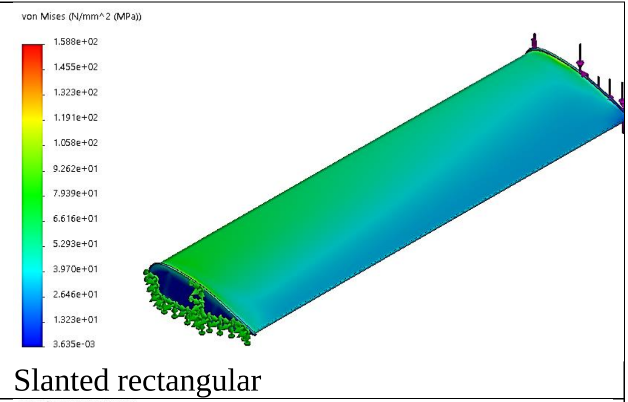

Slanted rectangular

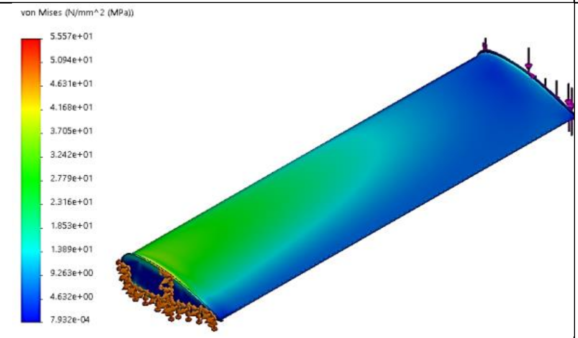

Trapezoid stiffer box

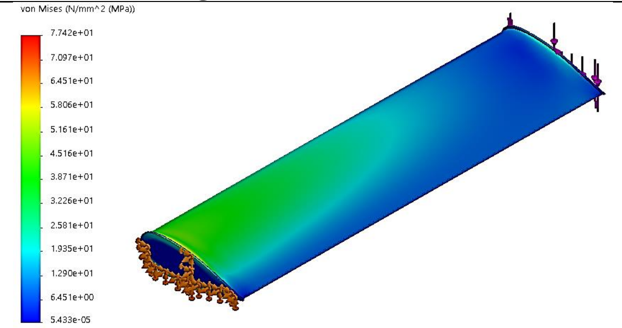

No stiffer box

Shear-torsion resultant displacement distribution of different stiffer box

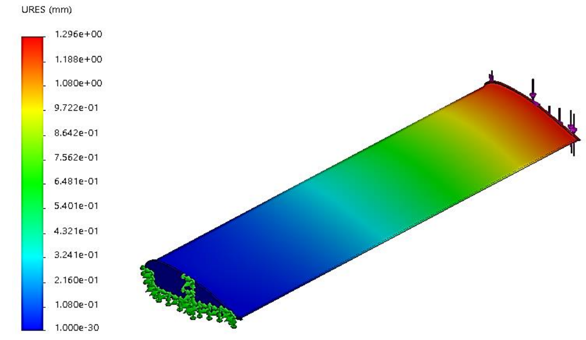

Rectangular stiffer box

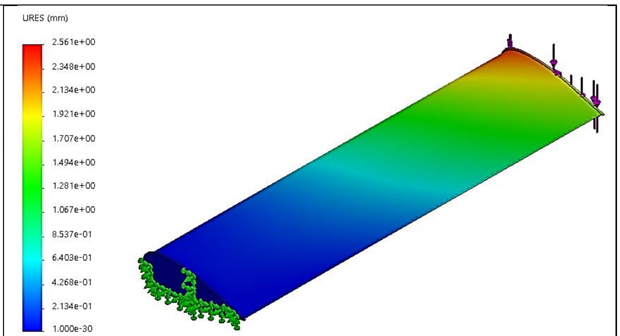

Slanted rectangular stiffer box

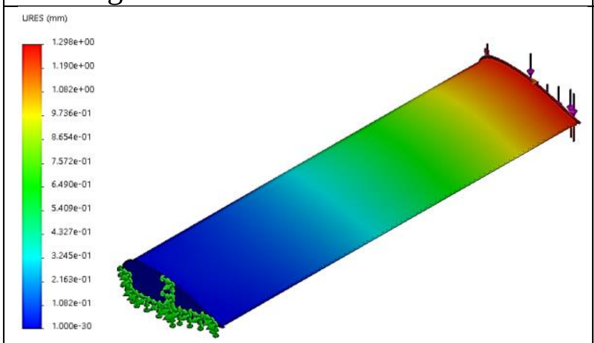

Trapezoid

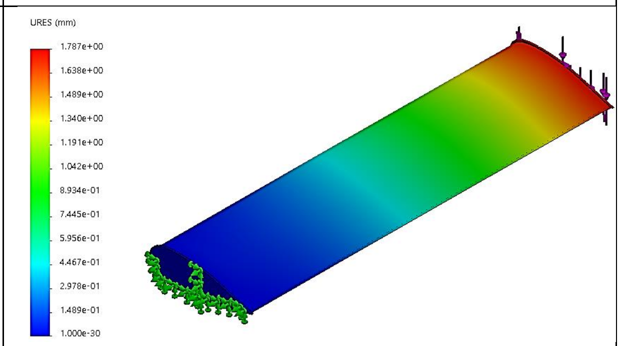

Without stiffer box

Bending-shear-torsion Von mise stress distribution of different stiffer box

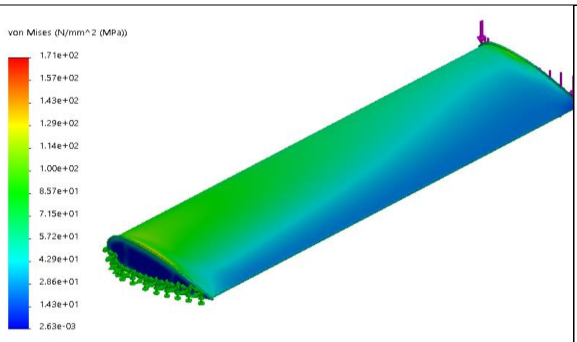

Rectangular stiffer box

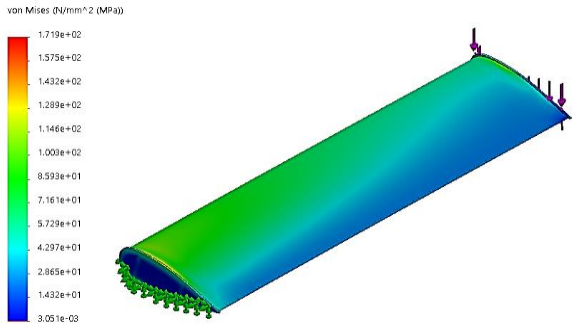

Slanted rectangular

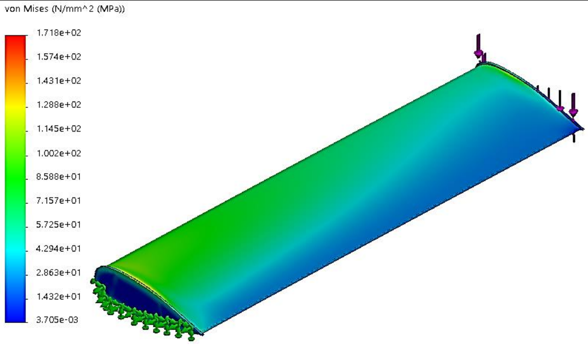

Trapezoid stiffer box

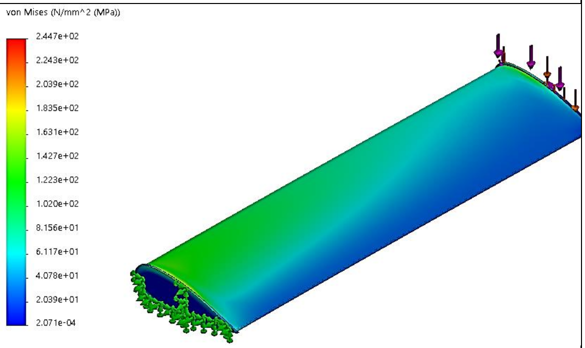

No stiffer box

Bending-shear-torsion resultant displacement distribution of different stiffer box

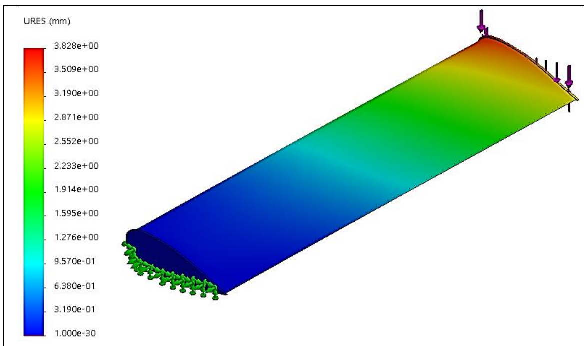

Rectangular stiffer box

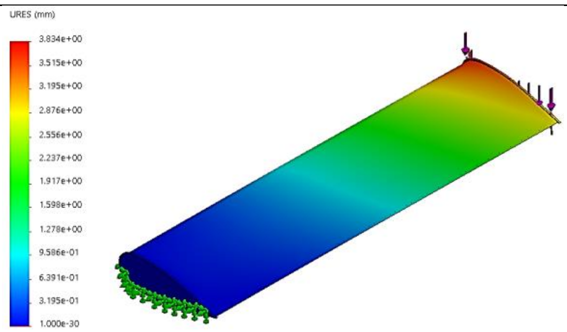

Slanted rectangular stiffer box

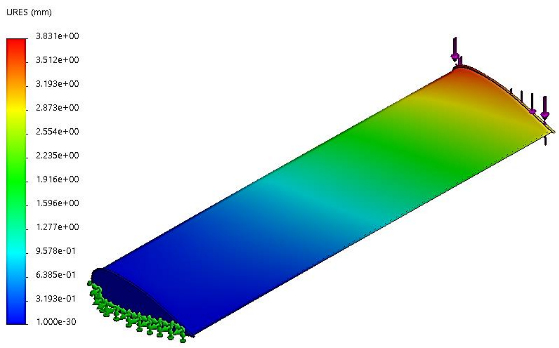

Trapezoid

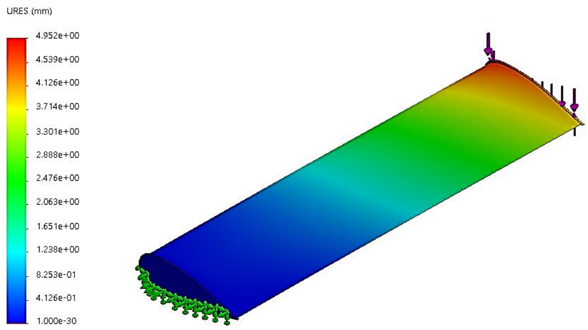

Without stiffer box

Appendix B

Asymmetric thin-walled composite beam simulation results

Pure bending von mise stress results of different stiffer boxes

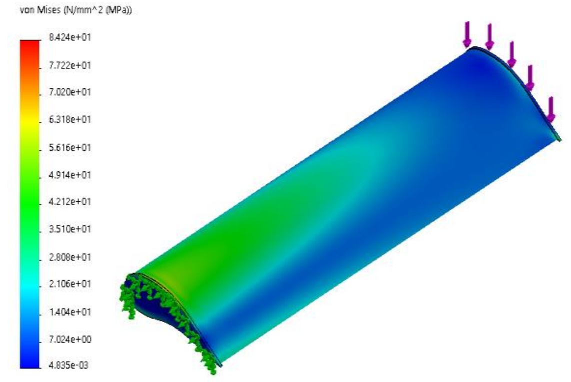

Without stiffer box

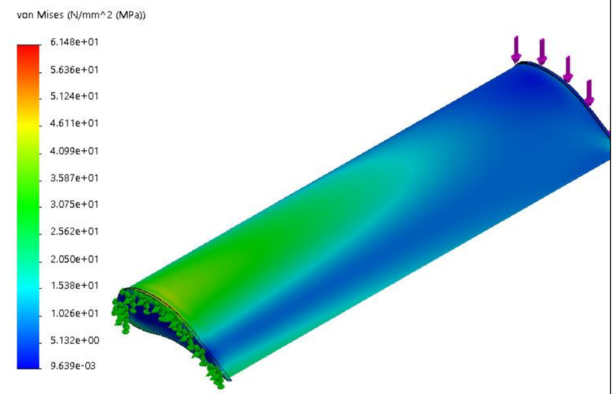

Rectangular stiffer box

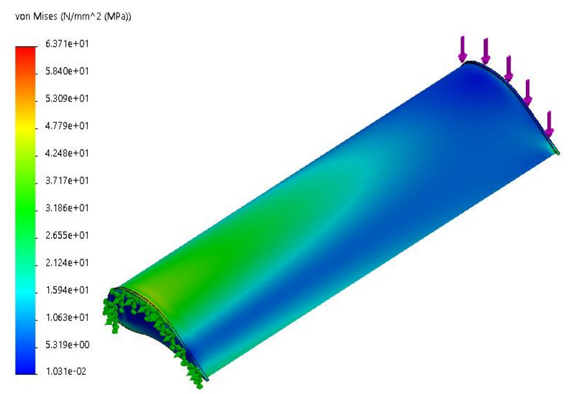

Left slanted rectangular stiffer box

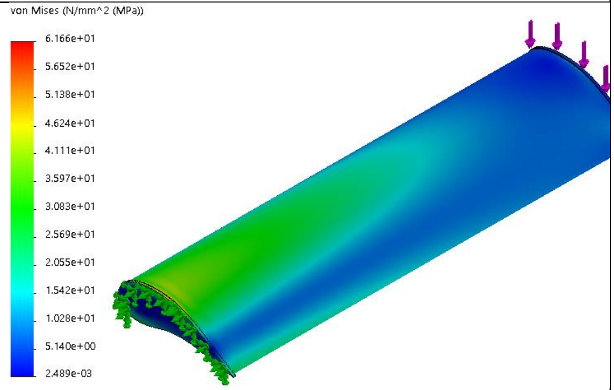

Right slanted rectangular stiffer box

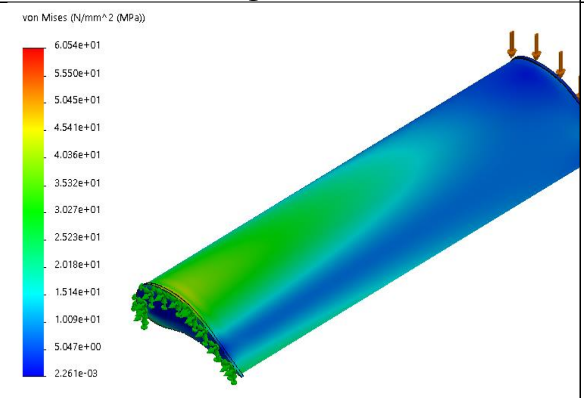

Downward trapezoid stiffer box

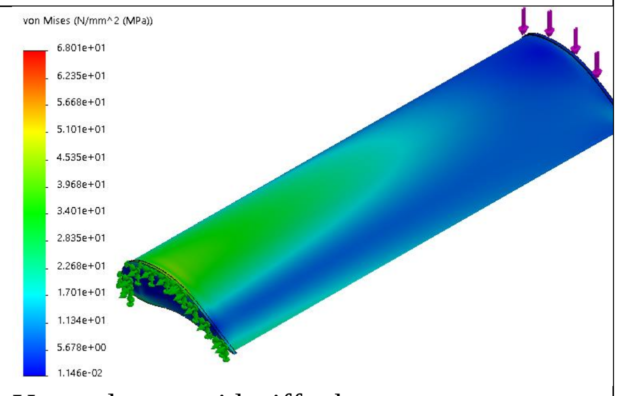

Upward trapezoid stiffer box

Pure bending resultant displacement results of different stiffer boxes

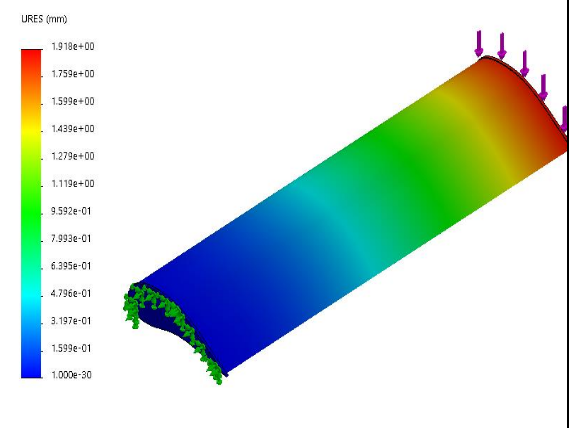

Without stiffer box

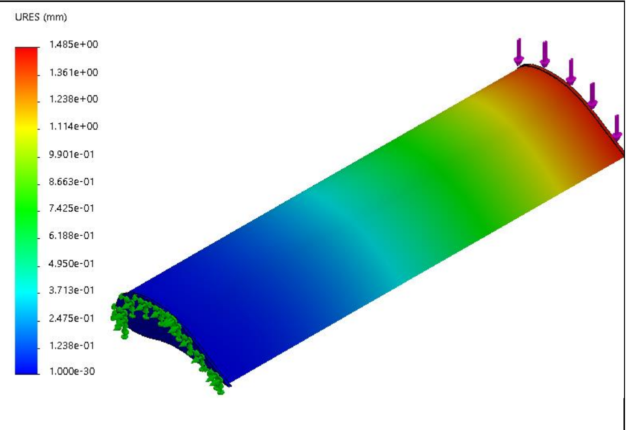

Rectangular stiffer box

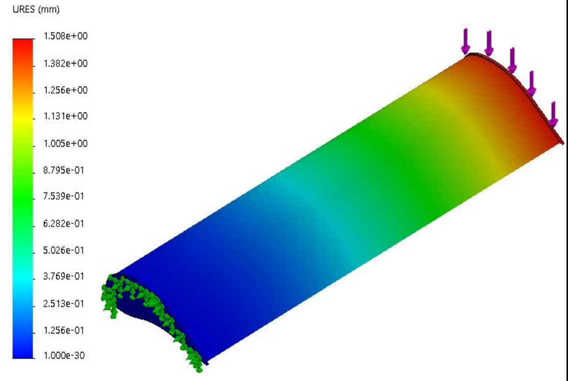

Left slanted rectangular stiffer box

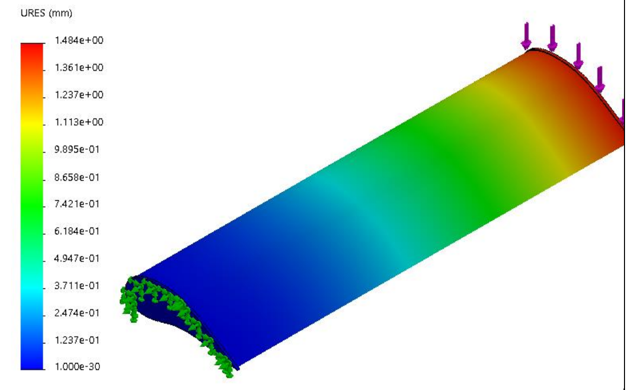

Right slanted rectangular stiffer box

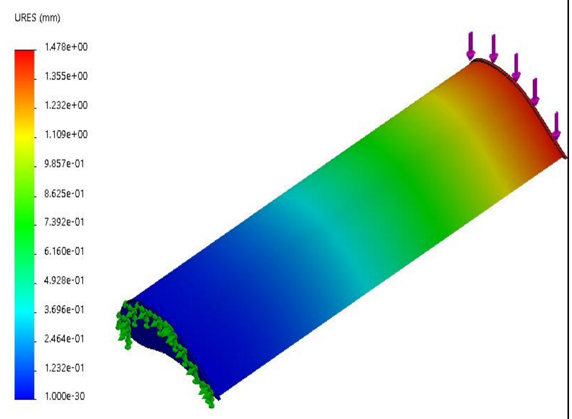

Downward trapezoid stiffer box

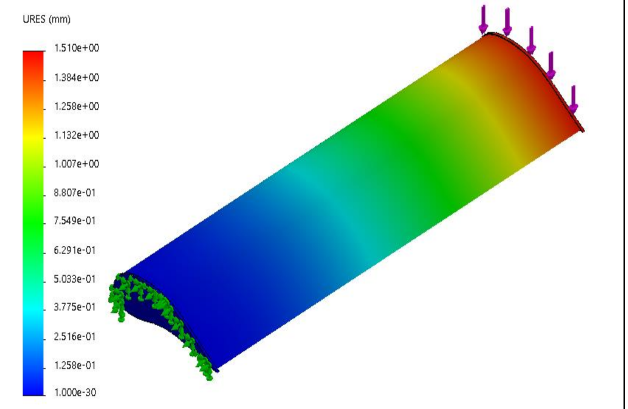

Upward trapezoid stiffer box

Pure shear von mise stress results of different stiffer boxes

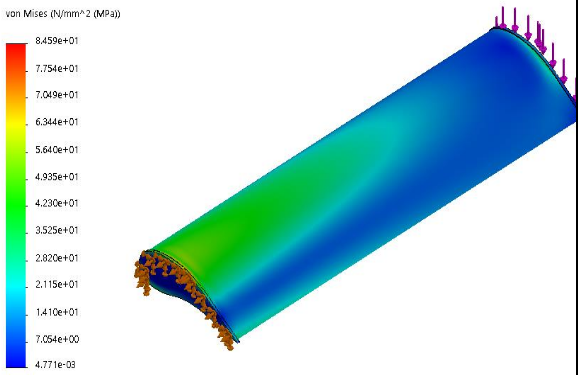

Without stiffer box

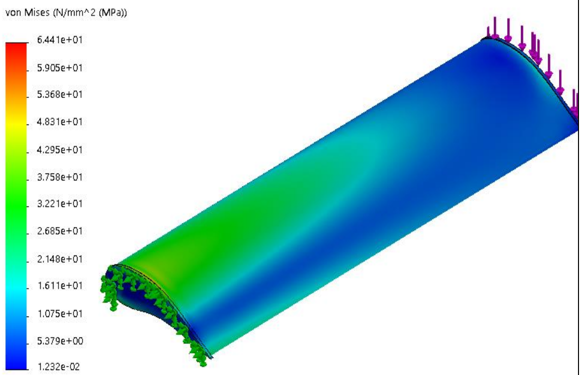

Rectangular stiffer box

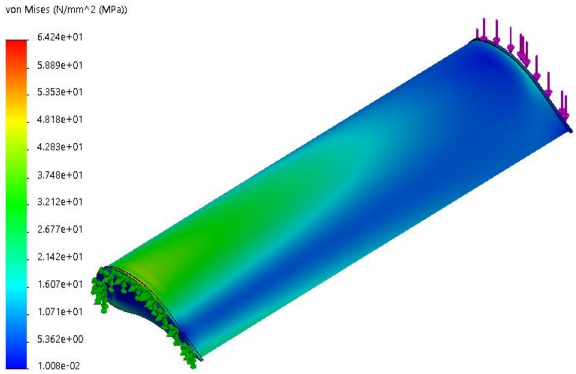

Left slanted rectangular stiffer box

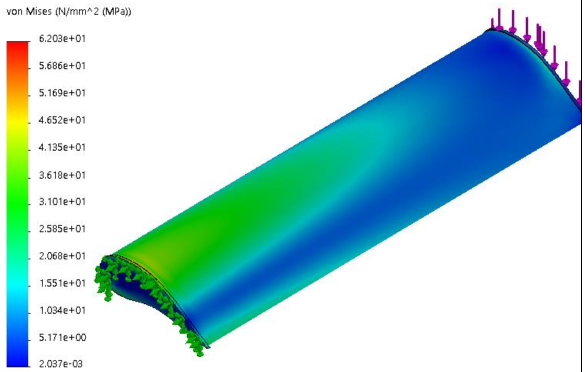

Right slanted rectangular stiffer box

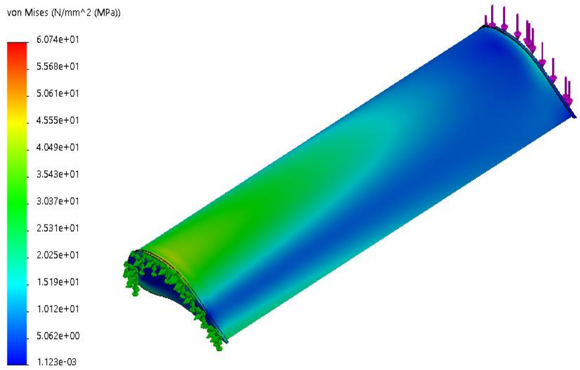

Downward trapezoid stiffer box

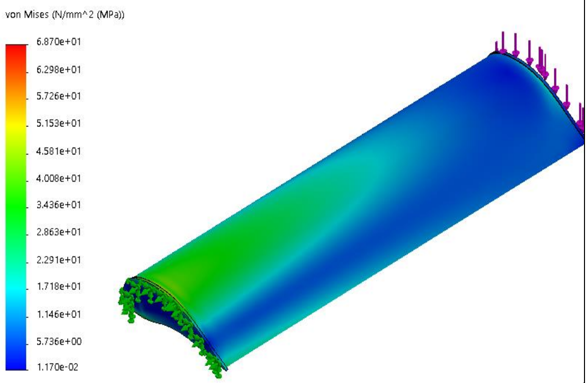

Upward trapezoid stiffer box

Pure shear resultant displacement results of different stiffer boxes

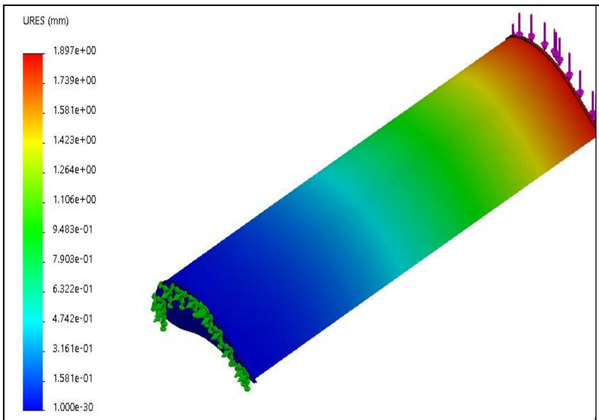

Without stiffer box

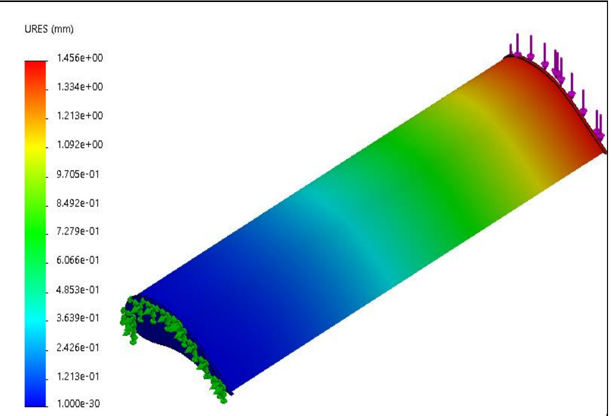

Rectangular stiffer box

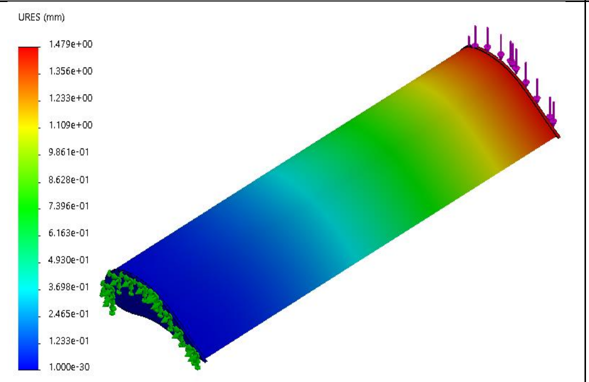

Left slanted rectangular stiffer box

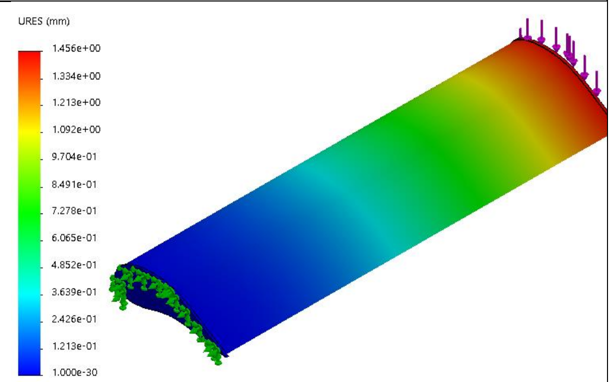

Right slanted rectangular stiffer box

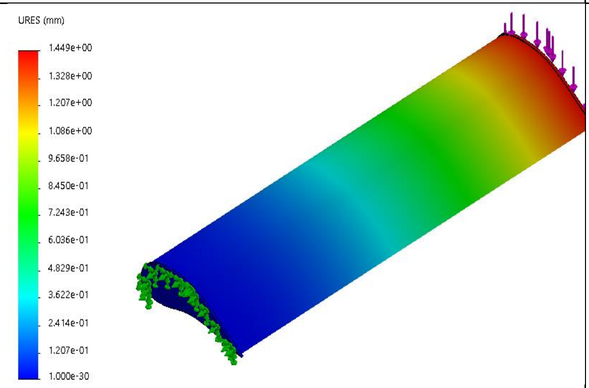

Downward trapezoid stiffer box

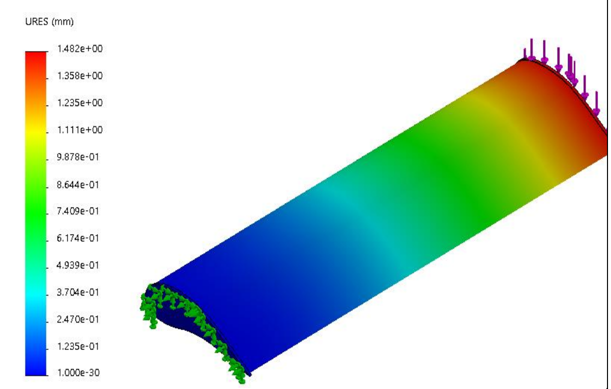

Upward trapezoid stiffer box

Pure torsion von mise stress results of different stiffer boxes

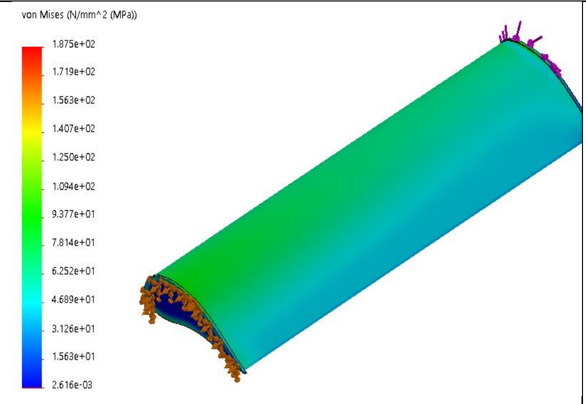

Without stiffer box

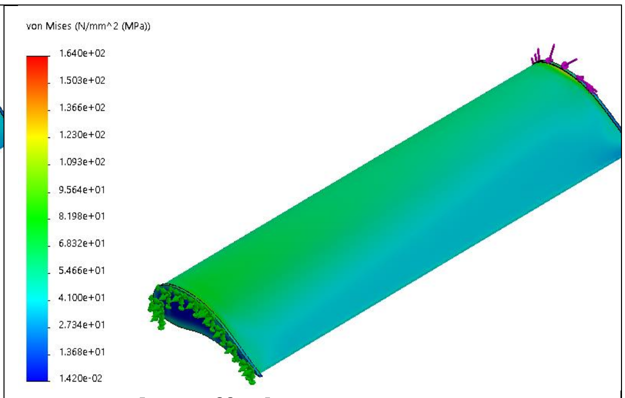

Rectangular stiffer box

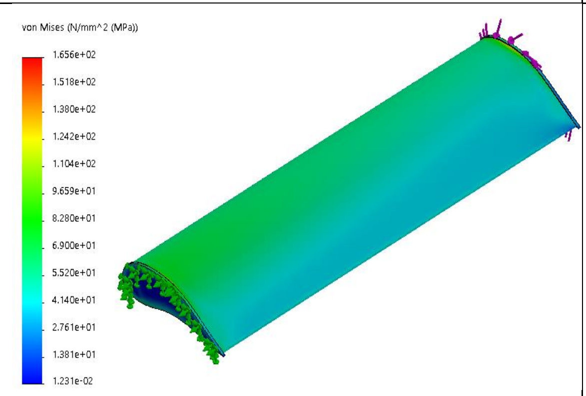

Left slanted rectangular stiffer box

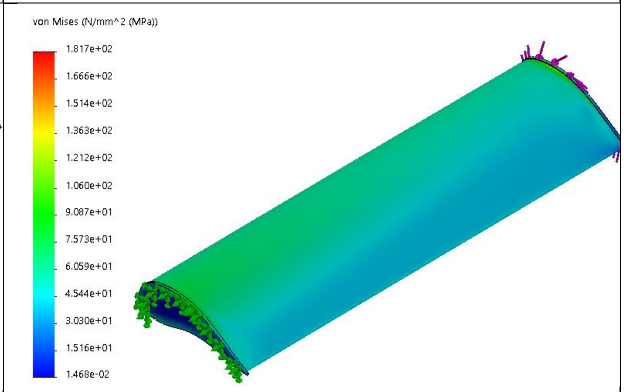

Right slanted rectangular stiffer box

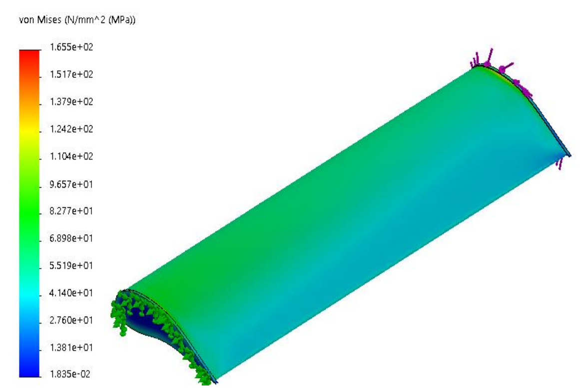

Downward trapezoid stiffer box

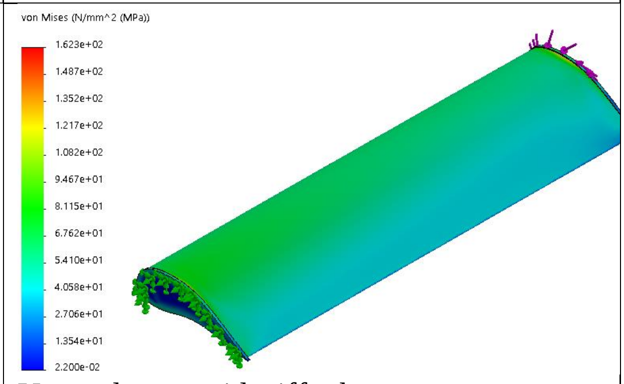

Upward trapezoid stiffer box

Pure torsion resultant displacement results of different stiffer boxes

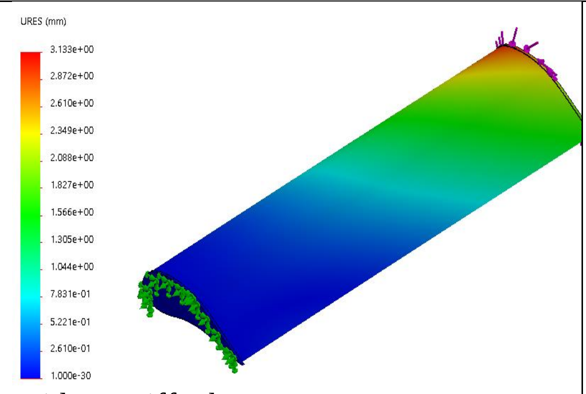

Without stiffer box

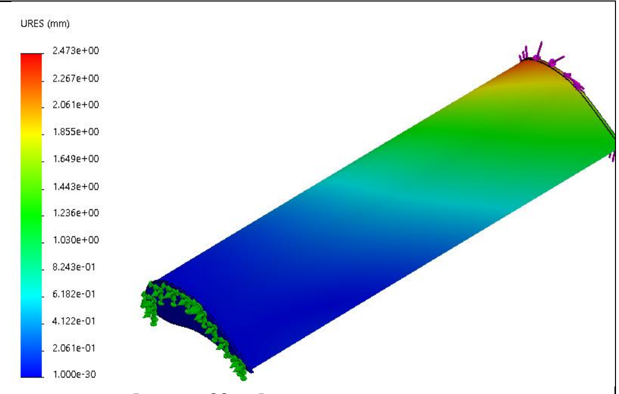

Rectangular stiffer box

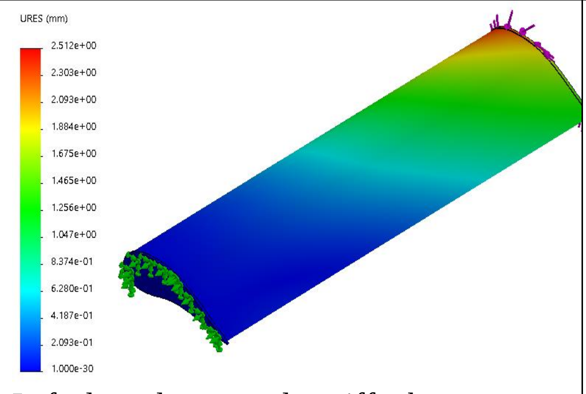

Left slanted rectangular stiffer box

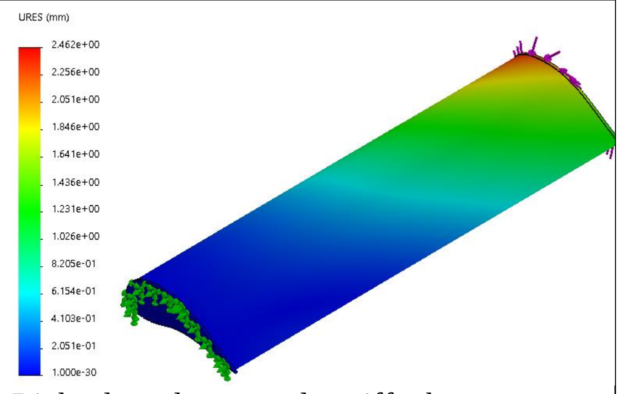

Right slanted rectangular stiffer box

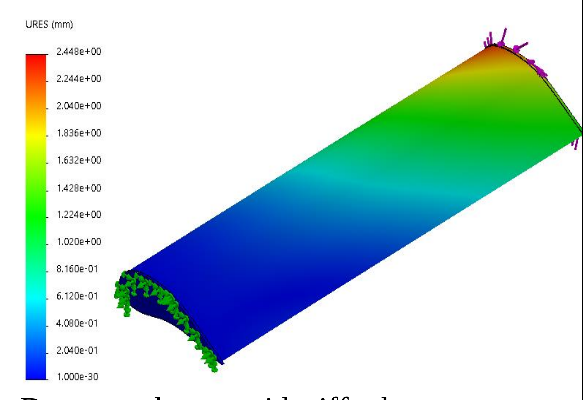

Downward trapezoid stiffer box

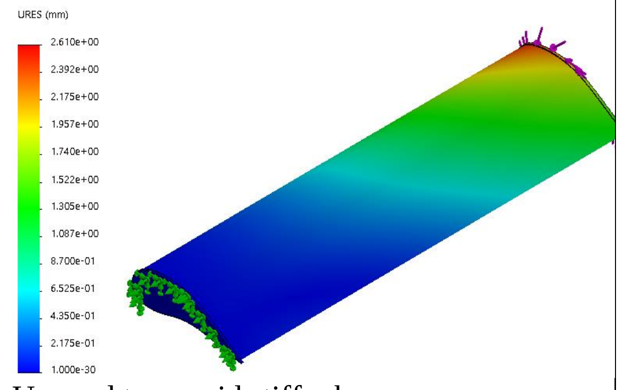

Upward trapezoid stiffer box

Bending-shear von mise stress results of different stiffer boxes

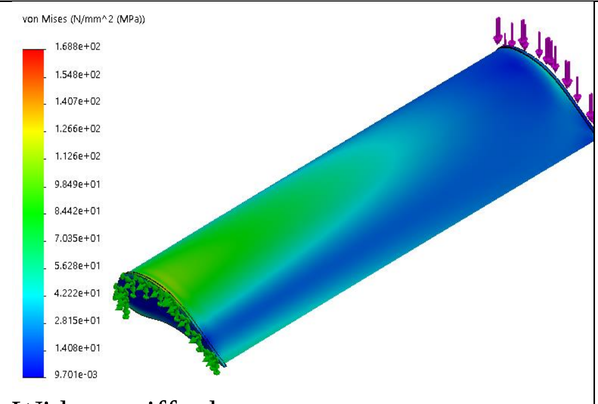

Without stiffer box

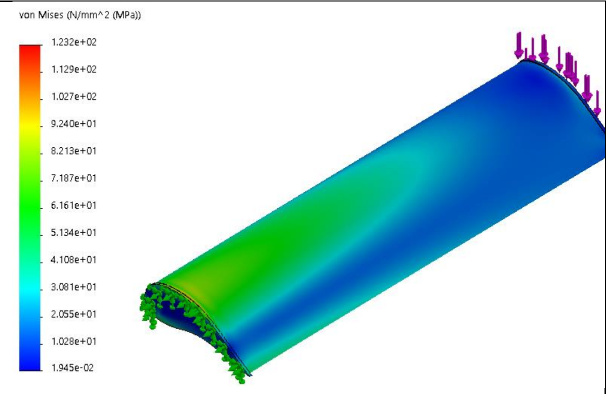

Rectangular stiffer box

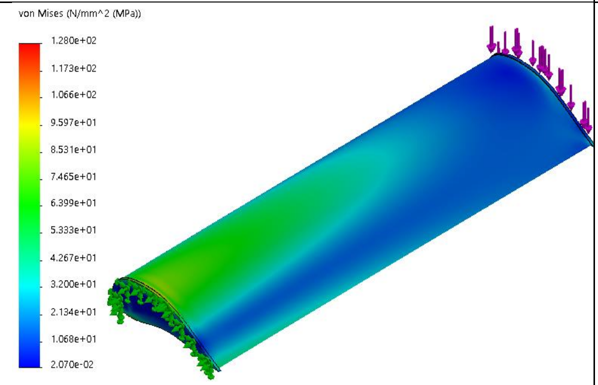

Left slanted rectangular stiffer box

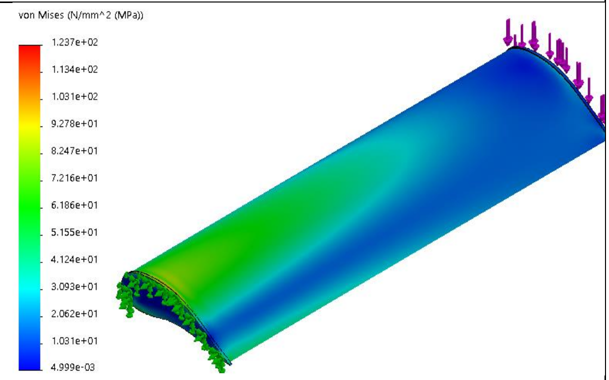

Right slanted rectangular stiffer box

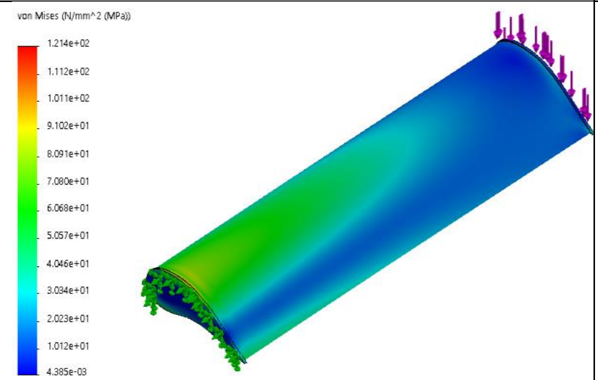

Downward trapezoid stiffer box

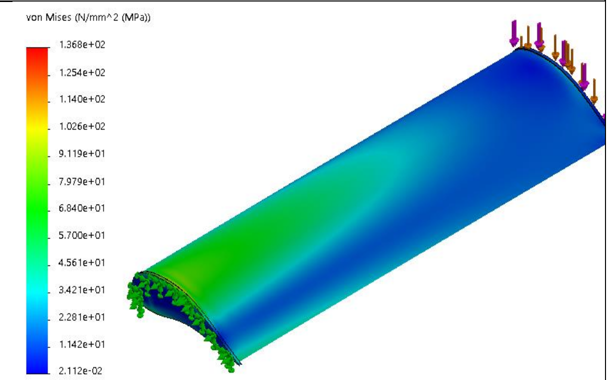

Upward trapezoid stiffer box

Bending-shear resultant displacement results of different stiffer boxes

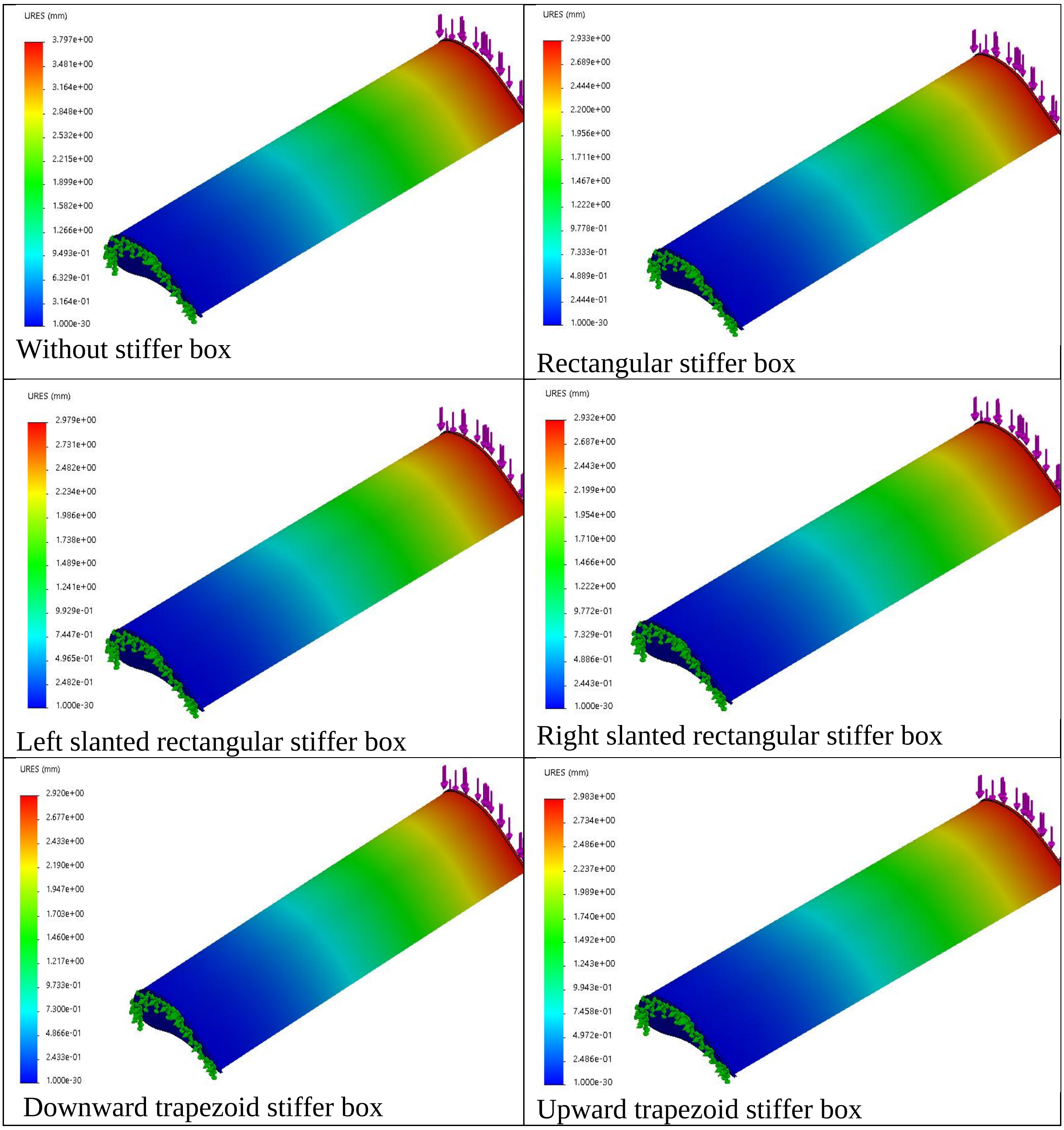

Bending-torsion von mise stress results of different stiffer boxes

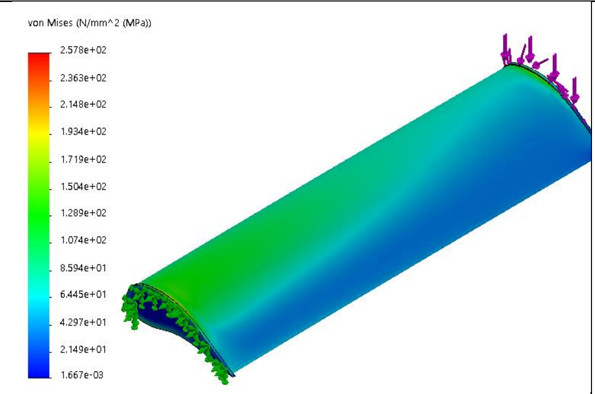

Without stiffer box

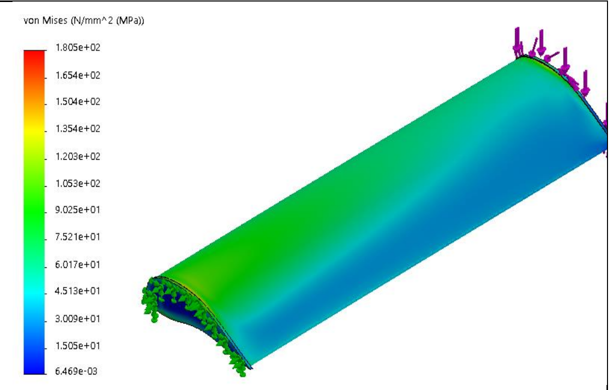

Rectangular stiffer box

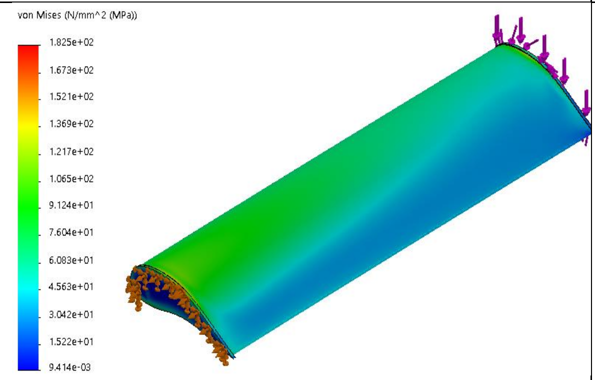

Left slanted rectangular stiffer box

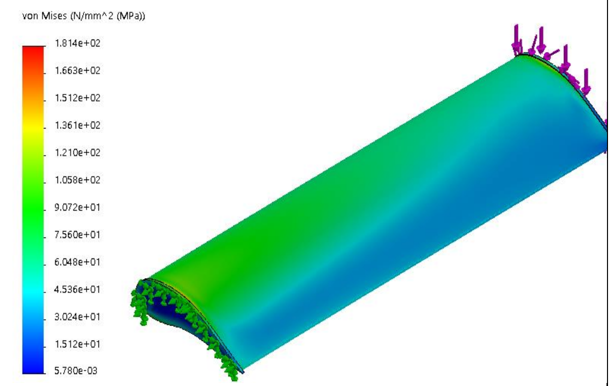

Right slanted rectangular stiffer box

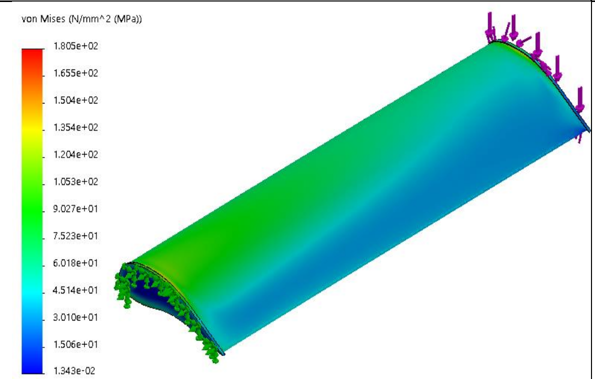

Downward trapezoid stiffer box

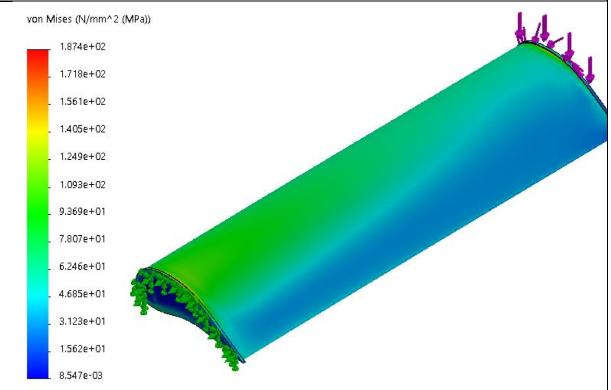

Upward trapezoid stiffer box

Bending-torsion resultant displacement results of different stiffer boxes

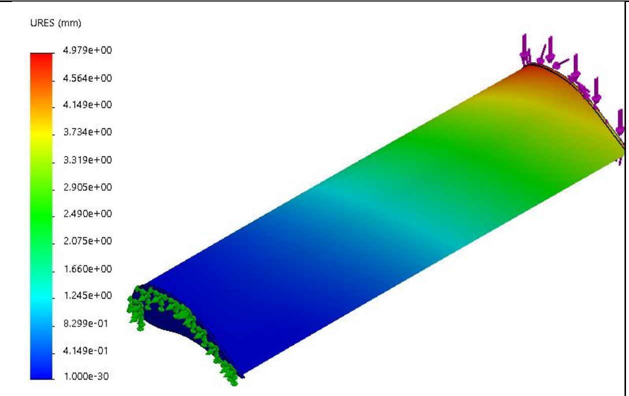

Without stiffer box

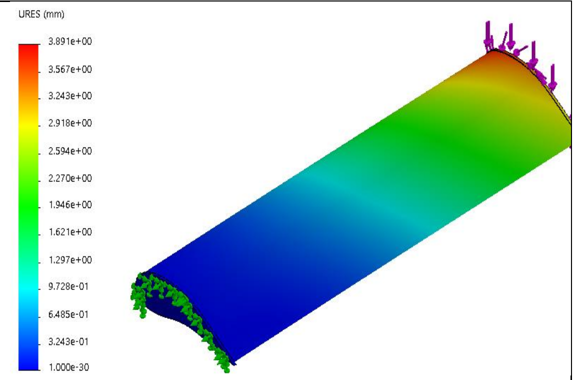

Rectangular stiffer box

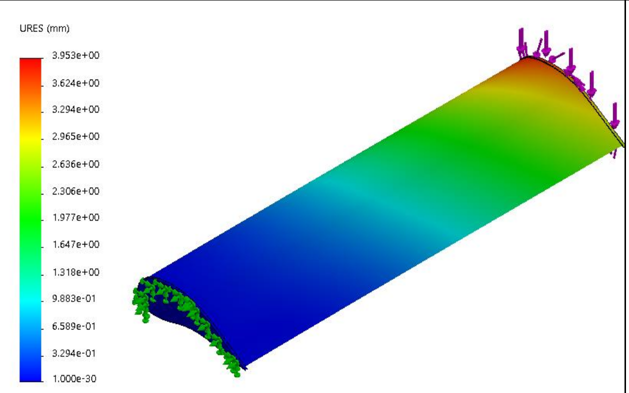

Left slanted rectangular stiffer box

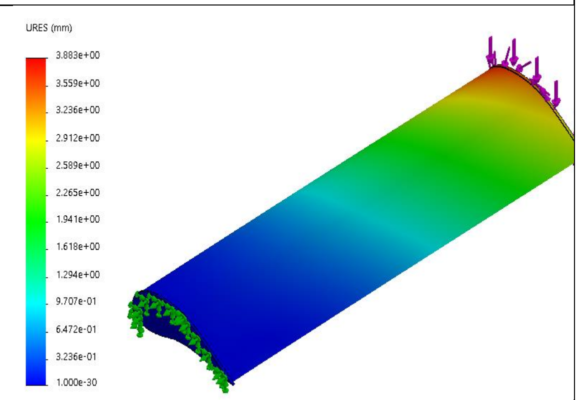

Right slanted rectangular stiffer box

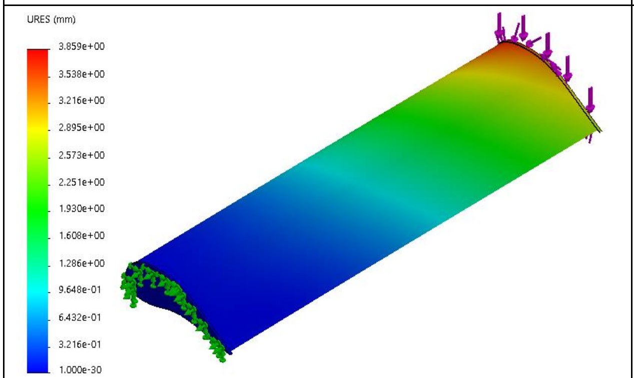

Downward trapezoid stiffer box

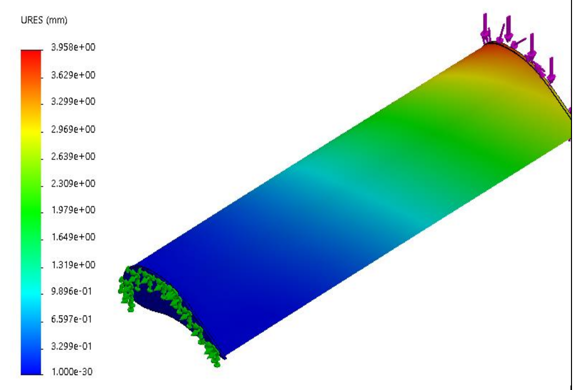

Upward trapezoid stiffer box

Shear-torsion von Mise stress results of different stiffer boxes

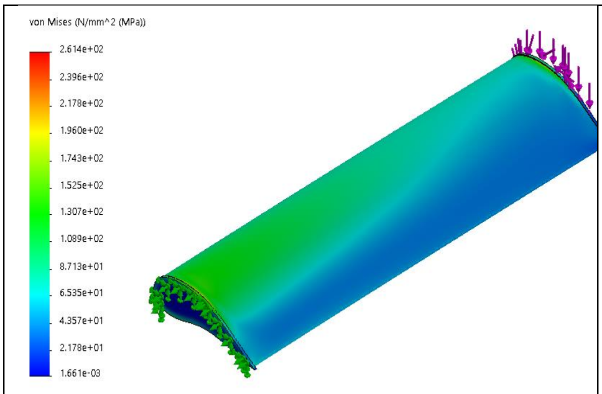

Without stiffer box

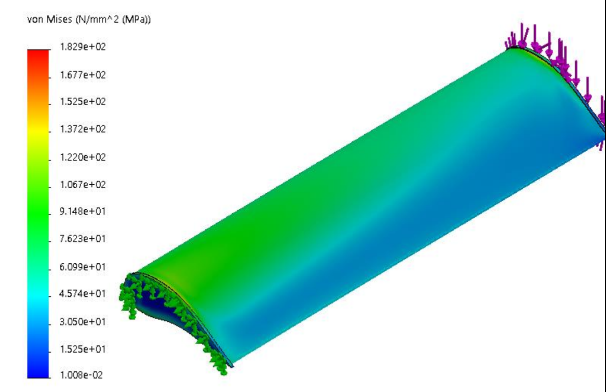

Rectangular stiffer box

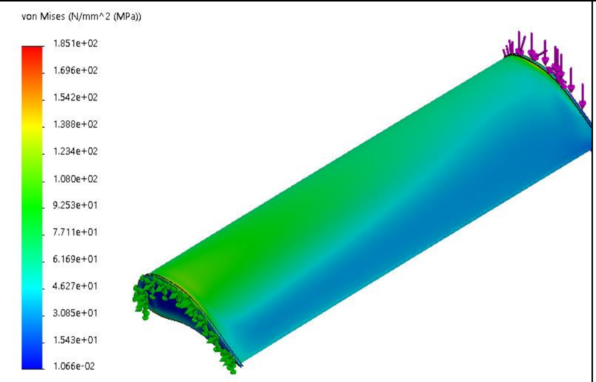

Left slanted rectangular stiffer box

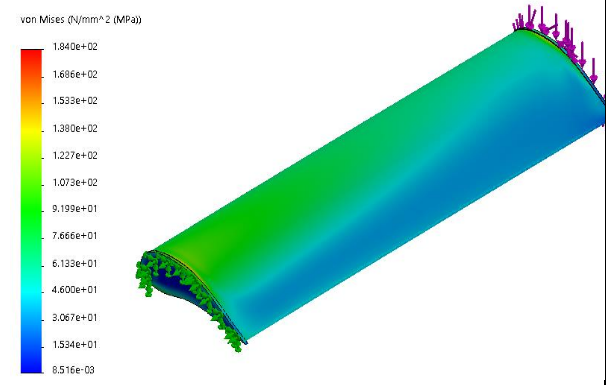

Right slanted rectangular stiffer box

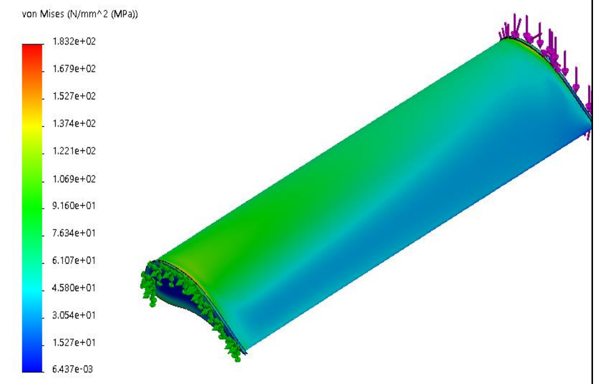

Downward trapezoid stiffer box

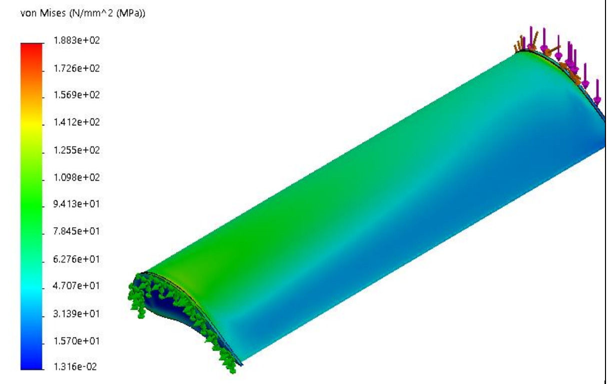

Upward trapezoid stiffer box

Shear-torsion resultant displacement results of different stiffer boxes

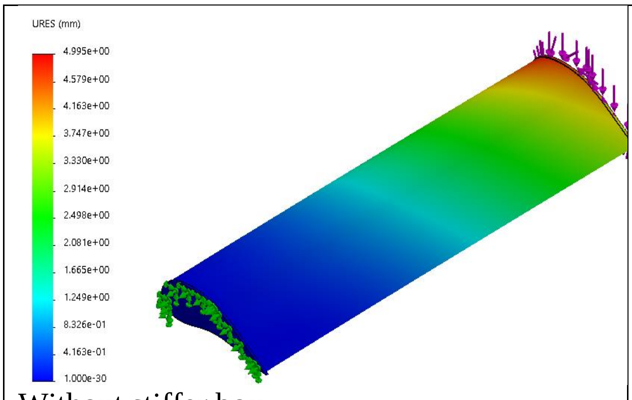

Without stiffer box

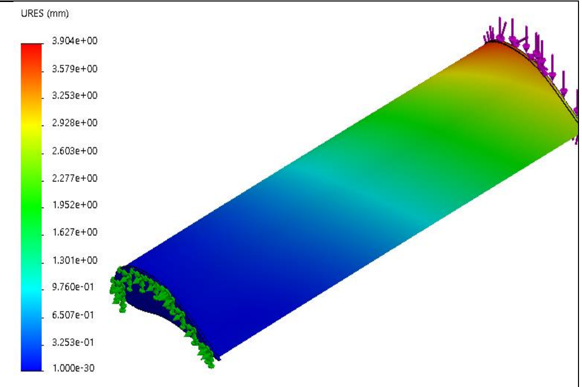

Rectangular stiffer box

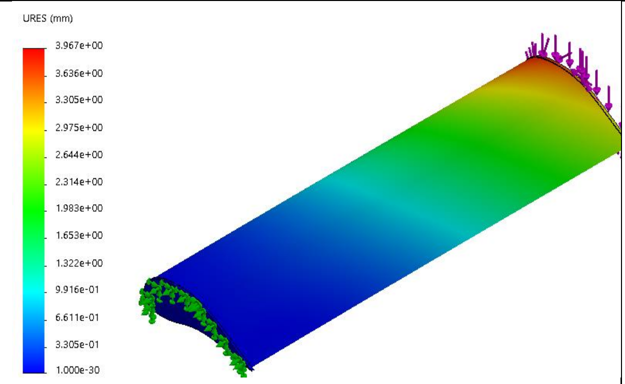

Left slanted rectangular stiffer box

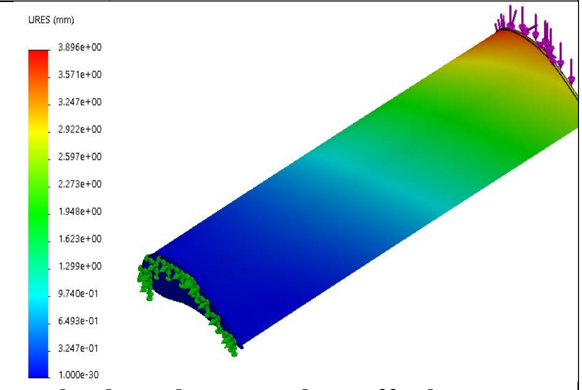

Right slanted rectangular stiffer box

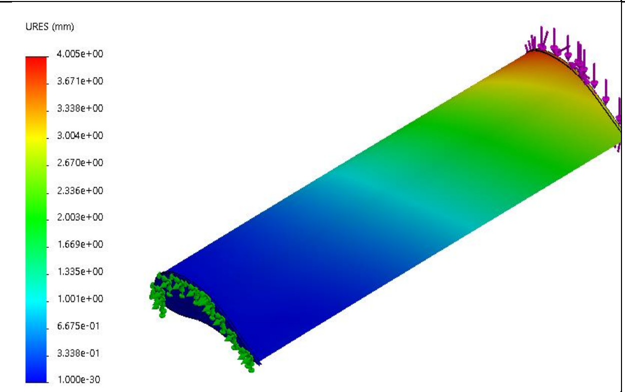

Downward trapezoid stiffer box

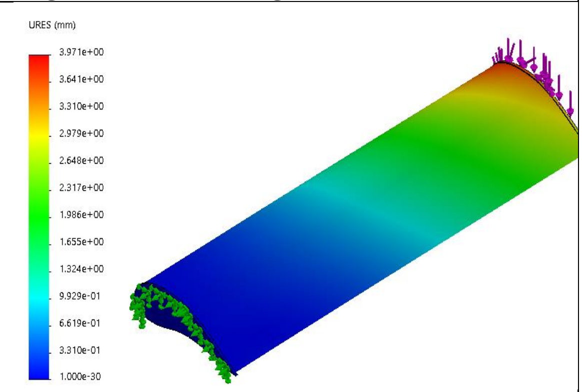

Upward trapezoid stiffer box

Bending-shear-torsion von mise stress results of different stiffer boxes

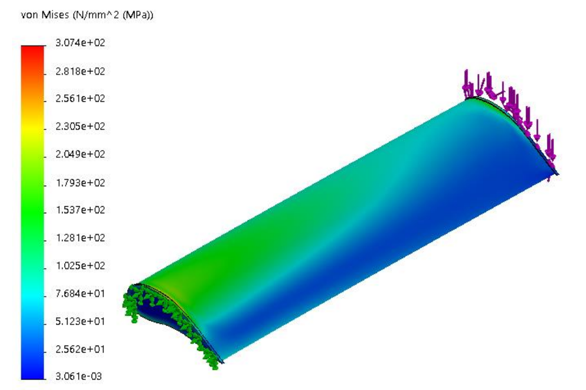

Without stiffer box

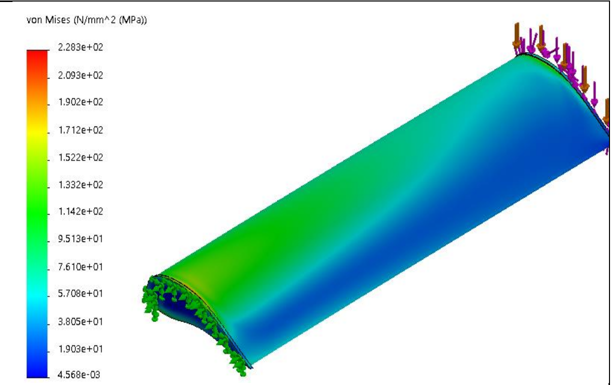

Rectangular stiffer box

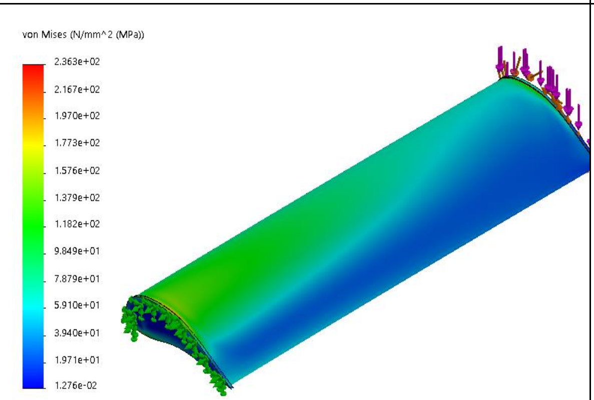

Left slanted rectangular stiffer box

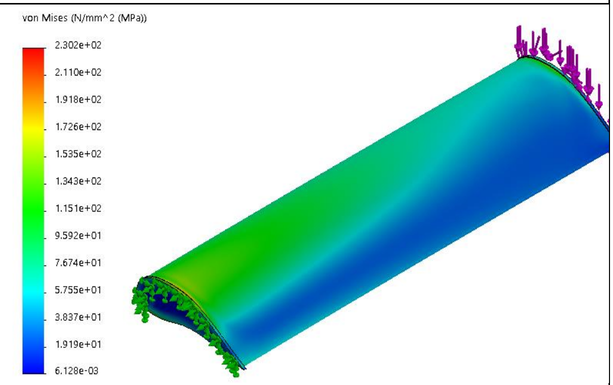

Right slanted rectangular stiffer box

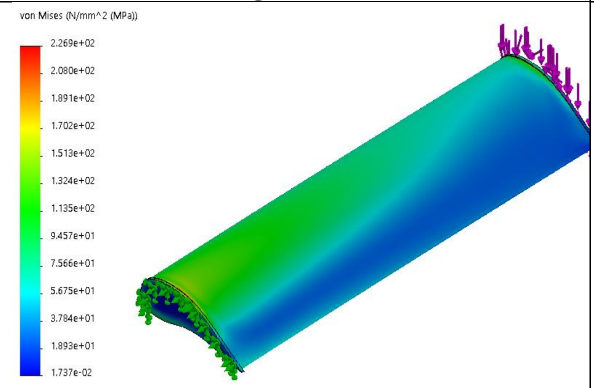

Downward trapezoid stiffer box

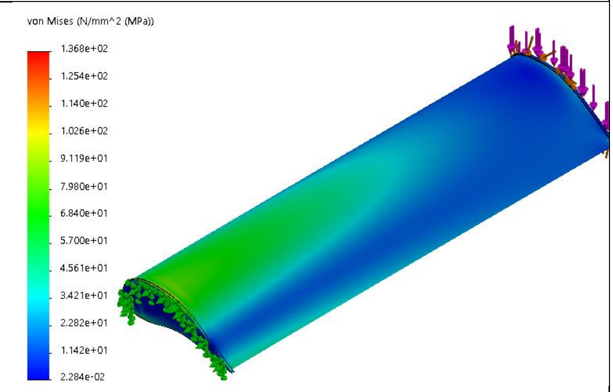

Upward trapezoid stiffer box

Bending-shear-torsion resultant displacement results of different stiffer boxes

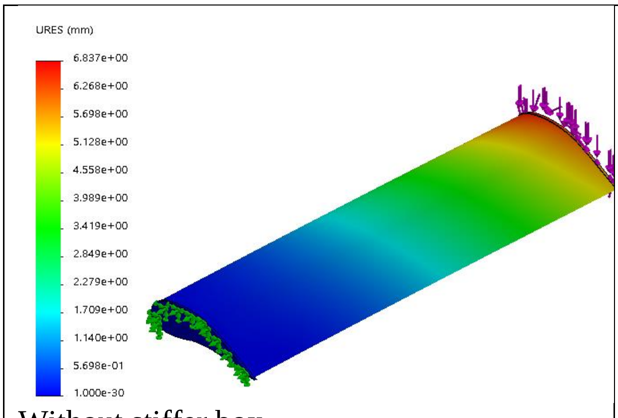

Without stiffer box

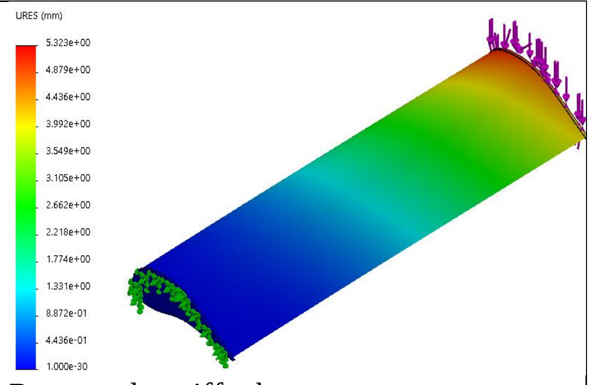

Rectangular stiffer box

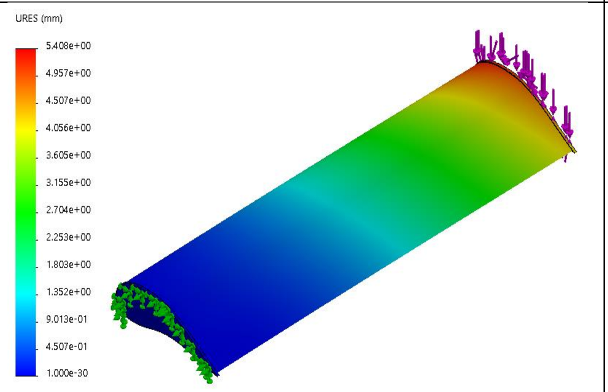

Left slanted rectangular stiffer box

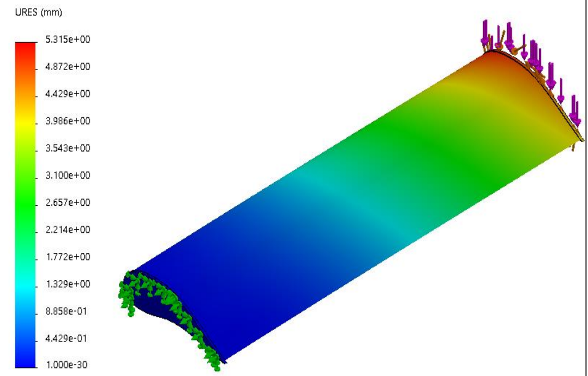

Right slanted rectangular stiffer box

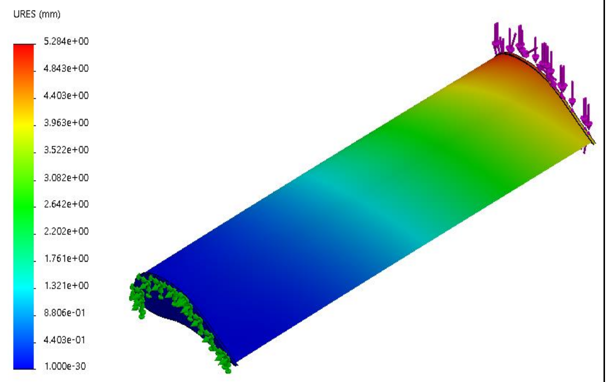

Downward trapezoid stiffer box

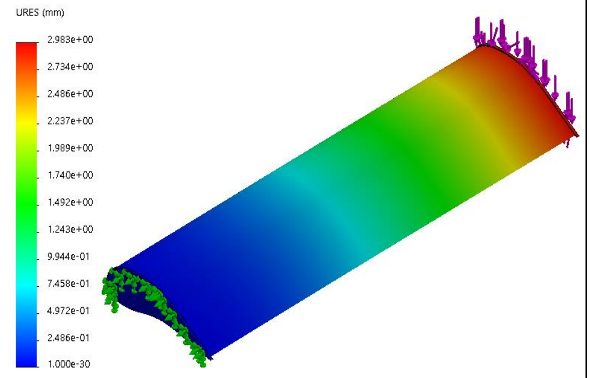

Upward trapezoid stiffer box